Karlsruhe Institute of Technology

Arc-dpa and NRT displacement cross-sections for neutron irradiation of materials from Be to Bi calculated using JEFF-4T1, ENDF/B-VIII, JENDL-5, and TENDL-2021 data

A.Yu. Konobeyev, D. Leichtle

KIT SCIENTIFIC WORKING PAPERS 190

INR, Karlsruhe Institute of Technology, 76344 Eggenstein-Leopoldshafen, Germany

Impressum

Karlsruher Institut für Technologie (KIT)
www.kit.edu

2022

ISSN: 2194-1629

Abstract

Atomic displacement cross-sections for an advanced assessment of radiation damage rates were calculated for materials from Be to Bi using the arc-dpa model and NRT model, and data from JEFF-4T1 test library, the ENDF/B-VIII, JENDL-5, and TENDL-2021 libraries at neutron incident energies from 10^{-5} eV to the maximum available energy.

Obtained cross-sections were extended to 200 MeV using TENDL-2021 data and earlier TENDL versions.

Data prepared in ENDF/B and ACE format are available on the site https://bit.ly/3L8ZlHQ

CONTENTS

page

1. **Introduction** ……………………………………………………………………….…… 1

2. **Data and tools used for calculations** …………..…………………..…..…..…….. 1

3. **Displacement cross-sections** ………………………...………..…..……….……..   3

   3.1 Data from 10^{-5} eV up to maximum available energy in files …..…...……… 3

   3.2 Data extended up to 200 MeV ………...……………………………………… 4

4. **Conclusion** ………………………………..……………………………….………….. 5

Acknowledgement ………………………..…………………………………….……... 5

References …….…………………….……………………................................. 11

Appendix Displacement cross-sections obtained using the arc-dpa and NRT models, and data from JEFF-4T1 …………...……………................................. 15

1. Introduction

In 2018, the atomic displacement cross-sections [1-4] were obtained using the arc-dpa model [5], the NRT model [6], and neutron data from the libraries ENDF/B-VIII [7], JEFF-3.3 [8], JENDL-4 [9], and TENDL-2017 [10]. Recently, new JENDL-5 [11] and TENDL-2021 [12] libraries have been published, a test library JEFF-4T1 [13] appeared.

The aim of this work is to obtain arc-dpa and NRT displacement cross-sections for neutron irradiation of materials from beryllium to bismuth using the new data.

The method for obtaining the arc-dpa parameters was recently proposed in Ref.[14]. The derived parameters [14] together with data from Refs.[5,15] were used to perform calculations of displacement cross-sections. For some materials, the calculation of the number of stable defects produced under irradiation using the arc-dpa model was supplemented by calculations applying the BCA approach. The numerical calculations were performed using the IOTA code [16] and SRIM code [17].

The resulting displacement cross-sections were recorded in ENDF/B and ACE formats.

Section 2 discusses the model parameters and tools used for calculations. Section 3 presents the obtained cross-sections.

2. Data and tools used for calculations

According to the arc-dpa model [5] the defect generation efficiency [18] can be approximated as following

$$\xi_{arcdpa}(T_{dam}) = \frac{1-c_{arcdpa}}{(2E_d/0.8)^{b_{arcdpa}}} T_{dam}^{b_{arcdpa}} + c_{arcdpa}, \qquad (1)$$

where b_{arcdpa} and c_{arcdpa} are parameters, E_d is the average threshold displacement energy, T_{dam} is the “damage energy”, the energy available to produce atom displacement by elastic collision [6] calculated using the Robinson formula [19].

For most of the materials, the c_{arcdpa} parameters and E_d values were taken from Ref.[14]. These data are shown in Figs.1,2. The value of b_{arcdpa} was taken equal to -0.82 [20].

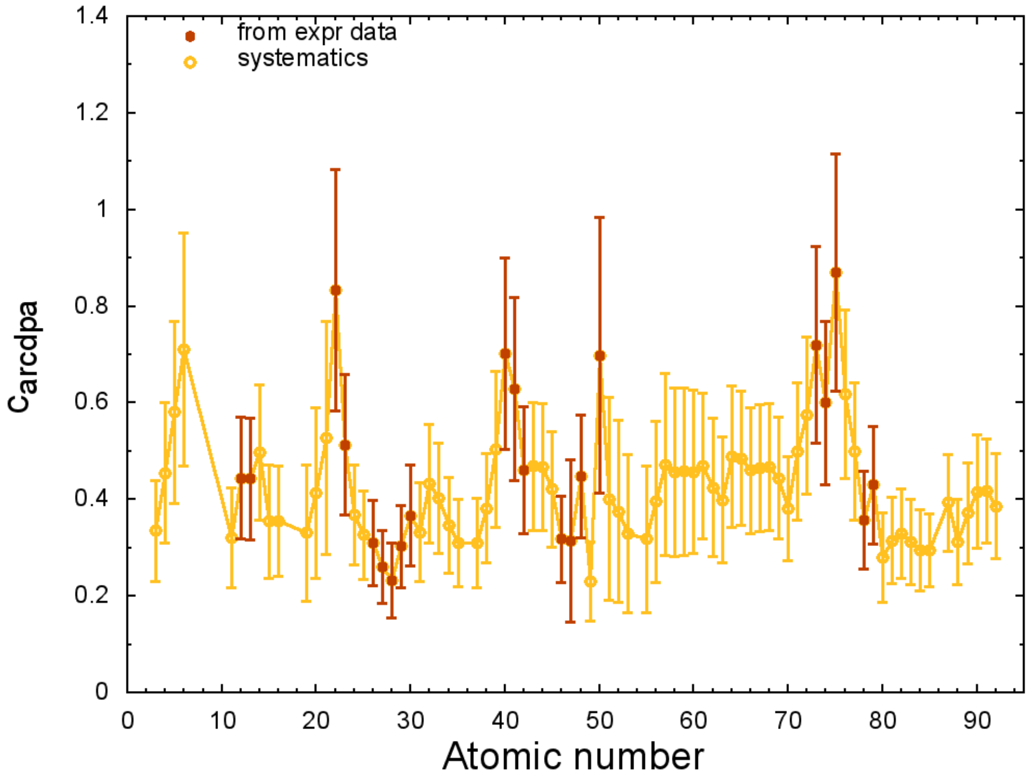

Fig.1 Estimated c_{arcdpa} parameters and experimental values discussed in Ref.[14].

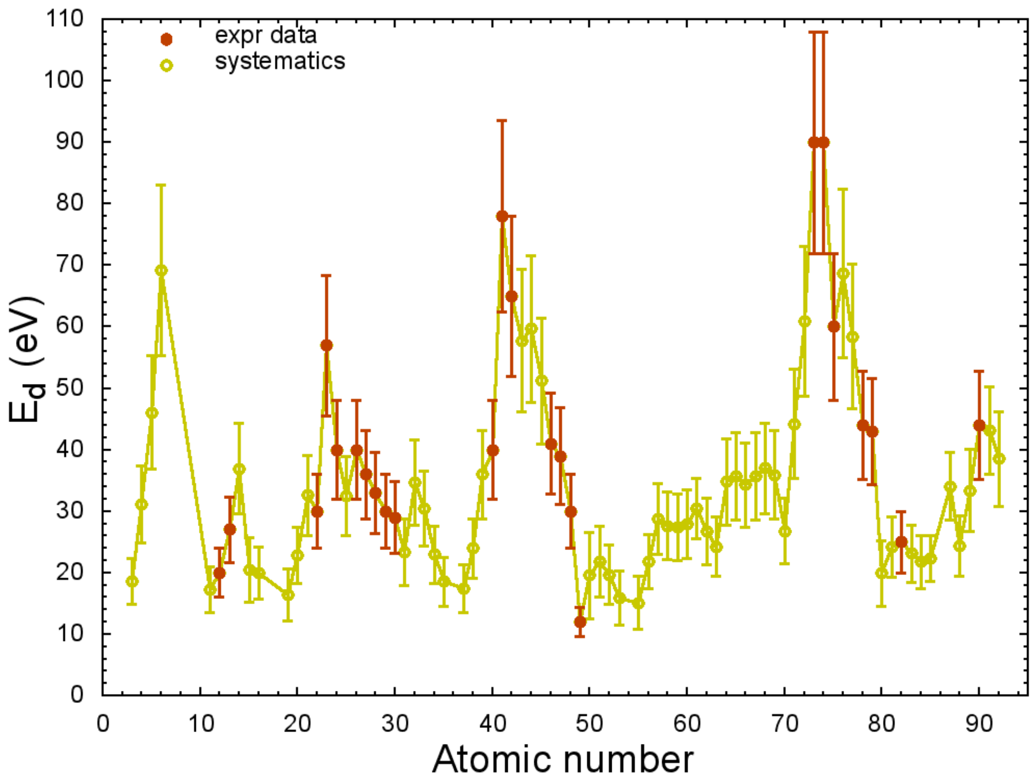

Fig.2 Estimated average threshold displacement energy and experimental data discussed in Ref.[14].

For beryllium b_{arcdpa}, c_{arcdpa}, and E_d values were taken from Ref.[21], for iron, nickel, copper, palladium, tungsten, and platinum from Nordlund and co-authors [5], and for silver and gold from Nordlund [15].

For beryllium, iron, copper, and tungsten additional calculations were performed using the combined arc-dpa - BCA approach [16]. In such calculations, the simulation of ion-ion interactions is performed using BCA until the kinetic energy of the ions drops to a certain energy, and at relatively low kinetic energy, the number of created defects is estimated according to the arc-dpa model with parameters discussed above. Figure 3 shows the example of such calculations for self-irradiation of beryllium. The results of MD simulation shown in Fig.3 were obtained in Ref.[22].

Displacement cross-sections were calculated using the last version of the NJOY-2016 code [23] with implemented subroutines for arc-dpa model calculations and for the use of results of joint arc-dpa and BCA simulations. Data from the test version JEFF-4T1, data from ENDF/B-VIII, JENDL-5, and TENDL-2021 were used to calculate recoil energy spectra and cross-sections.

The PREPRO-2021 code [24] and several service codes were applied to calculate displacement cross sections for natural mixtures of isotopes and other auxiliary calculations.

3. Displacement cross-sections

3.1 Data from 10^{-5} eV up to maximum available energy in files

Displacement cross-sections were obtained for all stable isotopes from Be to Bi and used for calculation of cross sections for natural isotope mixtures. Data from the libraries were used as they are, up to maximum available energy.

Calculations were performed using the arc-dpa and the NRT model. The example of data obtained are shown in Fig.4

No additional adjustments were made to avoid the possible data jumps around 20 – 30 MeV discussed in Ref.[25].

Displacement cross sections were written in the ENDF-6 format and processed in the ACE format with the NJOY code. Cross-sections are presented on a point-by-point basis, without averaging by energy intervals. The data obtained can be downloaded on the page Ref.[26].

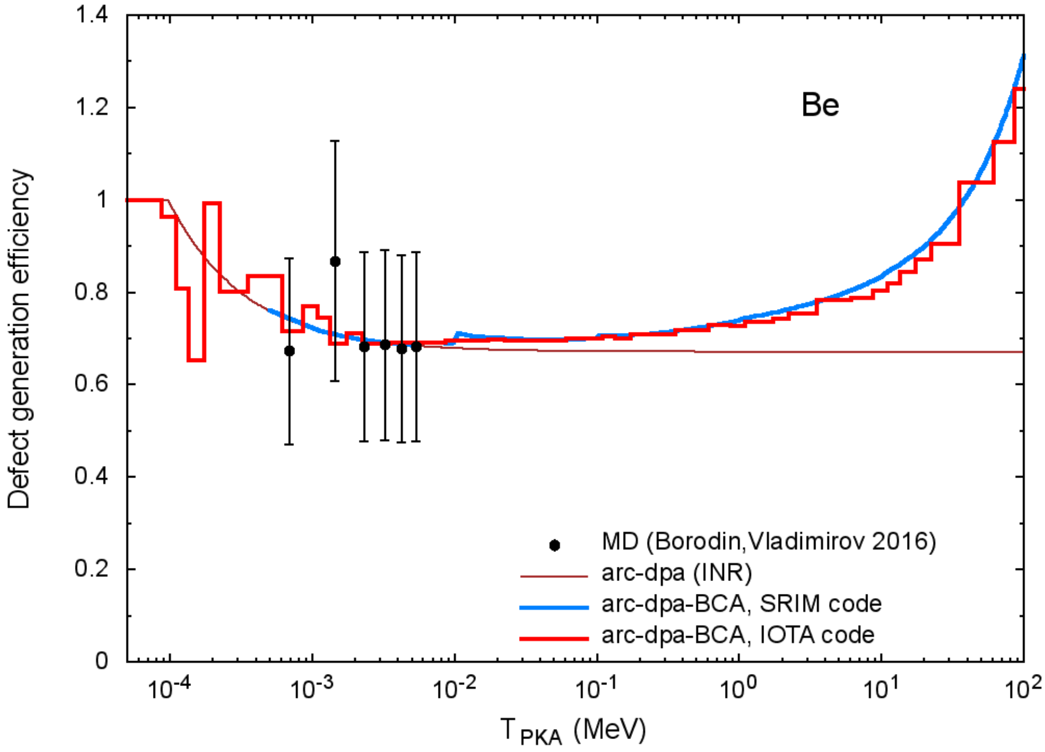

Fig.3 Defect production efficiency for Be-Be irradiation estimated using the arc-dpa model with INR parameters [21], calculated with the IOTA and SRIM codes [21], and obtained from MD modelling in Ref.[22]. The E_d value is equal to 31,2 eV.

3.2 Data extended up to 200 MeV

For a certain part of the data files in the libraries, the maximum energy at which data are available is below 200 MeV, see details in Ref.[25]. To simplify the possible high energy application of displacement cross-sections the data obtained in this work were extended up to 200 MeV for all targets between Be and Bi, if necessary.

For materials with atomic number above ten, the extension was performed using new TENDL-2021 files. The displacement cross-sections for lighter nuclei were extended using data prepared with earlier versions of TENDL, depending on the availability of evaluated data up to 200 MeV, see details in Ref.[27].

Additionally, the displacement cross-sections were corrected to avoid non-physical jumps and irregularities and providing a proper data combination. The smoothing was performed for targets with extended data only.

The examples of data extension are shown in Figs.5-12.

Obtained data in ENDF/B and ACE format are ready for download on the page [26].

Displacement cross-sections calculated using JEFF-4T1 data are shown in Appendix.

4. Conclusion

Displacement cross-sections were calculated for 78 materials from Be to Bi using the arc-dpa model and NRT model, and evaluated data from JEFF-4T1, ENDF/B-VIII, JENDL-5, and TENDL-2021.

The cross-sections obtained were extended using the TENDL data up to incident neutron energy 200 MeV.

Displacement cross sections were written in the ENDF-6 format, processed using the NJOY code and recorded in the ACE format.

Data are presented by points, without averaging over energy intervals.

The obtained displacement cross-sections can be downloaded on the page https://bit.ly/3L8ZlHQ [26].

Acknowledgement

This work has been carried out within the framework of the EUROfusion Consortium and has received funding from the Euratom research and training programme 2014-2018 and 2019-2020 under grant agreement No 633053. The views and opinions expressed herein do not necessarily reflect those of the European Commission.

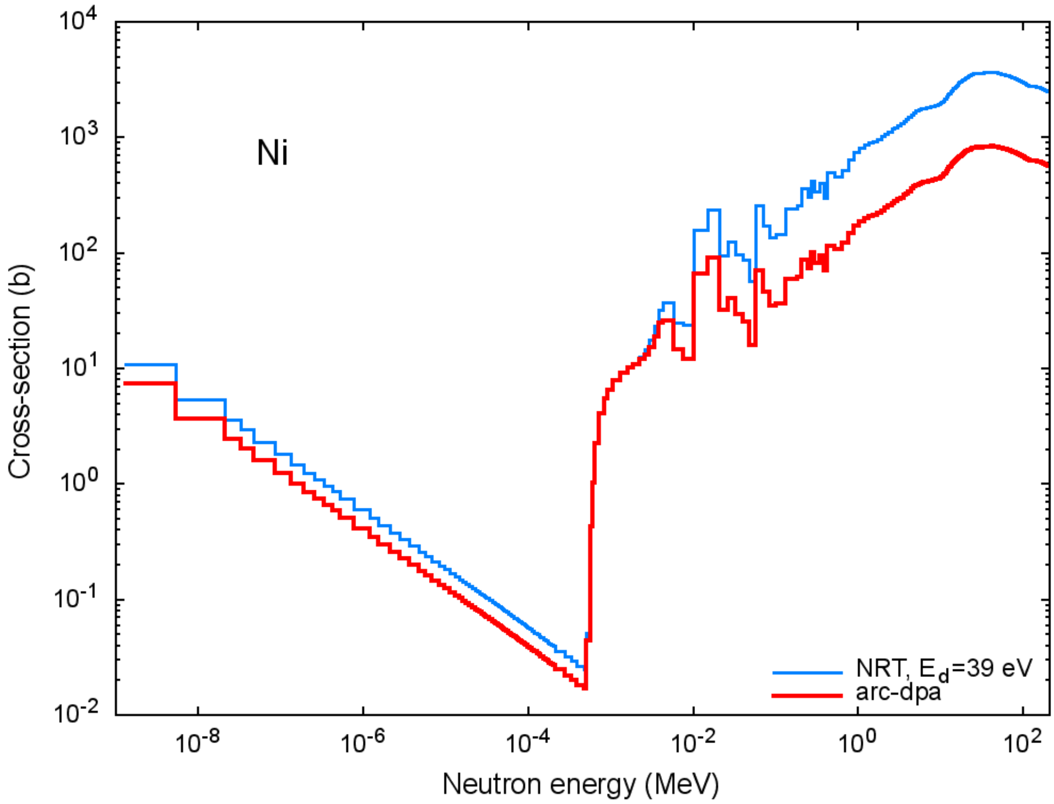

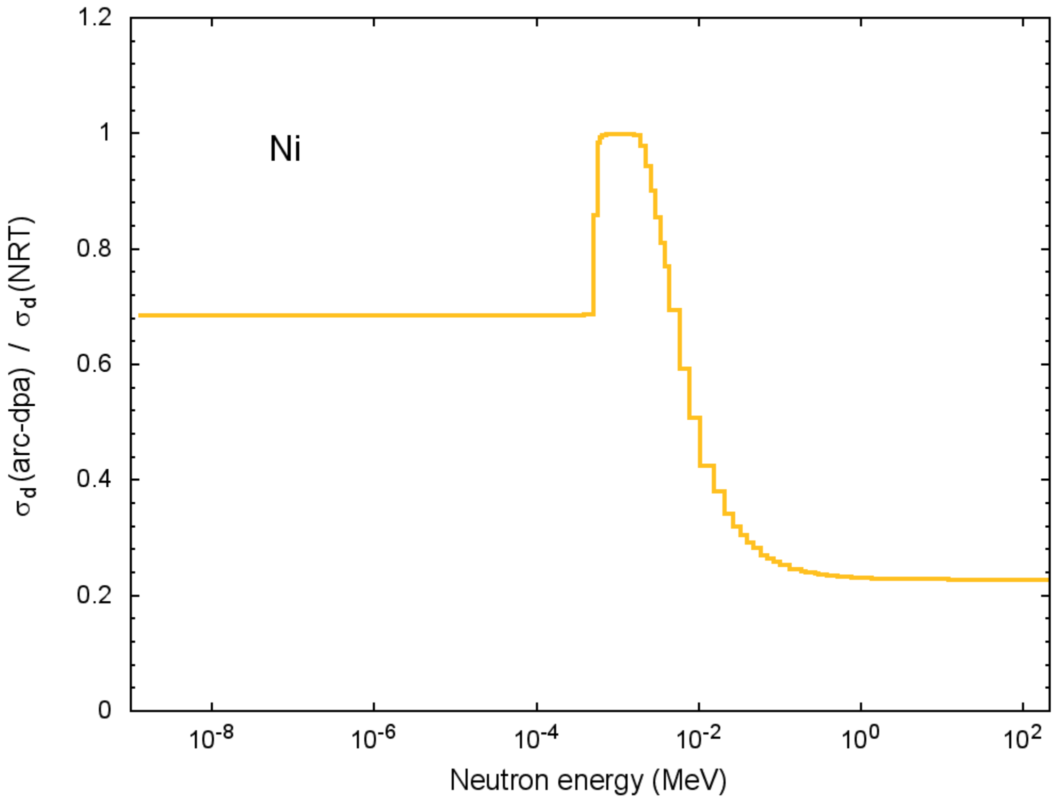

Fig.4 Displacement cross-sections (upper figure) for nickel obtained using the arc-dpa model and NRT model and data from JEFF-4T1 and the ratio of cross-sections (lower figure). For a better graphical representation, the cross sections were averaged using 304 energy groups.

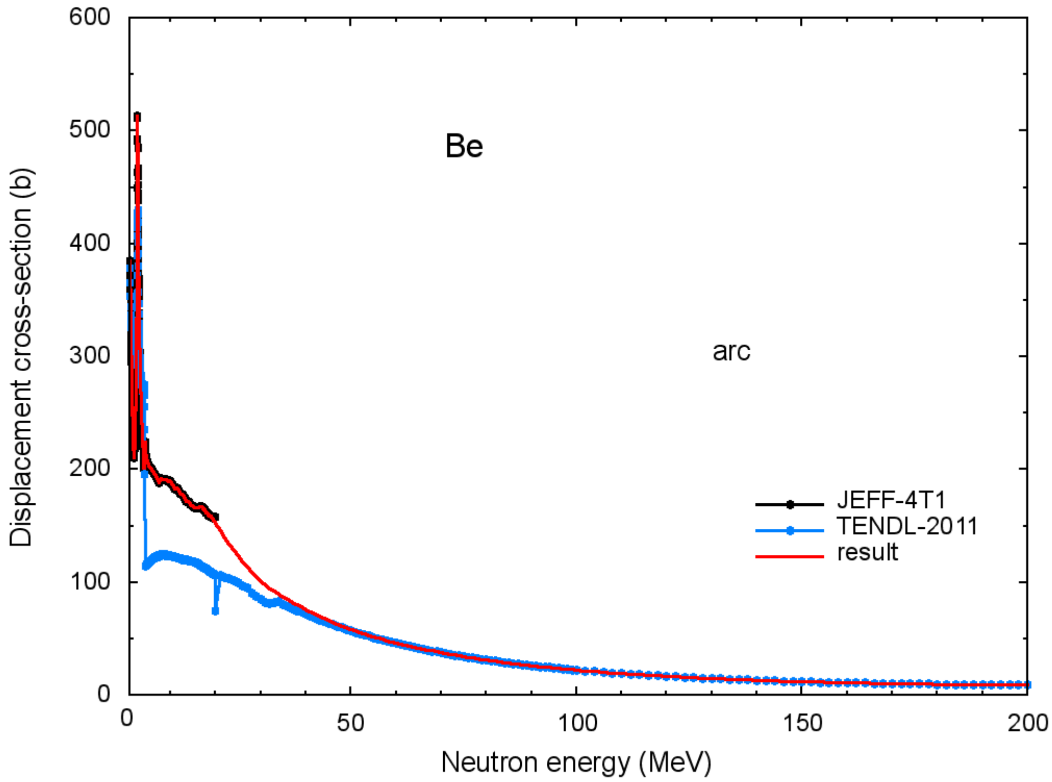

Fig.5 Example of the extension of arc-dpa displacement cross-sections for beryllium calculated using JEFF-4T1 applying data from TENDL.

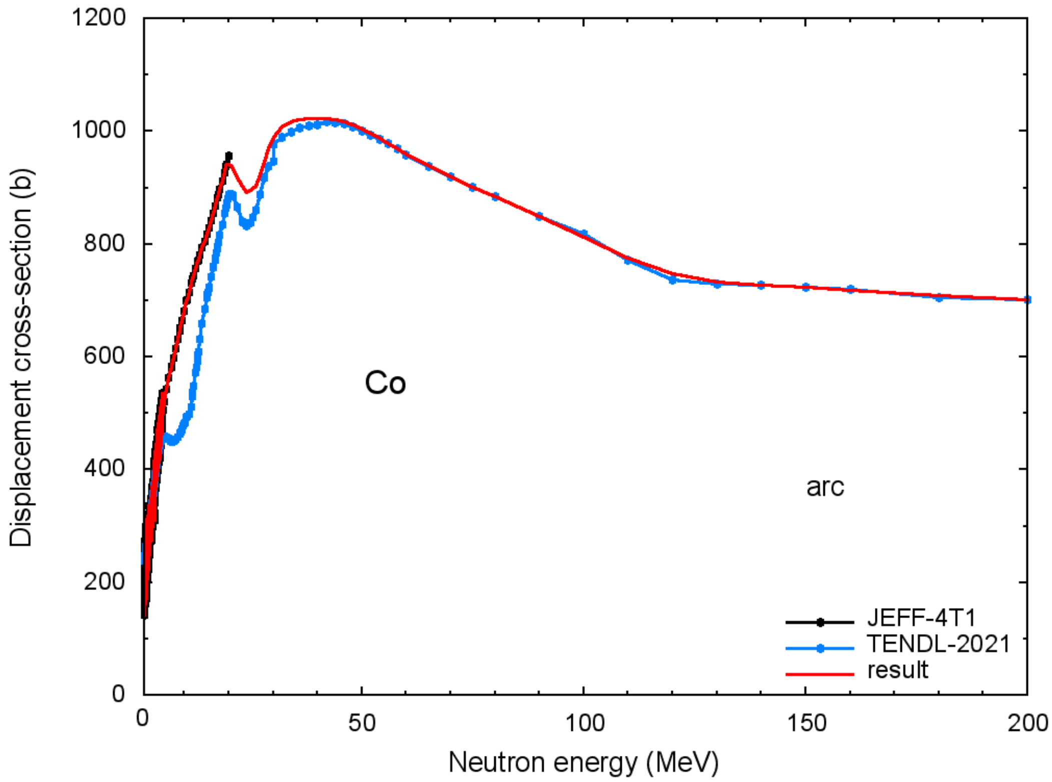

Fig.6 The same as in Fig.5 but for cobalt.

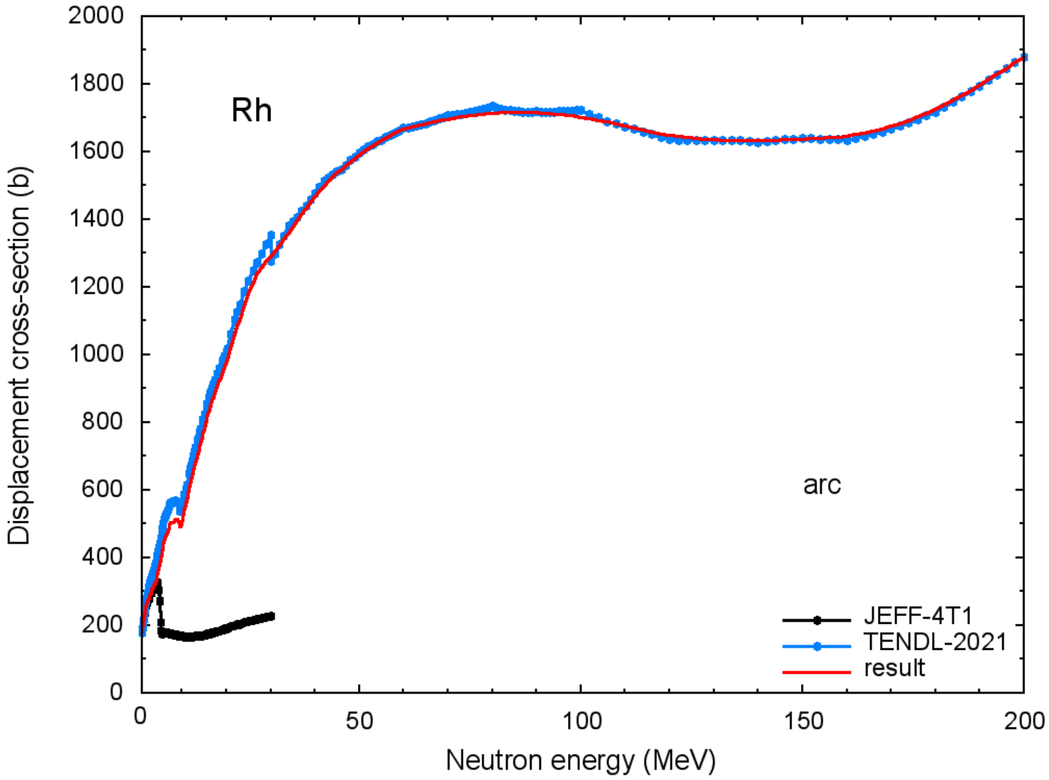

Fig.7 The same as in Fig.5 but for rhenium.

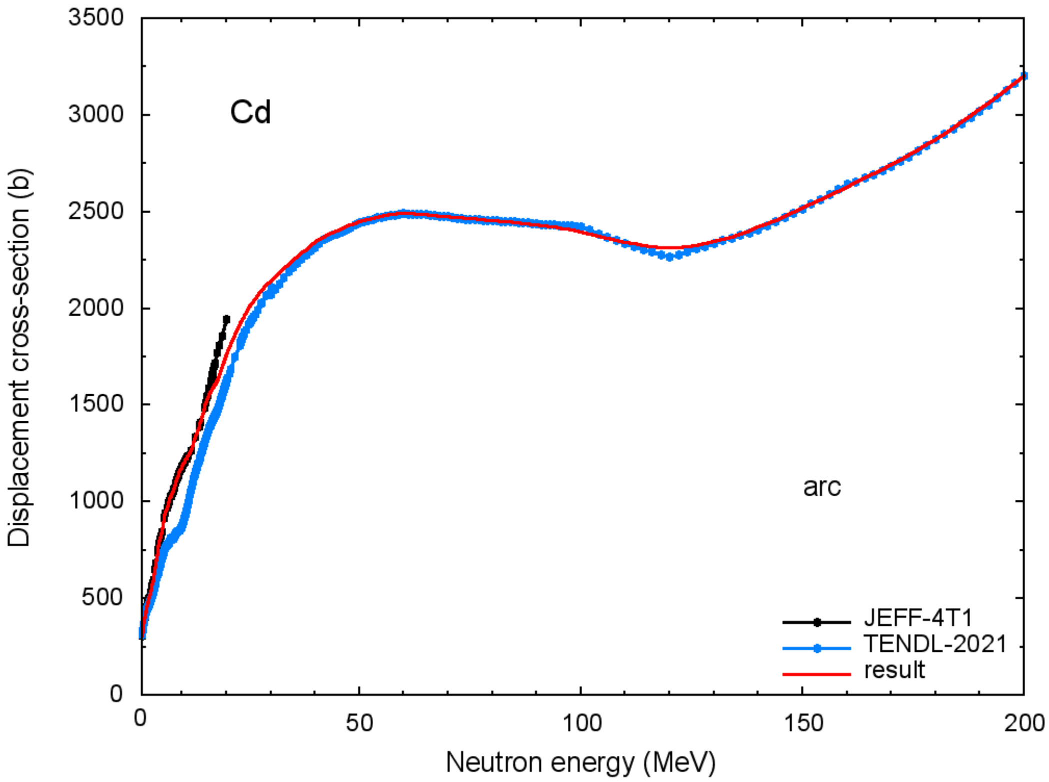

Fig.8 The same as in Fig.5 but for cadmium.

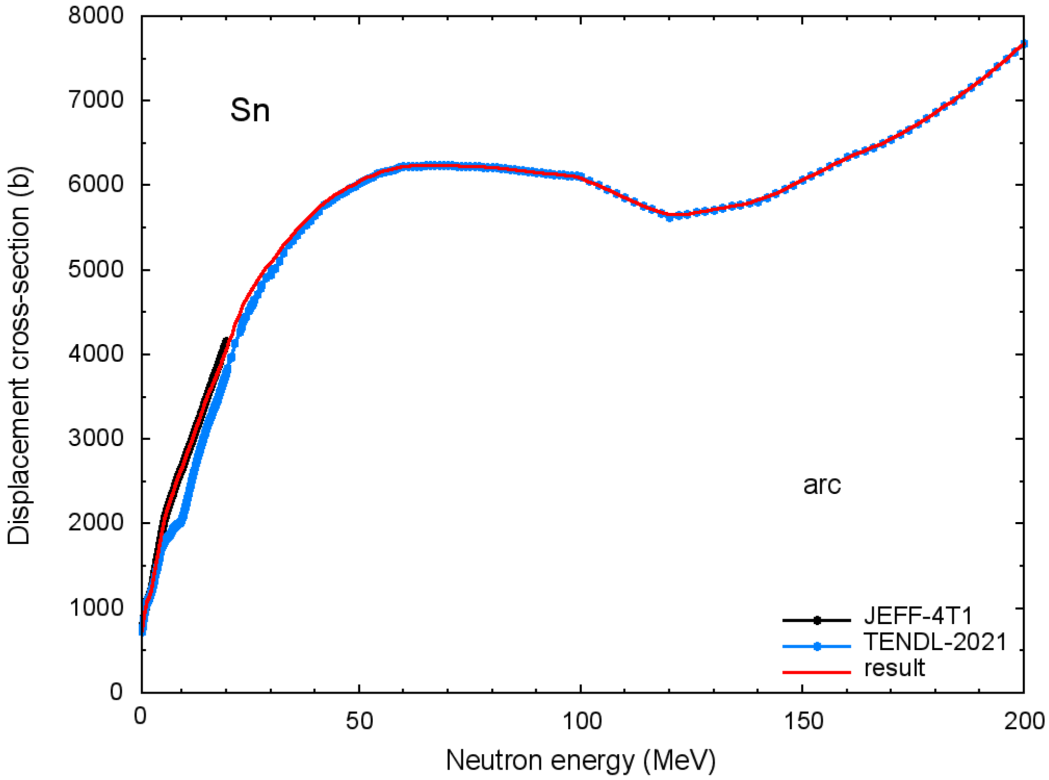

Fig.9 The same as in Fig.5 but for tin.

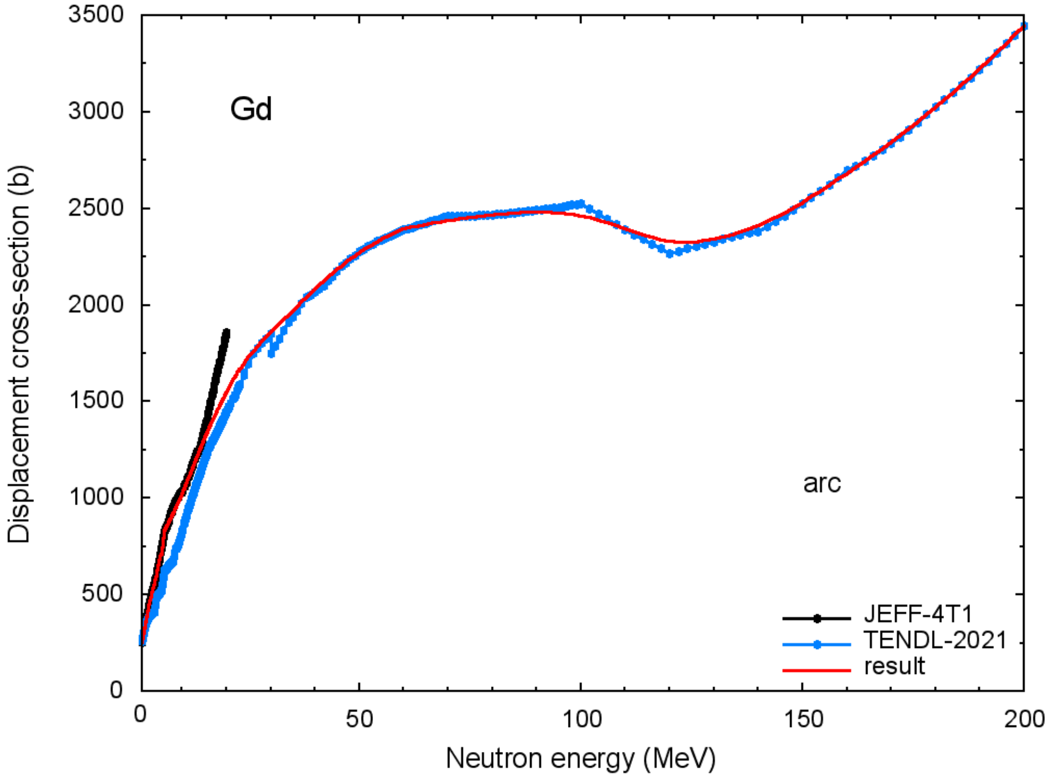

Fig.10 The same as in Fig.5 but for gadolinium.

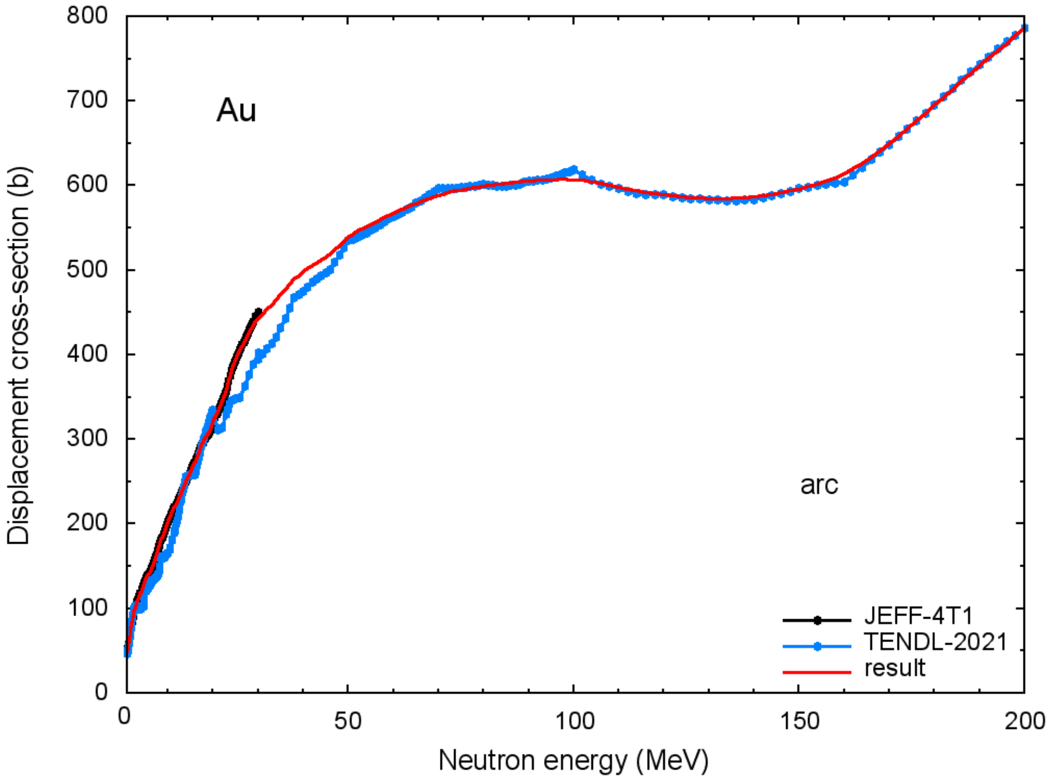

Fig.11 The same as in Fig.5 but for gold.

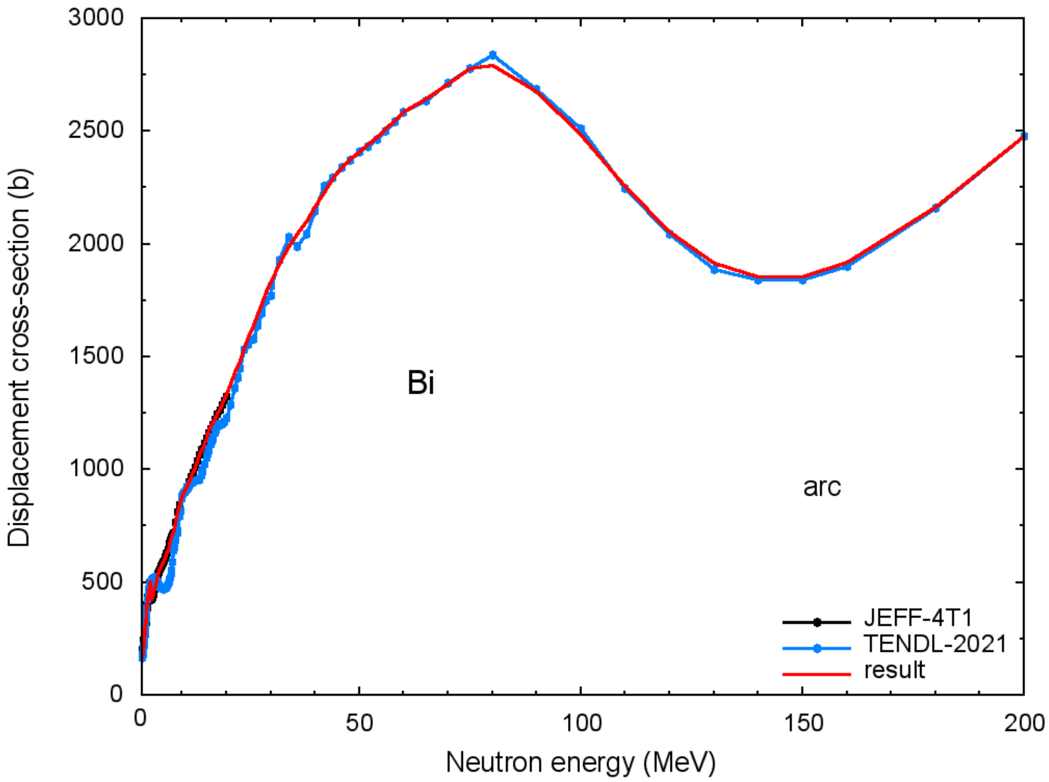

Fig.12 The same as in Fig.5 but for bismuth.

References

[1] A.Yu. Konobeyev, U. Fischer, P.E. Pereslavtsev, S.P. Simakov, Displacement cross-sections, DXS files (2018), https://www-nds.iaea.org/public/download-endf/DXS/

[2] A.Yu. Konobeyev, U. Fischer, S.P.,Simakov, Improved atomic displacement cross-sections for proton irradiation of aluminium, iron, copper, and tungsten at energies up to 10 GeV, *Nucl. Instr. Meth. Phys. Res.* B431 (2018) 55.

[3] A.Yu. Konobeyev, U. Fischer, S.P.,Simakov, Atomic displacement cross-sections for neutron irradiation of materials from Be to Bi calculated using the arc-dpa model, *Nuclear Engineering and Technology*, 51 (2019) 170.

[4] The Joint Evaluated Fission and Fusion File, JEFF-3.3 (2017), https://www.oecd-nea.org/dbdata/jeff/jeff33/index.html#dpa

[5] K. Nordlund, S.J. Zinkle, A.E. Sand, F. Granberg, R.S. Averback, R. Stoller, T. Suzudo, L. Malerba, F. Banhart, W.J. Weber, F. Willaime, S.L. Dudarev, D. Simeone, Improving atomic displacement and replacement calculations with physically realistic damage models, *Nature Communications,* 9 (2018) 1084, https://doi.org/10.1038/s41467-018-03415-5

[6] M.J. Norgett, M.T. Robinson, I.M. Torrens, A proposed method of calculating displacement dose rates, *Nucl. Eng. Des.* 33 (1975) 50.

[7] D.A. Brown, M.B. Chadwick, R. Capote, A.C. Kahler, A. Trkov, M.W. Herman, A.A. Sonzogni, Y. Danon, A.D. Carlson, M. Dunn, D.L. Smith, G.M. Hale, G. Arbanas, R. Arcilla, C.R. Bates, B. Beck, B. Becker, F. Brown, R.J. Casperson, J. Conlin, D.E. Cullen, M.-A. Descalle, R. Firestone, T. Gaines, K.H. Guber, A.I. Hawari, J. Holmes, T.D. Johnson, T. Kawano, B.C. Kiedrowski, A.J. Koning, S. Kopecky, L. Leal, J.P. Lestone, C. Lubitz, J.I. Márquez Damián, C.M. Mattoon, E.A. McCutchan, S. Mughabghab, P. Navratil, D. Neudecker, G.P.A. Nobre, G. Noguere, M. Paris, M.T. Pigni, A.J. Plompen, B. Pritychenko, V.G. Pronyaev, D. Roubtsov, D. Rochman, P. Romano, P. Schillebeeckx, S. Simakov, M. Sin, I. Sirakov, B. Sleaford, V. Sobes, E.S. Soukhovitskii, I. Stetcu, P. Talou, I. Thompson, S. van der Marck, L. Welser-Sherrill, D. Wiarda, M. White, J.L. Wormald, R.Q. Wright, M. Zerkle, G. Žerovnik, Y. Zhu, ENDF/B-VIII.0: The 8^{th} major release of the nuclear reaction data library with CIELO-project cross sections, new standards and thermal scattering data, *Nuclear Data Sheets*, 148, (2018) 1.

[8] A.J.M. Plompen, O.Cabellos, C.De Saint Jean, M. Fleming, A. Algora, M. Angelone, P. Archier, E. Bauge, O. Bersillon, A. Blokhin, F. Cantargi, A. Chebboubi, C. Diez, H. Duarte, E. Dupont, J. Dyrda, B. Erasmus, L. Fiorito, U. Fischer, D. Flammini, D. Foligno, M. R. Gilbert, J. R. Granada, W. Haeck, F.-J. Hambsch, P. Helgesson, S. Hilaire, I. Hill, M. Hursin, R. Ichou, R. Jacqmin, B. Jansky, C. Jouanne, M. A. Kellett, D. H. Kim, H. I. Kim, I. Kodeli, A. J. Koning, A. Yu. Konobeyev, S. Kopecky, B. Kos, A. Krása, L. C. Leal, N. Leclaire, P. Leconte, Y. O. Lee, H. Leeb, O. Litaize, M. Majerle, J. I Márquez Damián, F. Michel-Sendis, R. W. Mills, B. Morillon, G. Noguère, M. Pecchia, S. Pelloni, P. Pereslavtsev, R. J. Perry, D. Rochman, A. Röhrmoser, P. Romain, P. Romojaro, D. Roubtsov, P. Sauvan, P. Schillebeeckx, K. H. Schmidt, O. Serot, S. Simakov, I. Sirakov, H. Sjöstrand, A. Stankovskiy, J. C. Sublet, P. Tamagno, A. Trkov, S. van der Marck, F. Álvarez-Velarde, R. Villari, T. C. Ware, K. Yokoyama, G. Žerovnik, The joint evaluated fission and fusion nuclear data library, JEFF-3.3, *Eur. Phys. J. A*, 56 (2020) 181.

[9] K. Shibata, O. Iwamoto, T. Nakagawa, N. Iwamoto, A. Ichihara, S. Kunieda, S. Chiba, K. Furutaka, N. Otuka, T. Ohsawa, T. Murata, H. Matsunobu, A. Zukeran, S. Kamada, J. Katakura: JENDL-4.0: A new library for nuclear science and engineering, *J. Nucl. Sci. Technol.*, 48(1) (2011) 1.

[10] A.J. Koning and D. Rochman, Modern nuclear data evaluation with the TALYS code system, *Nuclear Data Sheets* 113 (2012) 2841; TENDL-2017 (December 30, 2017), https://tendl.web.psi.ch/tendl_2017/tendl2017.html

[11] O. Iwamoto, N. Iwamoto, K. Shibata, A. Ichihara, S. Kunieda, F. Minato, S. Nakayama, Status of JENDL, *EPJ Web of Conferences*, 239 (2020) 09002_1-6; JENDL-5 (December 2021), https://wwwndc.jaea.go.jp/jendl/j5/j5.html

[12] A.J. Koning, D. Rochman, J. Sublet, N. Dzysiuk, M. Fleming, S. van der Marck, TENDL: complete nuclear data library for innovative nuclear science and technology, *Nuclear Data Sheets* 155 (2019) 1; TENDL-2021 (December 30, 2021), https://tendl.web.psi.ch/tendl_2021/tendl2021.html

[13] Joint Evaluated Fission and Fusion (JEFF) Nuclear Data Library, JEFF-4T1 (Test library) (February 2022), https://www.oecd-nea.org/dbdata/jeff/jeff40/t1/

[14] A.Yu. Konobeyev, U. Fischer, Yu.A. Korovin, S.P. Simakov, Evaluation of effective threshold displacement energies and other data required for the calculation of advanced atomic displacement cross-sections, *Nuclear Energy and Technology*, 3 (2017) 169.

[15] K. Nordlund, private communication (2016).

[16] A.Yu. Konobeyev, U. Fischer, Yu.A. Korovin, S.P. Simakov, IOTA-2017: a code for the simulation of ion transport in materials, KIT Scientific Working Papers 63 (2017), https://publikationen.bibliothek.kit.edu/1000077011

[17] J.F. Ziegler, SRIM - The stopping and range of ions in matter, http://srim.org/

[18] C.H.M. Broeders, A.Yu. Konobeyev, Defect production efficiency in metals under neutron irradiation, *J. Nucl. Mater.* 328 (2004) 197.

[19] M.T. Robinson, Basic physics of radiation damage production, *J. Nucl. Mater.* 216 (1994) 1.

[20] A. Yu. Konobeyev, U. Fischer, S. P. Simakov, Neutron displacement cross-sections for materials from Be to U calculated using the arc-dpa concept, Proc. 13th International Topical Meeting on the Applications of Accelerators (AccApp'17), July 31-August 4, 2017, Quebec, http://accapp17.org/wp-content/2017/data/pdfs/110-22892.pdf; https://goo.gl/3swcvs

[21] A.Yu. Konobeyev, U. Fischer, S.P. Simakov, Status of the evaluation of n+^{9}Be displacement cross-section using advance defect production model, NEA Nuclear Data Week, 25-29 November 2019, EFFDOC-1411 (2019), https://www.oecd-nea.org/dbdata/nds_effdoc/effdoc-1411.pdf; https://bit.ly/3sqC9O2

[22] V.A. Borodin, P.V. Vladimirov, Damage production in atomic displacement cascades in beryllium, *Nuclear Materials and Energy,* 9 (2016) 216.

[23] The NJOY Nuclear Data Processing System, version 2016, NJOY2016.66 (November 2021), https://github.com/njoy/NJOY2016

[24] D.E. Cullen, PREPRO 2021, 2021 ENDF/B Pre-processing Codes, IAEA-NDS-0238, (July 14, 2021), https://www-nds.iaea.org/public/endf/prepro/

[25] A.Yu. Konobeyev, D.Leichtle, Status of the work for neutron displacement cross-sections for JEFF-4T1, Nuclear Data Week, April 2022, EFFDOC-1471 (2022), https://dx.doi.org/10.13140/RG.2.2.34427.80161

[26] A.Yu. Konobeyev, D. Leichtle, Evaluated atomic displacement cross-sections using arc-dpa and NRT model (May 2022), https://bit.ly/3L8ZlHQ

[27] A.Yu. Konobeyev, U. Fischer, S.P. Simakov, Status of the work for evaluation of arc-dpa cross-sections for high priority elements, NEA Nuclear Data Week-JEFF Meeting, 24–27 April 2017, EFFDOC-1317 (2017), https://www.oecd-nea.org/dbdata/nds_effdoc/effdoc-1317.pdf

Appendix

Displacement cross-sections obtained using the arc-dpa model and NRT model and data from JEFF-4T1

For a better graphical representation, the data were averaged using 304 energy groups

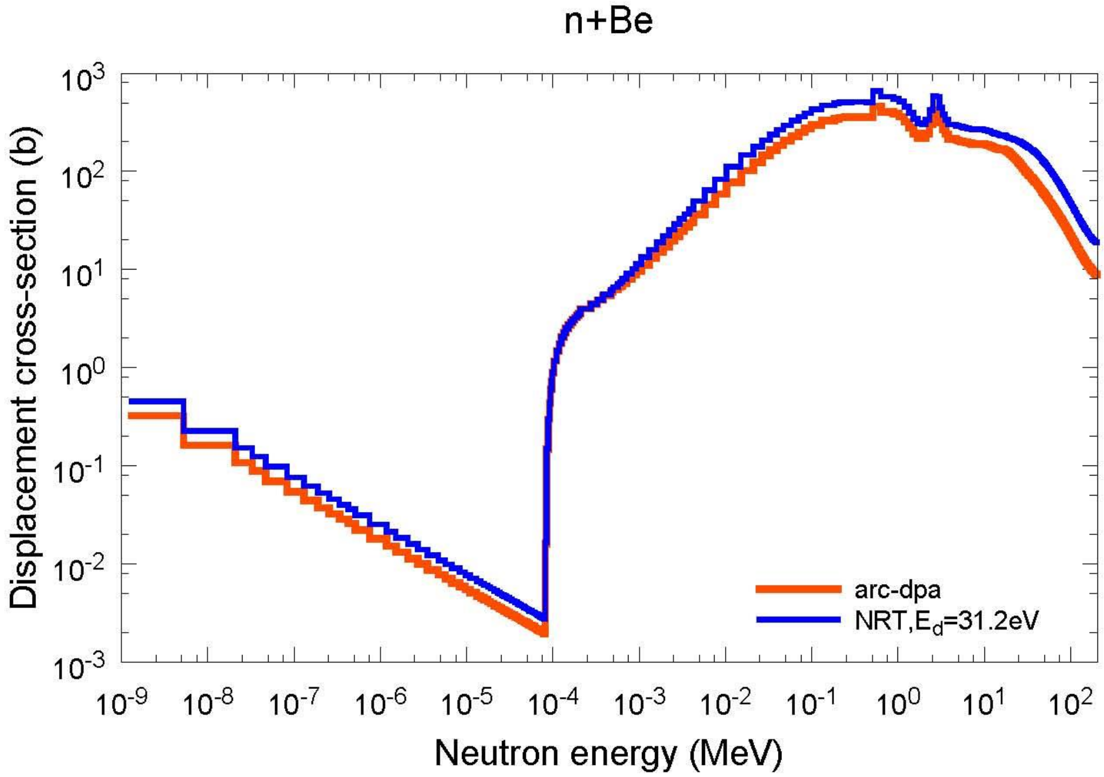
n+Be
Displacement cross-section (b)
Neutron energy (MeV)
arc-dpa
NRT,E$_d$=31.2eV

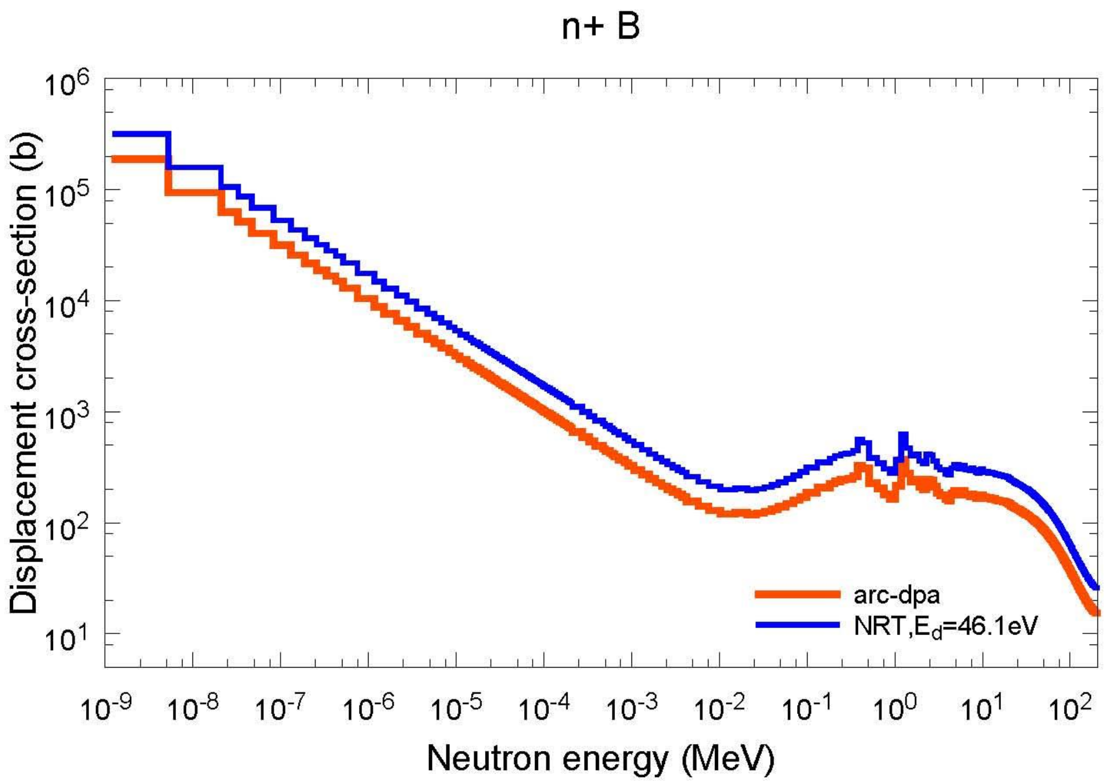
n+ B
Displacement cross-section (b)
Neutron energy (MeV)
arc-dpa
NRT,E$_d$=46.1eV

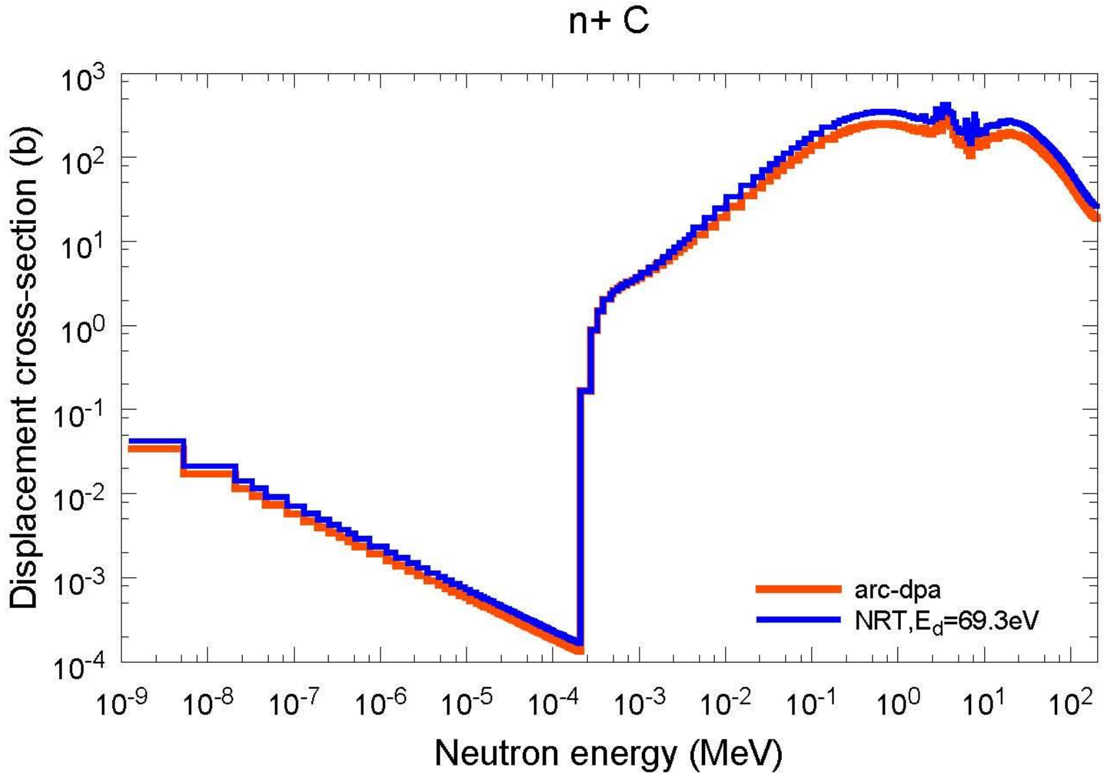
n+ C
Displacement cross-section (b)
Neutron energy (MeV)
arc-dpa
NRT,E$_d$=69.3eV

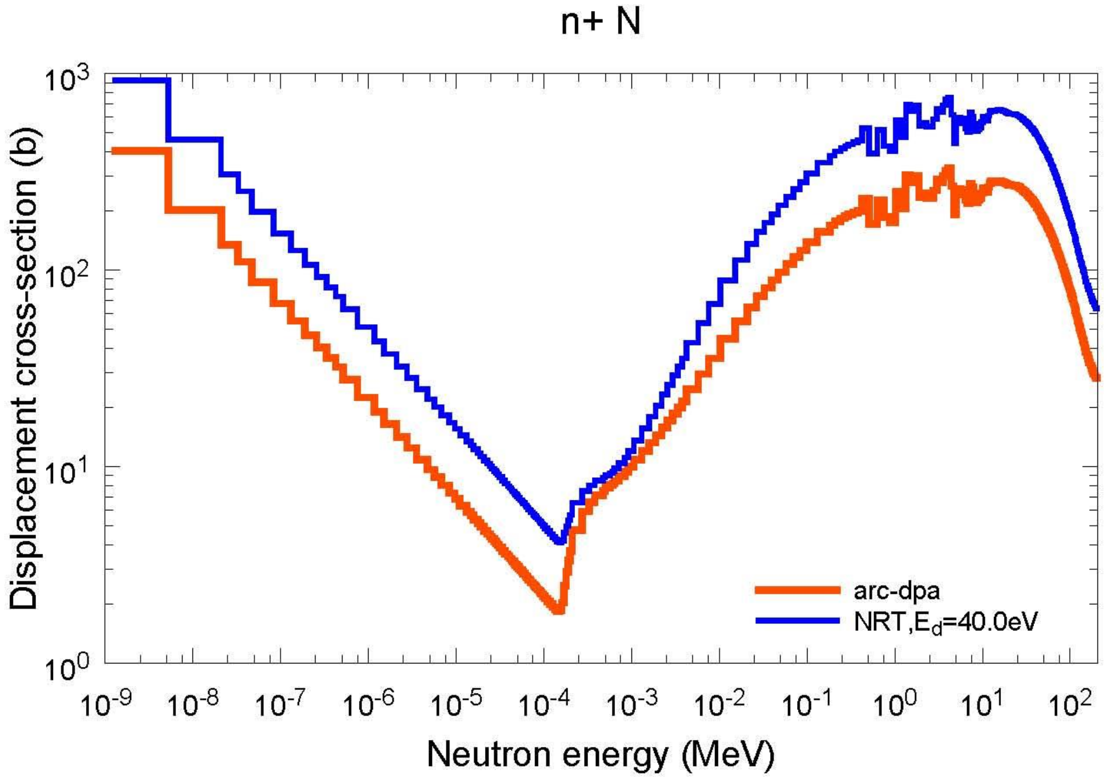
n+ N
Displacement cross-section (b)
Neutron energy (MeV)
arc-dpa
NRT,E$_d$=40.0eV

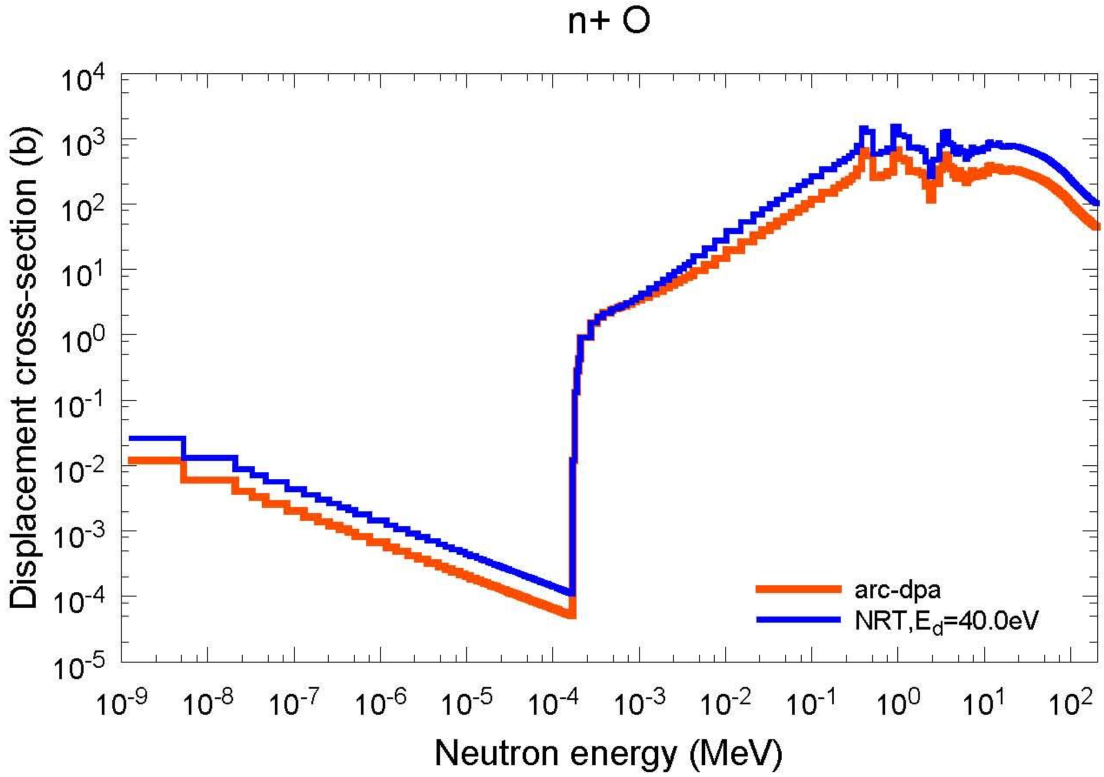
n+ O
Displacement cross-section (b)
Neutron energy (MeV)
arc-dpa
NRT,E_d=40.0eV

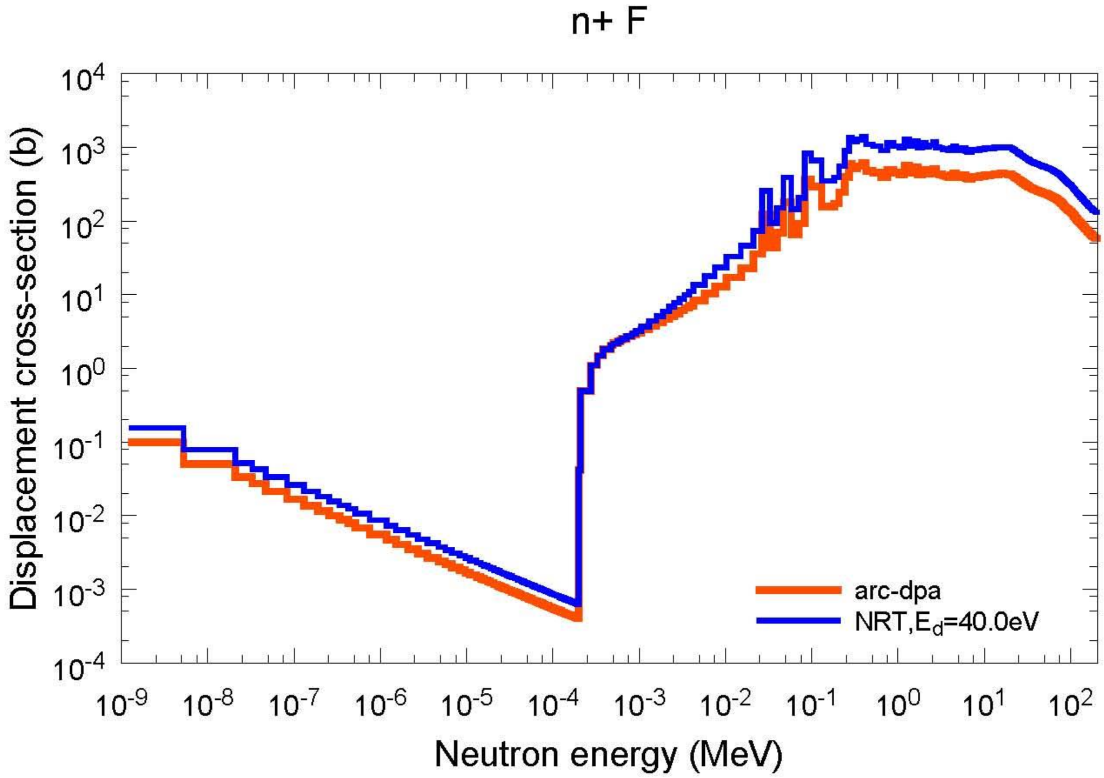
n+ F
Displacement cross-section (b)
Neutron energy (MeV)
arc-dpa
NRT,E_d=40.0eV

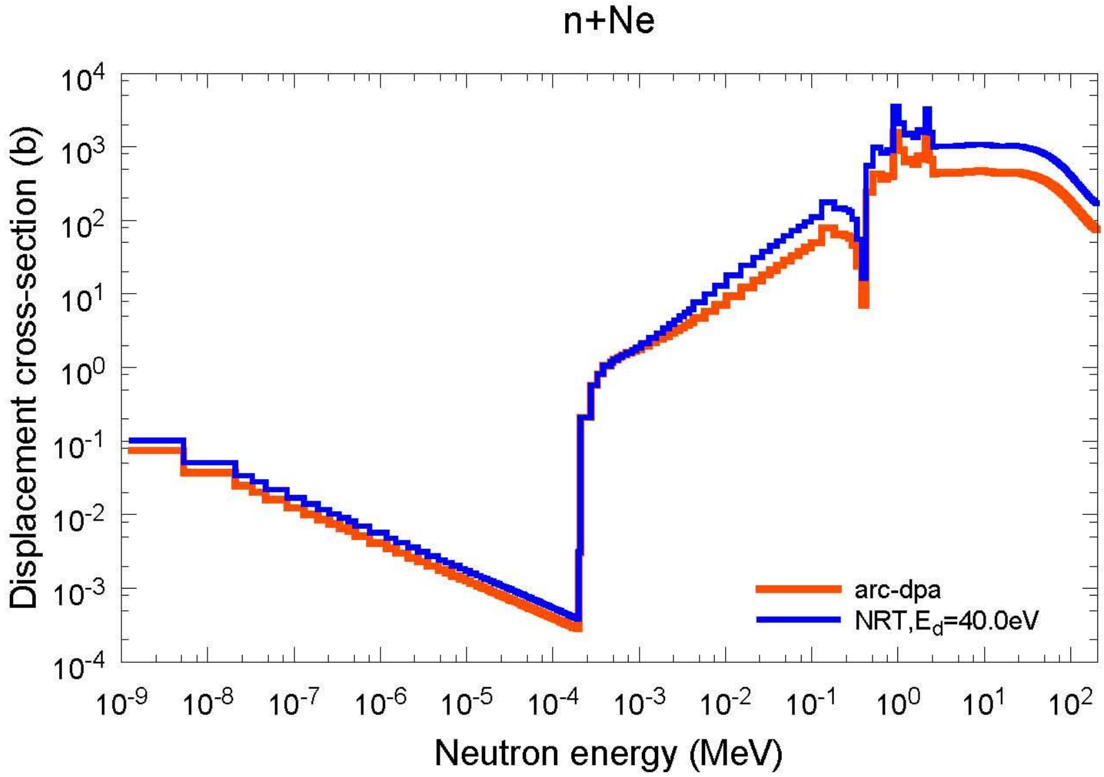
n+Ne
Displacement cross-section (b)
arc-dpa
NRT,E_d=40.0eV
Neutron energy (MeV)

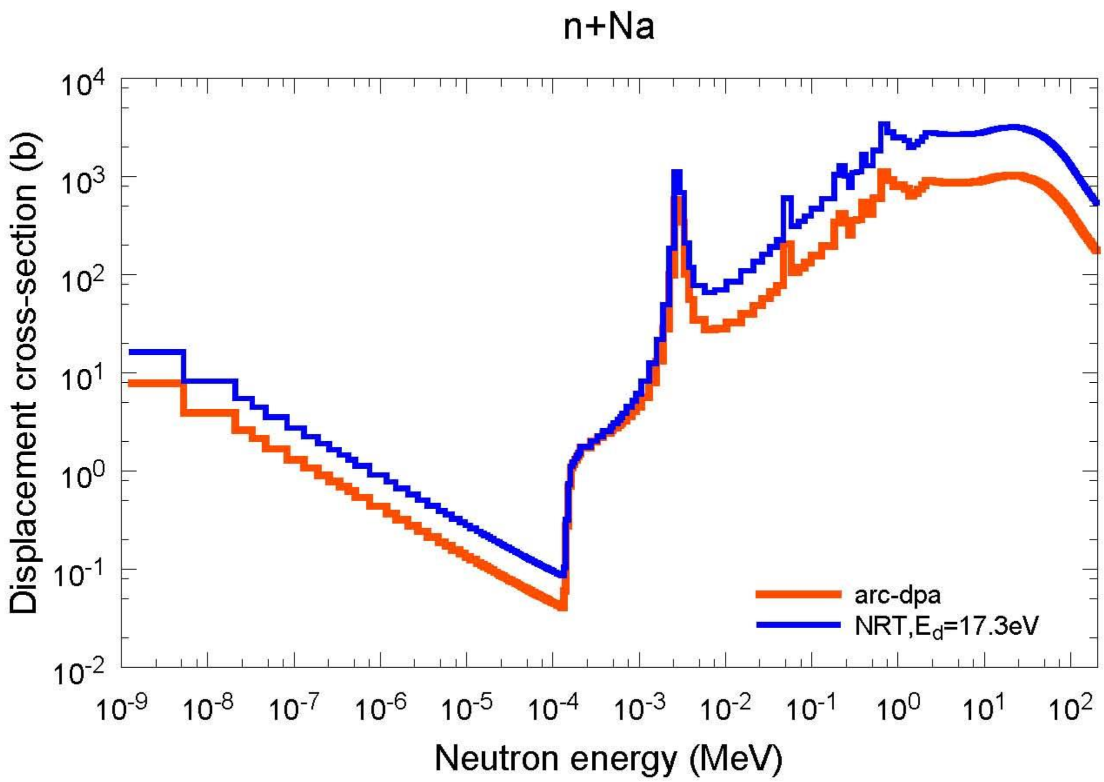
n+Na
Displacement cross-section (b)
arc-dpa
NRT,E_d=17.3eV
Neutron energy (MeV)

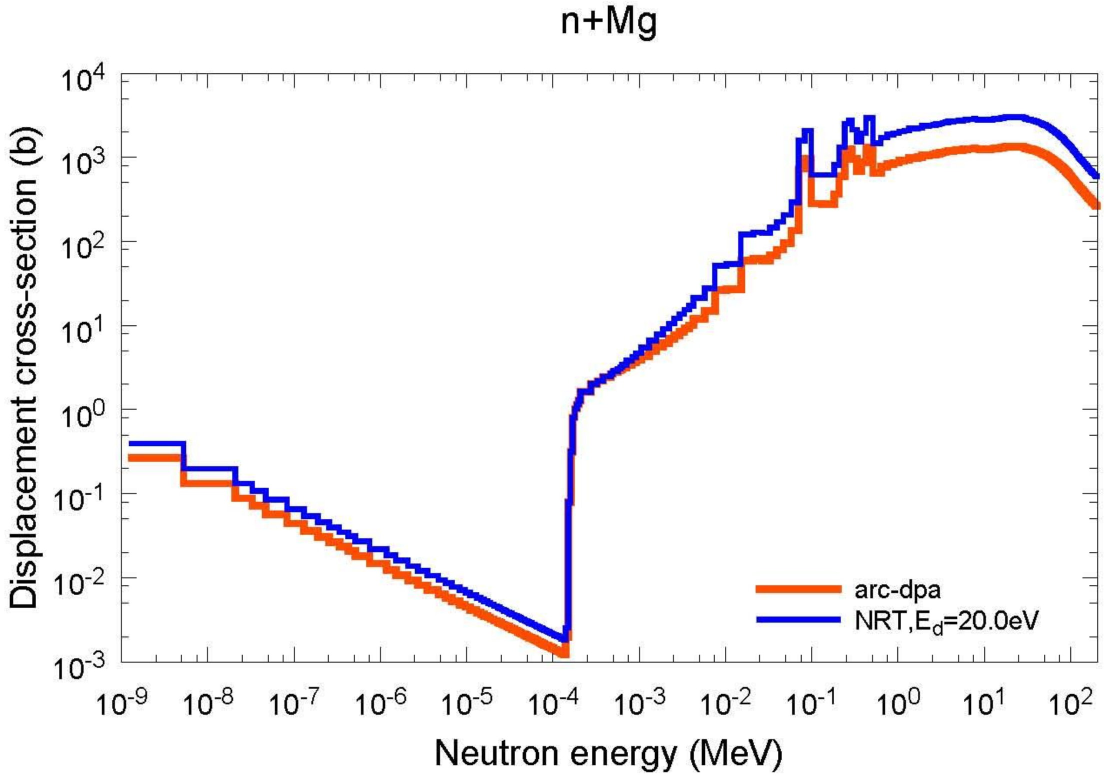
n+Mg
Displacement cross-section (b)
Neutron energy (MeV)
arc-dpa
NRT,E$_d$=20.0eV

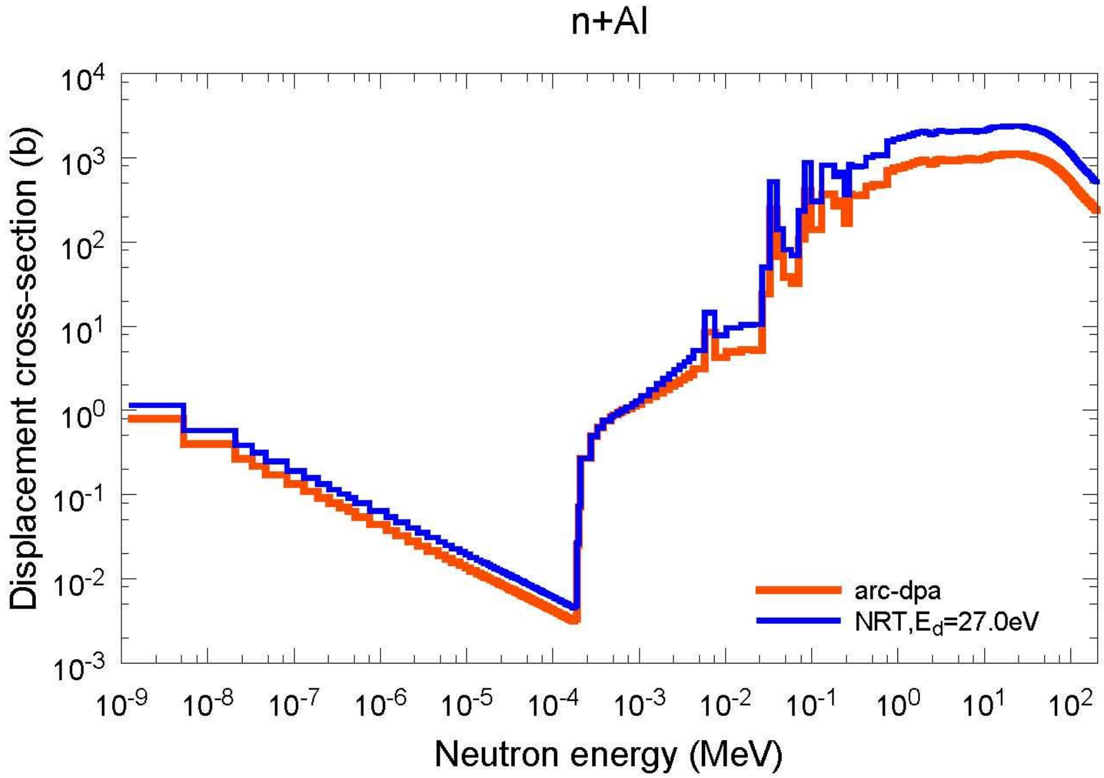
n+Al
Displacement cross-section (b)
Neutron energy (MeV)
arc-dpa
NRT,E$_d$=27.0eV

n+Si

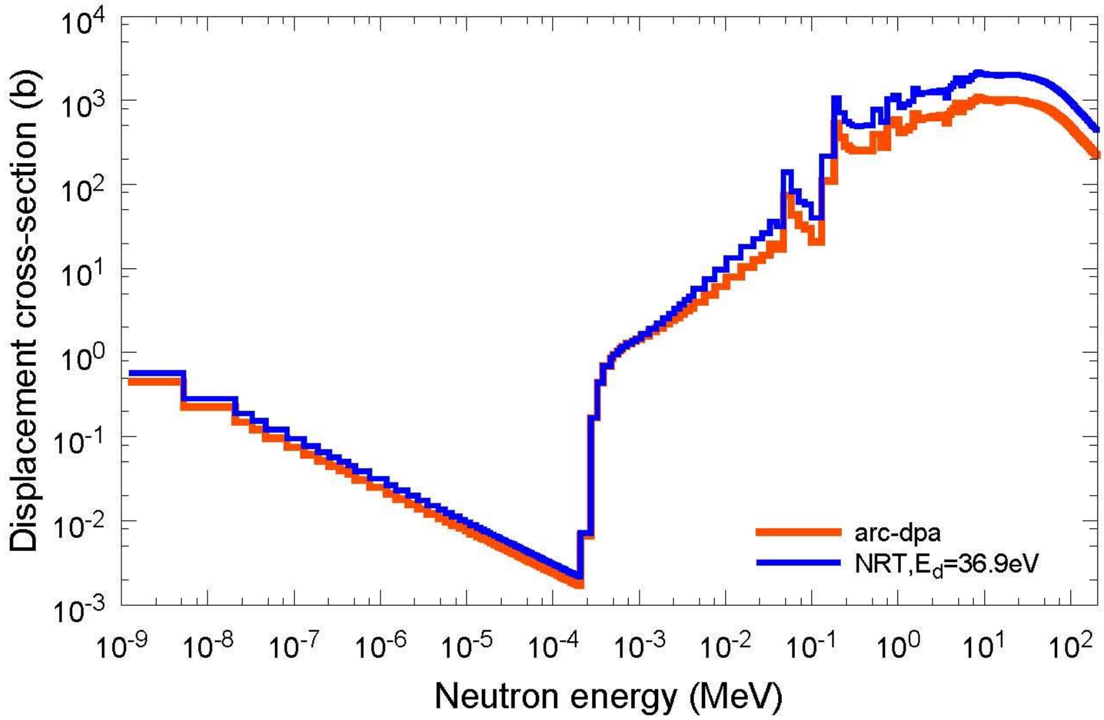

Displacement cross-section (b)
Neutron energy (MeV)
arc-dpa
NRT,E$_d$=36.9eV

n+ P

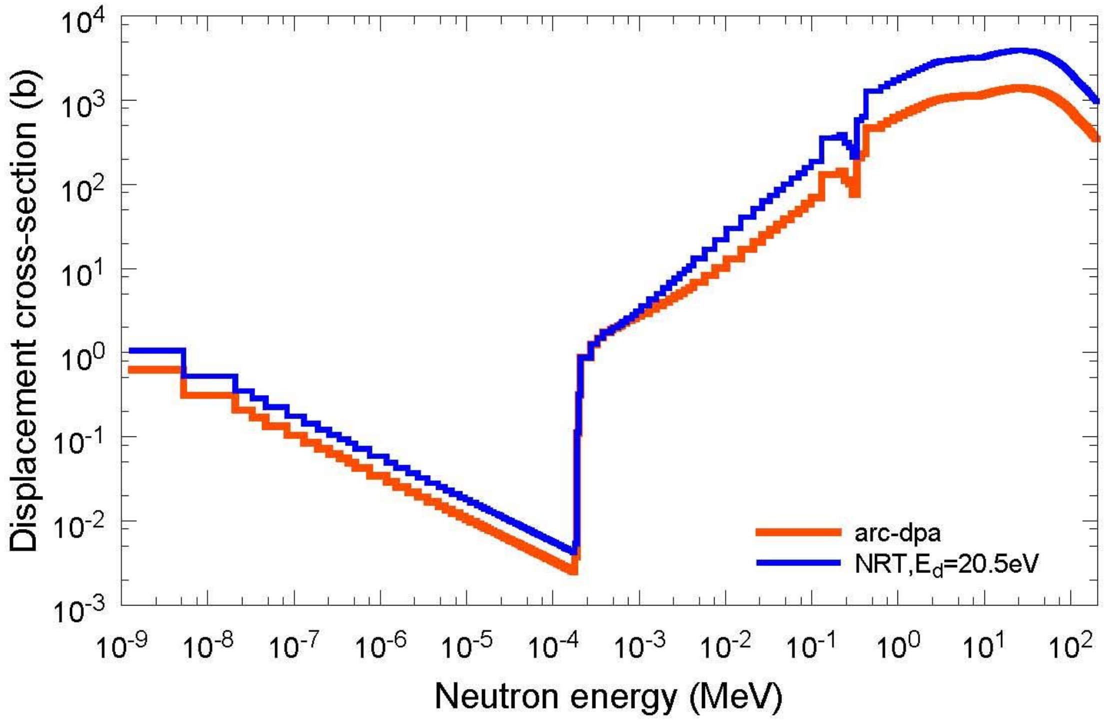

Displacement cross-section (b)
Neutron energy (MeV)
arc-dpa
NRT,E$_d$=20.5eV

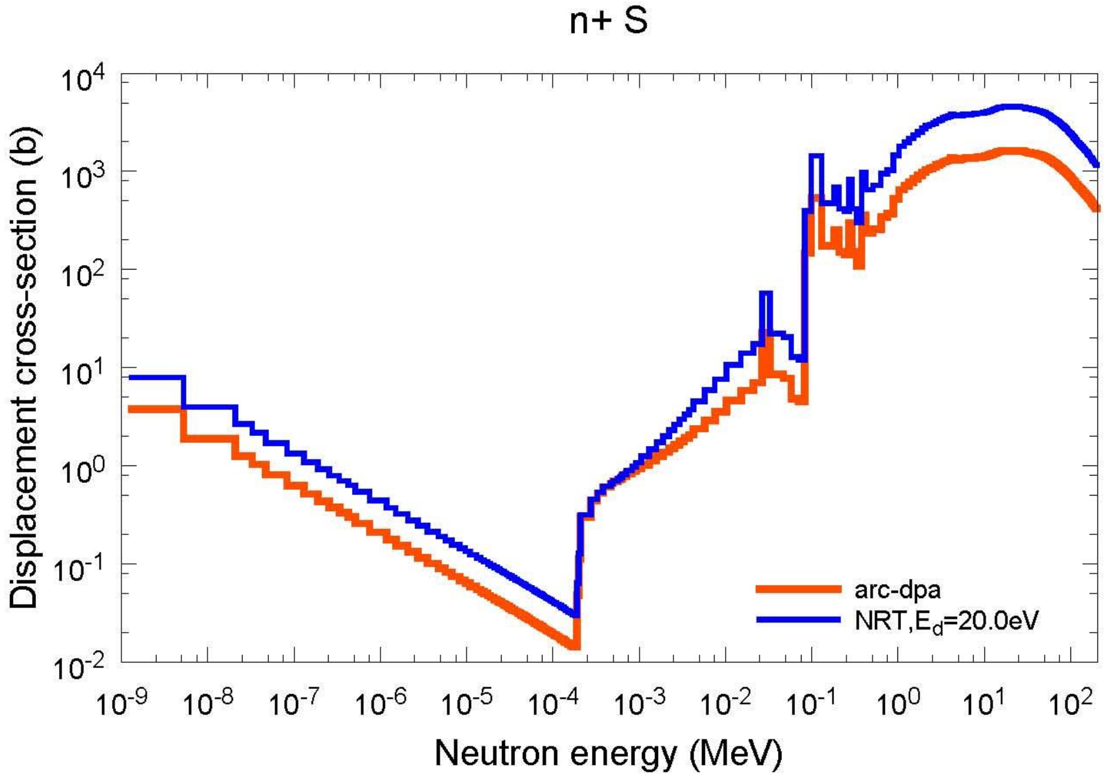
n+ S
Displacement cross-section (b)
10^{4}
10^{3}
10^{2}
10^{1}
10^{0}
10^{-1}
10^{-2}
10^{-9} 10^{-8} 10^{-7} 10^{-6} 10^{-5} 10^{-4} 10^{-3} 10^{-2} 10^{-1} 10^{0} 10^{1} 10^{2}
Neutron energy (MeV)
arc-dpa
NRT,E_d=20.0eV

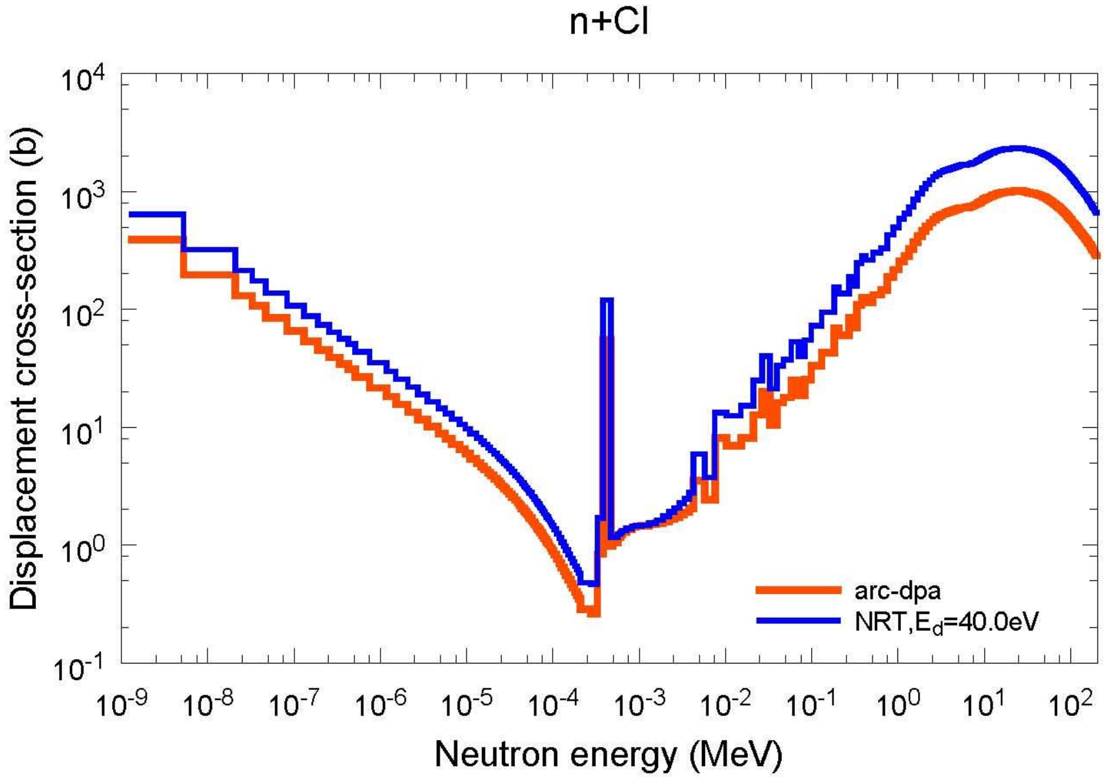
n+Cl
Displacement cross-section (b)
10^{4}
10^{3}
10^{2}
10^{1}
10^{0}
10^{-1}
10^{-9} 10^{-8} 10^{-7} 10^{-6} 10^{-5} 10^{-4} 10^{-3} 10^{-2} 10^{-1} 10^{0} 10^{1} 10^{2}
Neutron energy (MeV)
arc-dpa
NRT,E_d=40.0eV

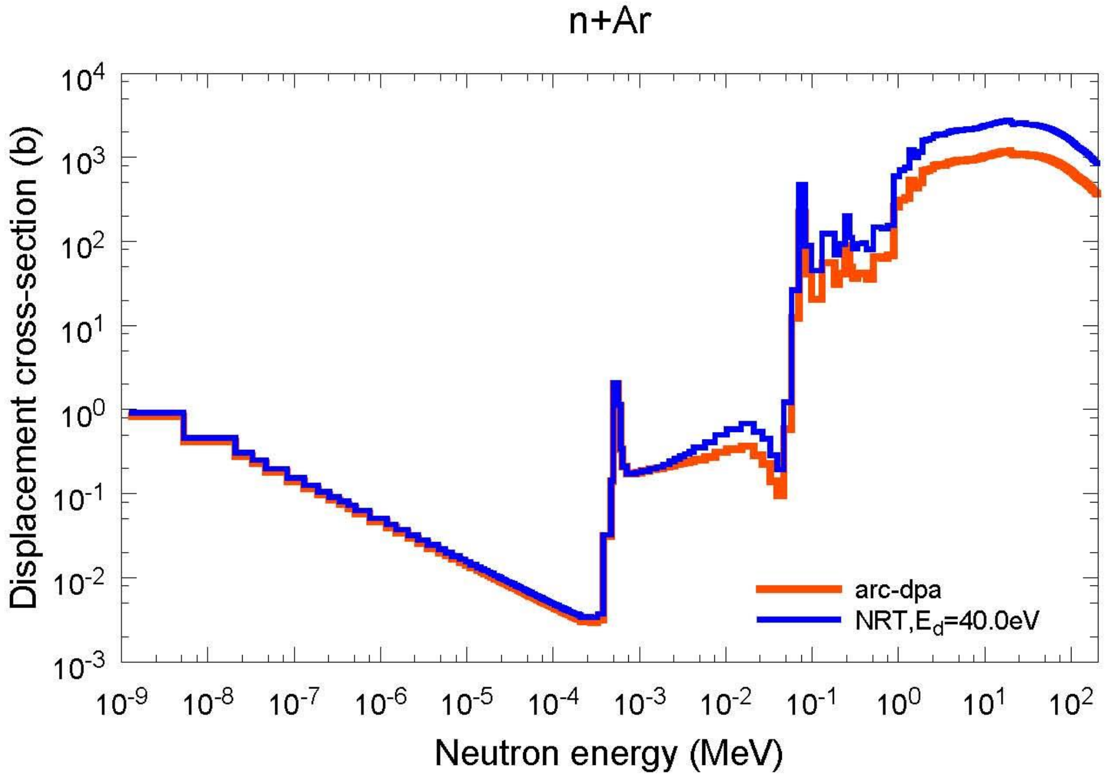
n+Ar
Displacement cross-section (b)
Neutron energy (MeV)
arc-dpa
NRT,E_d=40.0eV

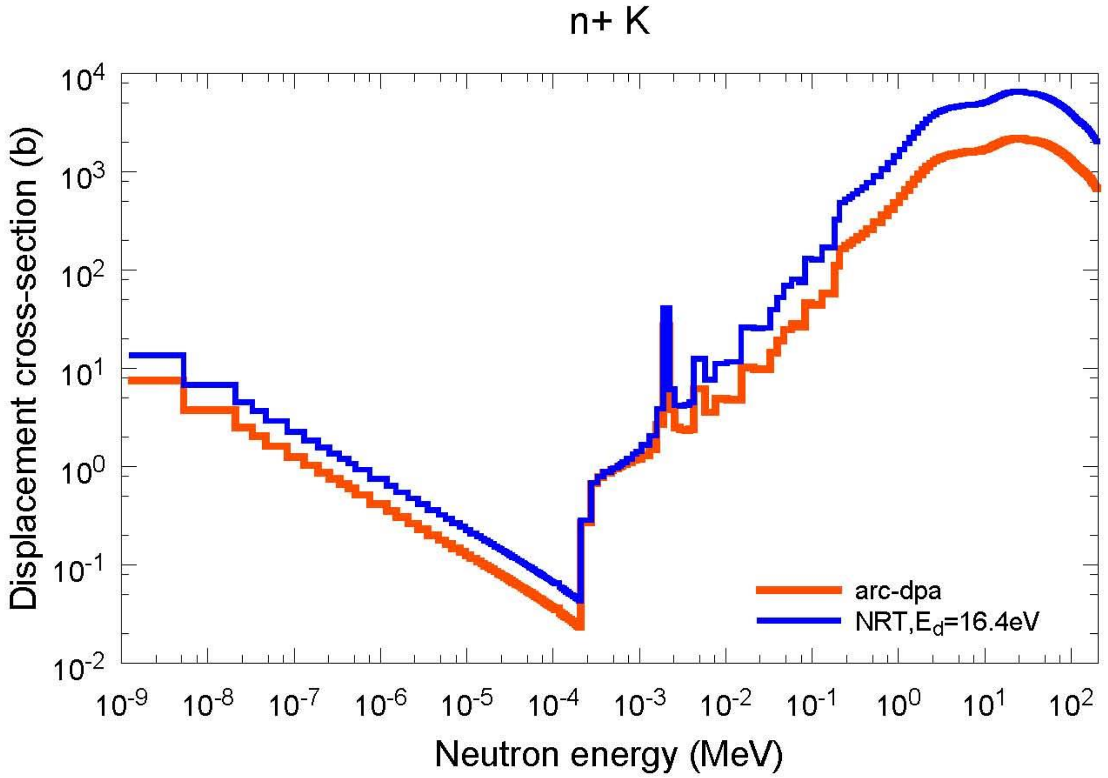
n+ K
Displacement cross-section (b)
Neutron energy (MeV)
arc-dpa
NRT,E_d=16.4eV

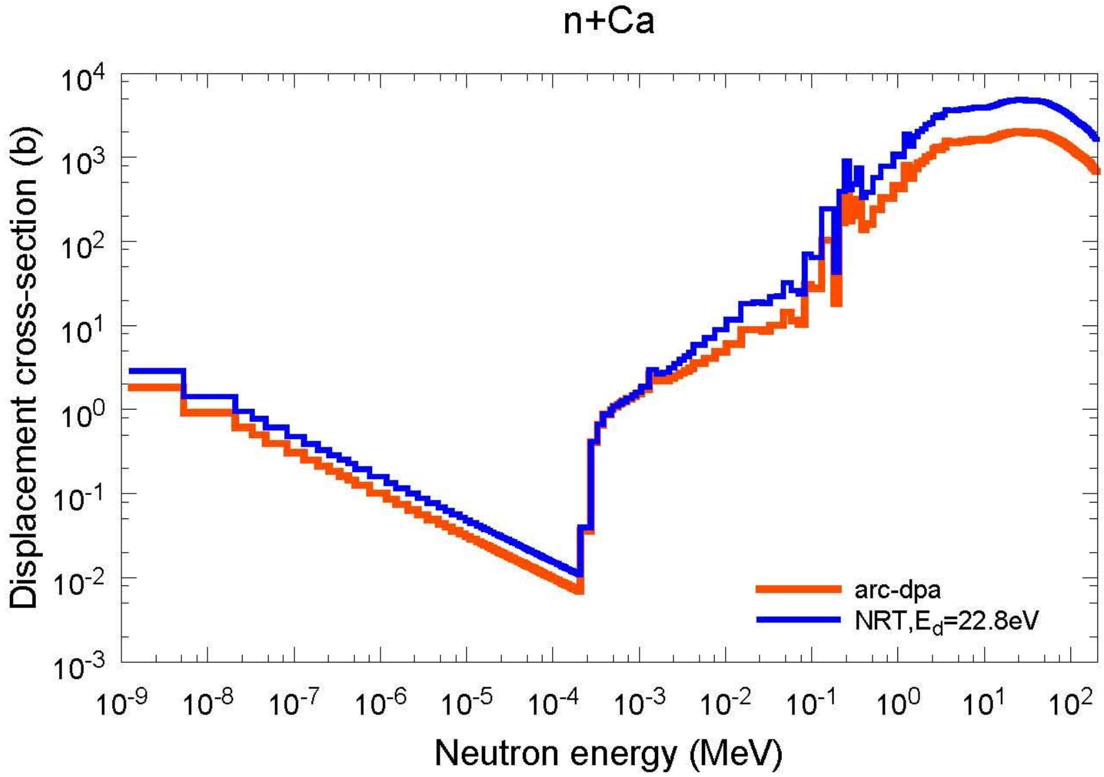
n+Ca
Displacement cross-section (b)
Neutron energy (MeV)
arc-dpa
NRT,E_d=22.8eV

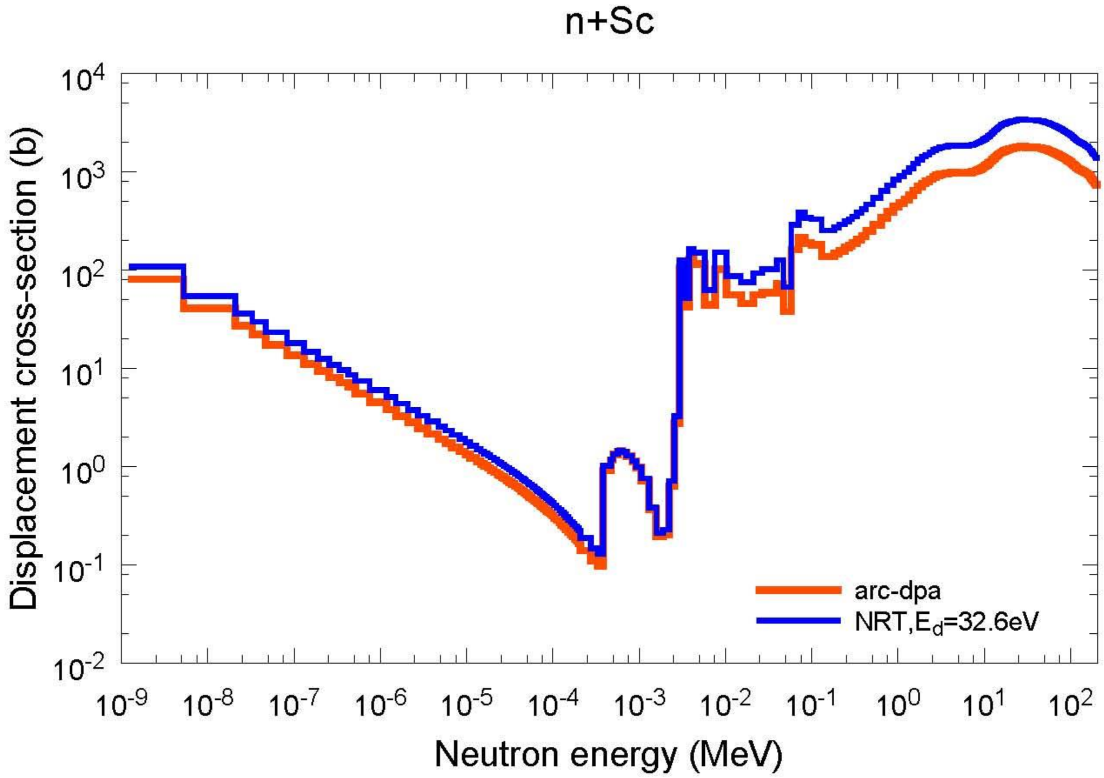
n+Sc
Displacement cross-section (b)
Neutron energy (MeV)
arc-dpa
NRT,E_d=32.6eV

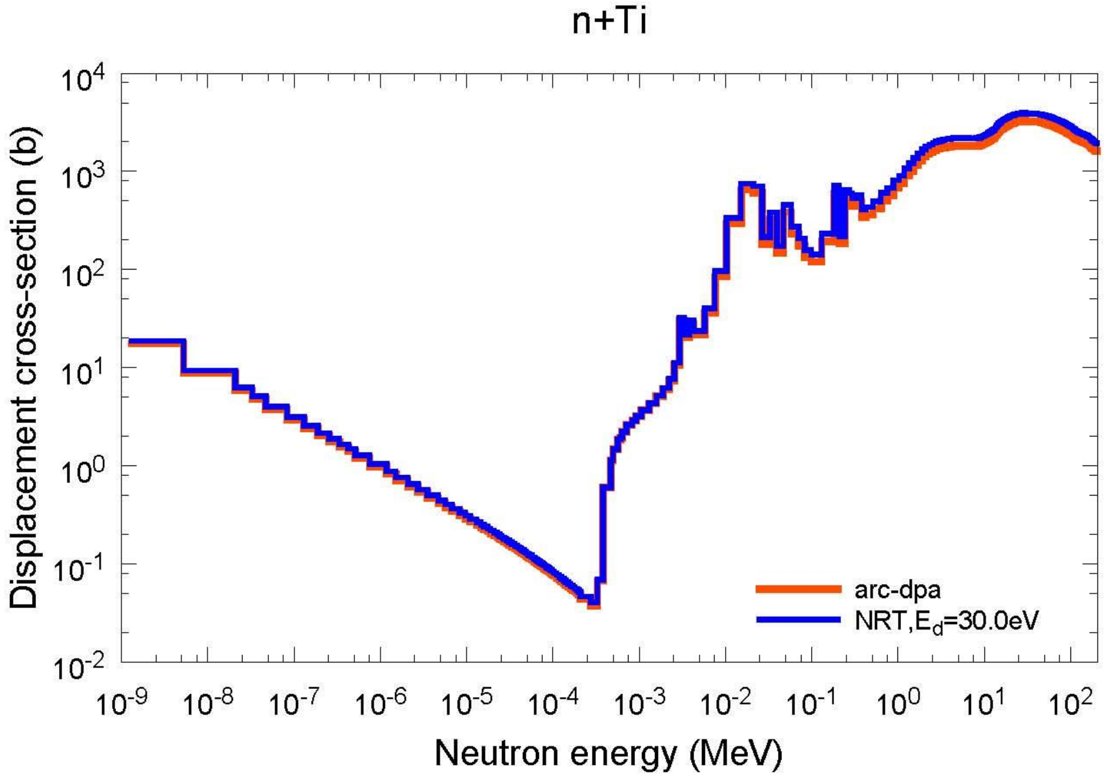
n+Ti
Displacement cross-section (b)
Neutron energy (MeV)
arc-dpa
NRT,E$_d$=30.0eV

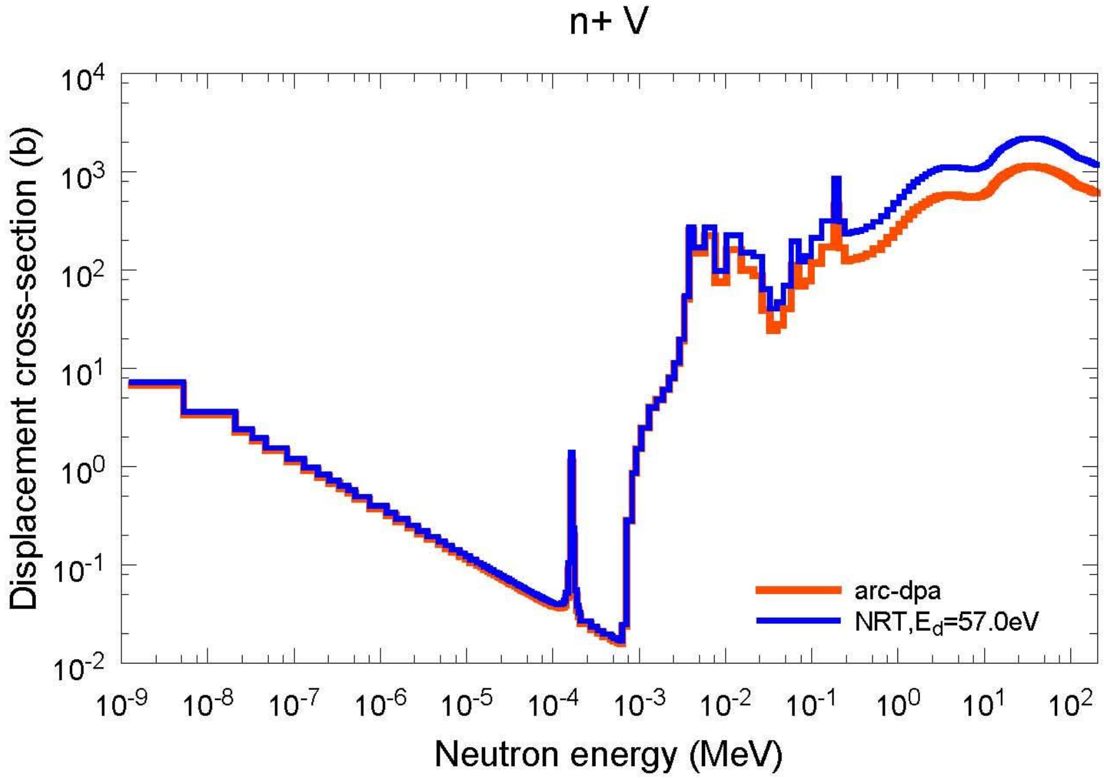
n+ V
Displacement cross-section (b)
Neutron energy (MeV)
arc-dpa
NRT,E$_d$=57.0eV

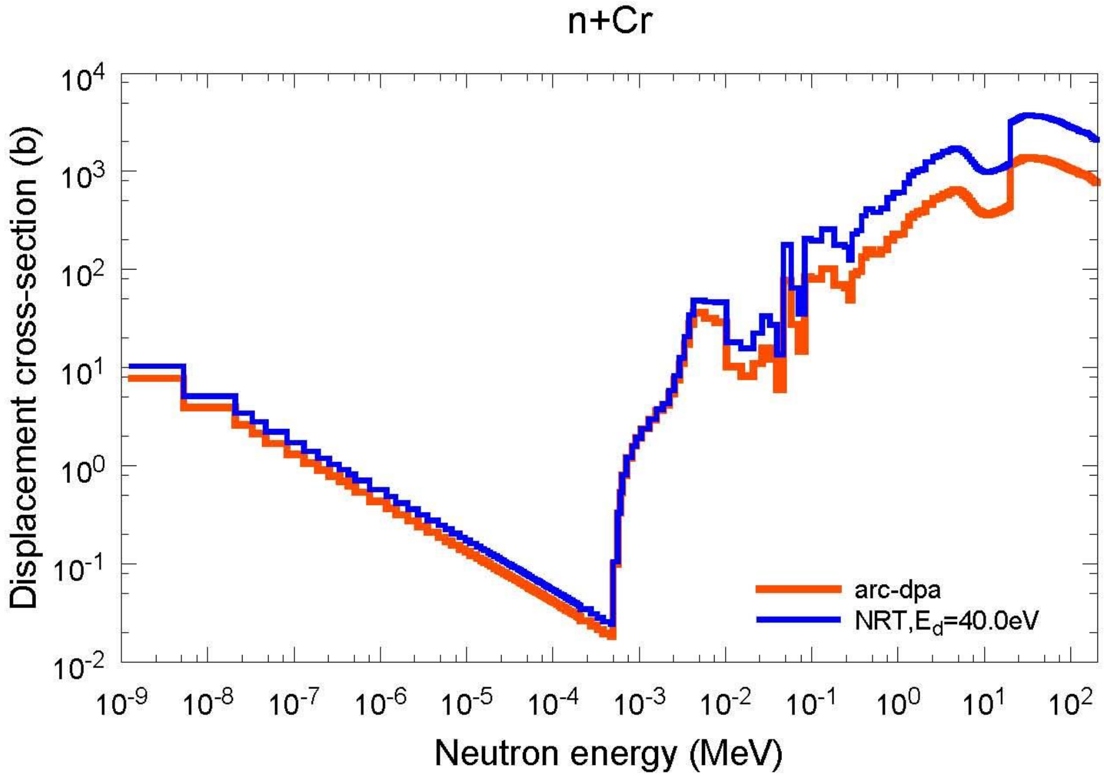
n+Cr
Displacement cross-section (b)
Neutron energy (MeV)
arc-dpa
NRT,E$_d$=40.0eV

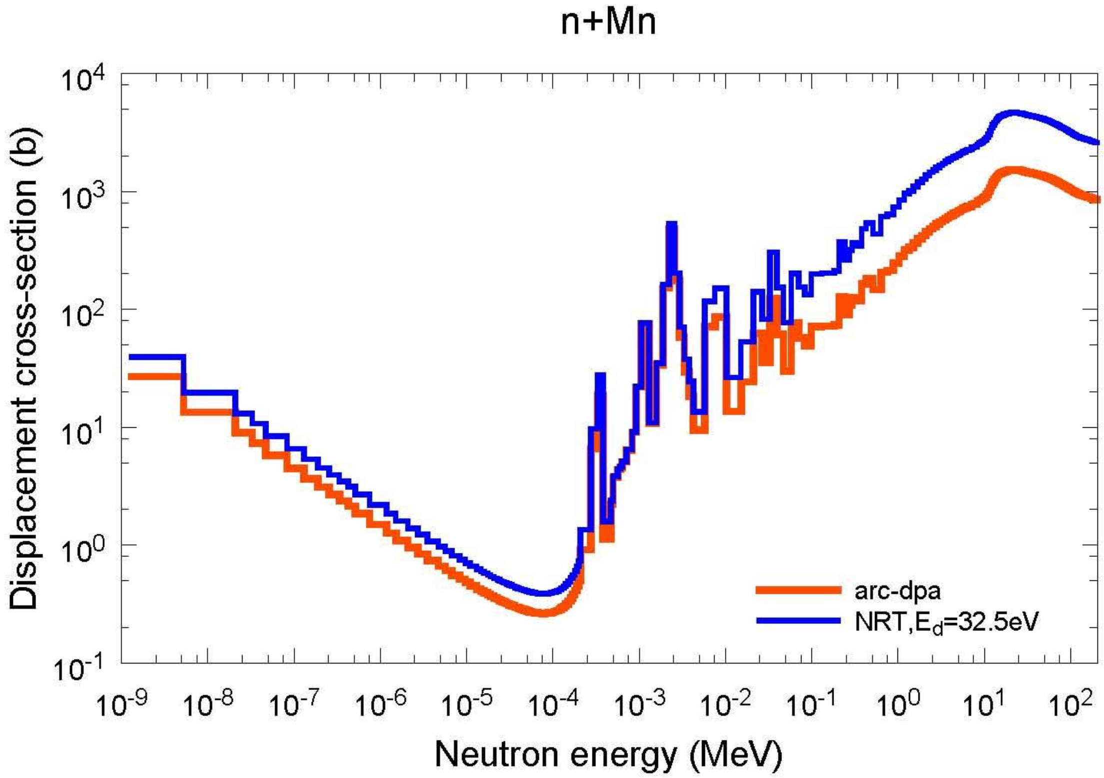
n+Mn
Displacement cross-section (b)
Neutron energy (MeV)
arc-dpa
NRT,E$_d$=32.5eV

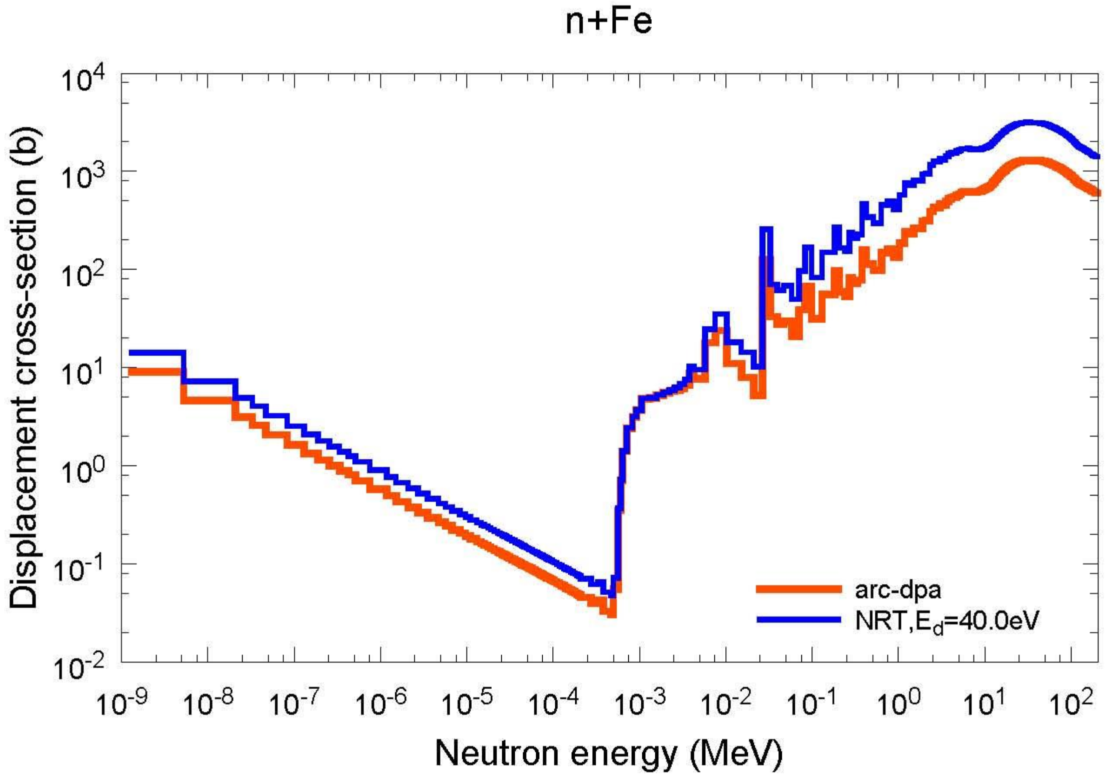
n+Fe
Displacement cross-section (b)
Neutron energy (MeV)
arc-dpa
NRT,E$_d$=40.0eV

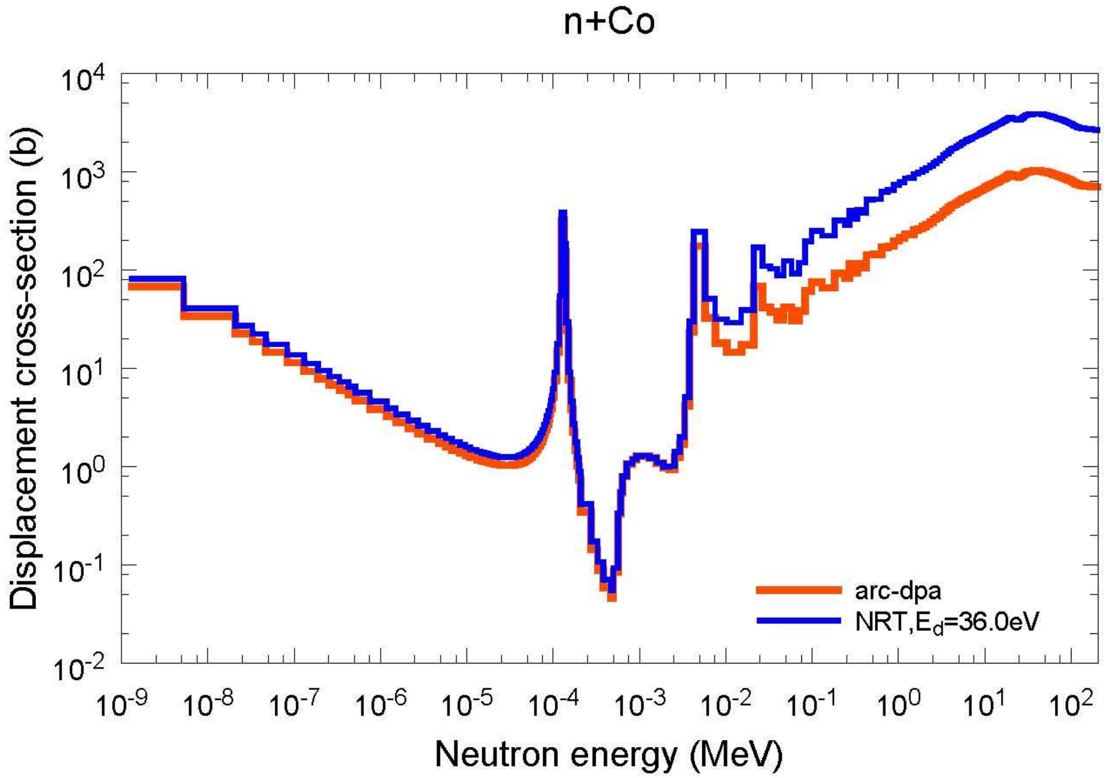
n+Co
Displacement cross-section (b)
Neutron energy (MeV)
arc-dpa
NRT,E$_d$=36.0eV

n+Ni

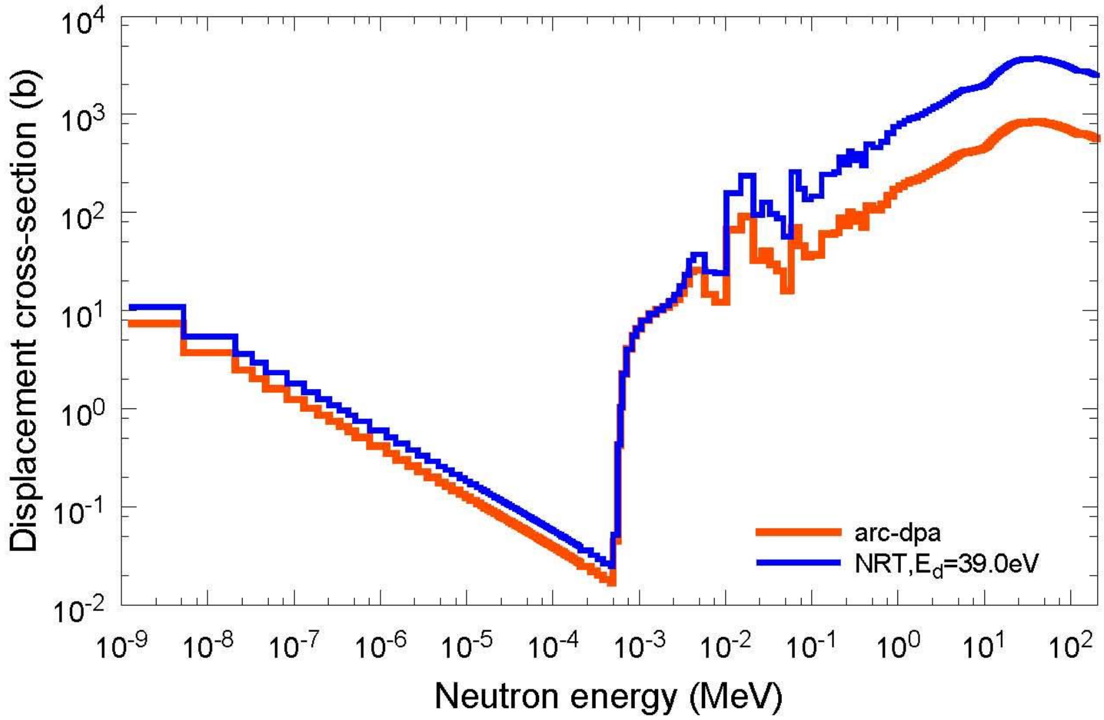

Displacement cross-section (b)
10^4
10^3
10^2
10^1
10^0
10^{-1}
10^{-2}
10^{-9} 10^{-8} 10^{-7} 10^{-6} 10^{-5} 10^{-4} 10^{-3} 10^{-2} 10^{-1} 10^0 10^1 10^2
Neutron energy (MeV)
arc-dpa
NRT,E_d=39.0eV

n+Cu

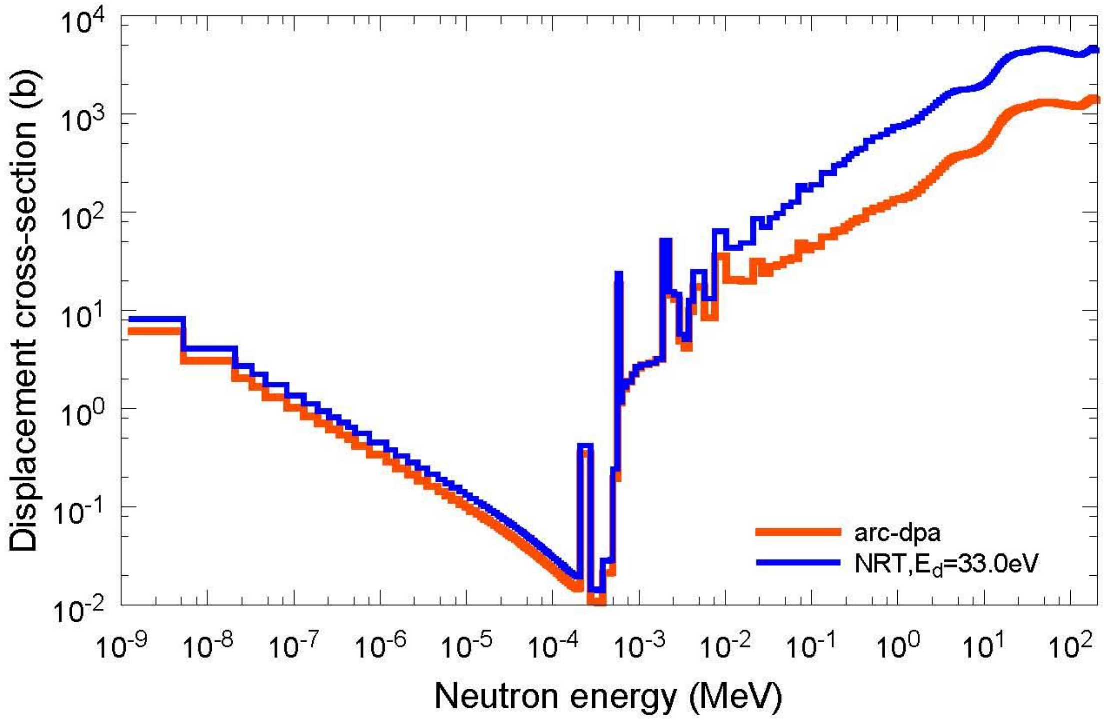

Displacement cross-section (b)
10^4
10^3
10^2
10^1
10^0
10^{-1}
10^{-2}
10^{-9} 10^{-8} 10^{-7} 10^{-6} 10^{-5} 10^{-4} 10^{-3} 10^{-2} 10^{-1} 10^0 10^1 10^2
Neutron energy (MeV)
arc-dpa
NRT,E_d=33.0eV

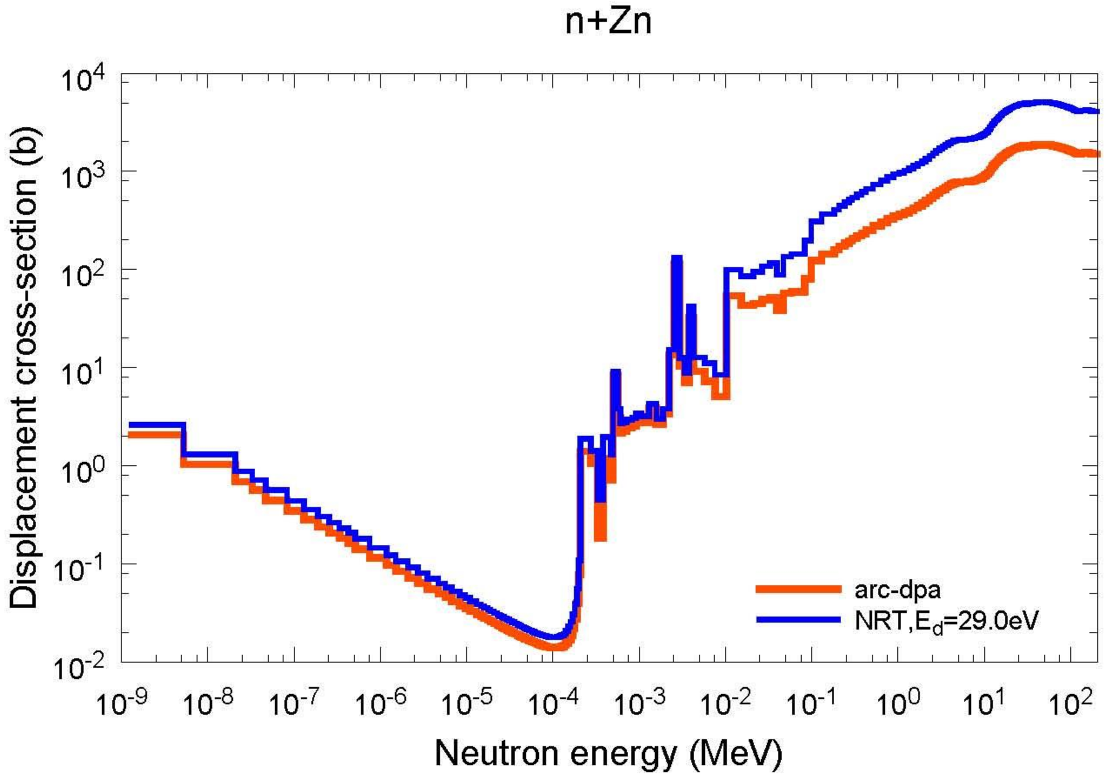
n+Zn
Displacement cross-section (b)
Neutron energy (MeV)
arc-dpa
NRT,E_d=29.0eV

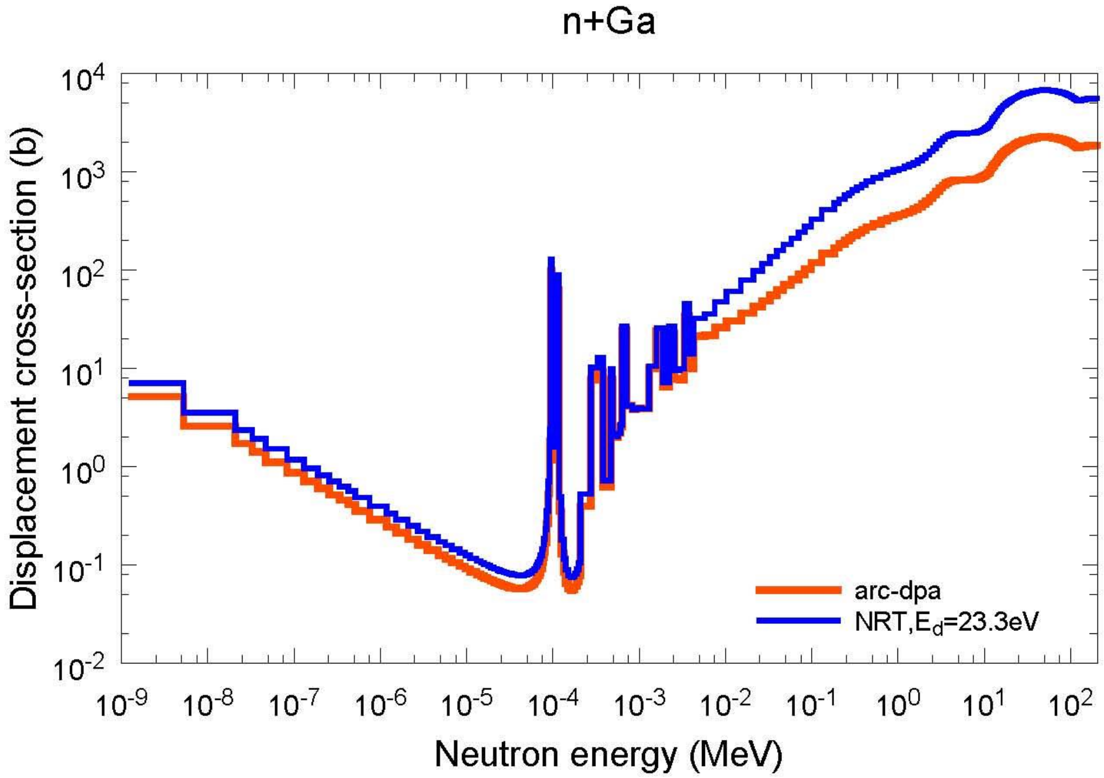
n+Ga
Displacement cross-section (b)
Neutron energy (MeV)
arc-dpa
NRT,E_d=23.3eV

n+Ge

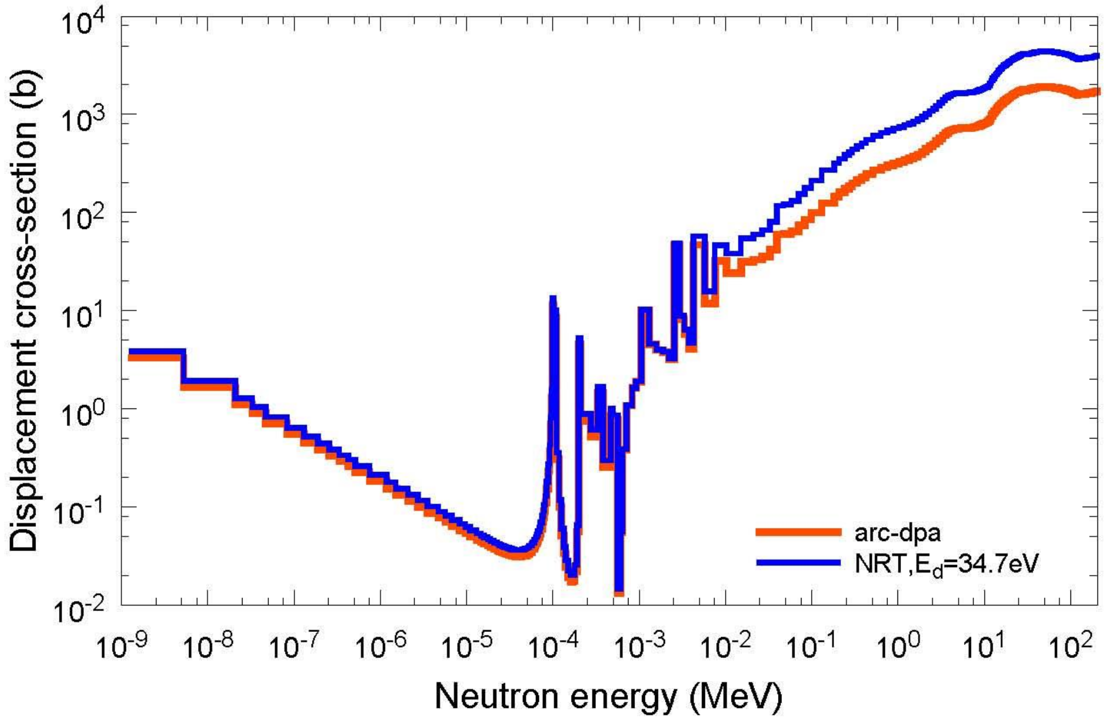

Displacement cross-section (b)
Neutron energy (MeV)
arc-dpa
NRT,E_d=34.7eV

n+As

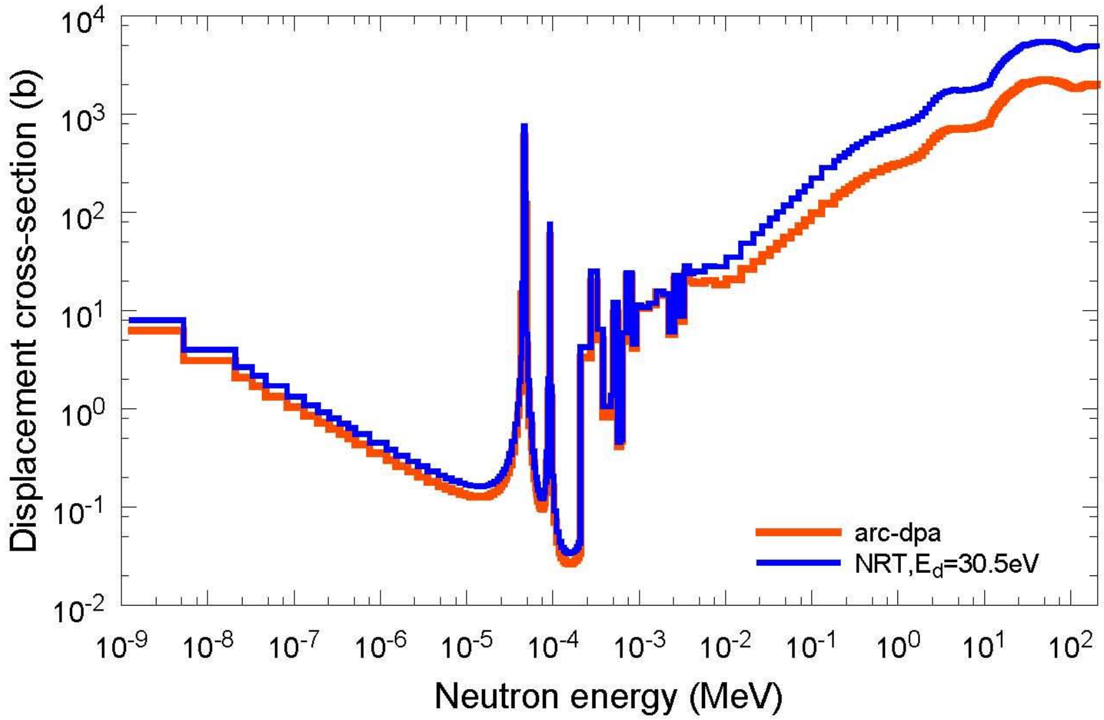

Displacement cross-section (b)
Neutron energy (MeV)
arc-dpa
NRT,E_d=30.5eV

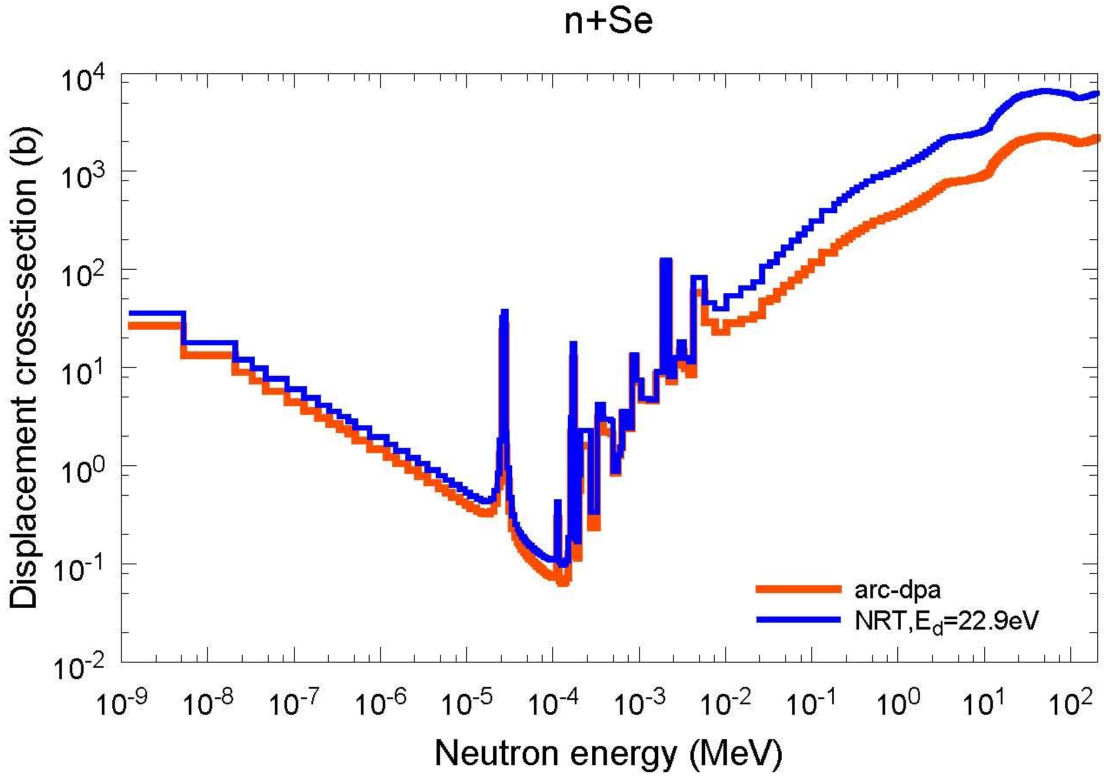
n+Se
Displacement cross-section (b)
Neutron energy (MeV)
arc-dpa
NRT,E$_d$=22.9eV

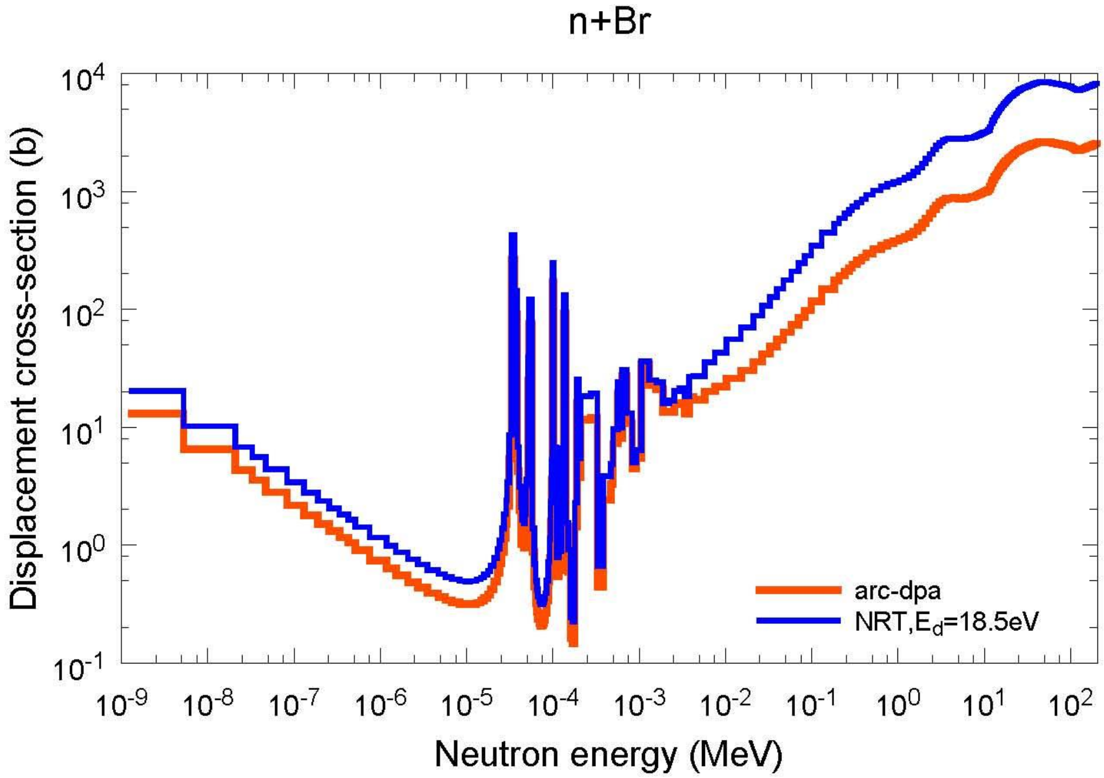
n+Br
Displacement cross-section (b)
Neutron energy (MeV)
arc-dpa
NRT,E$_d$=18.5eV

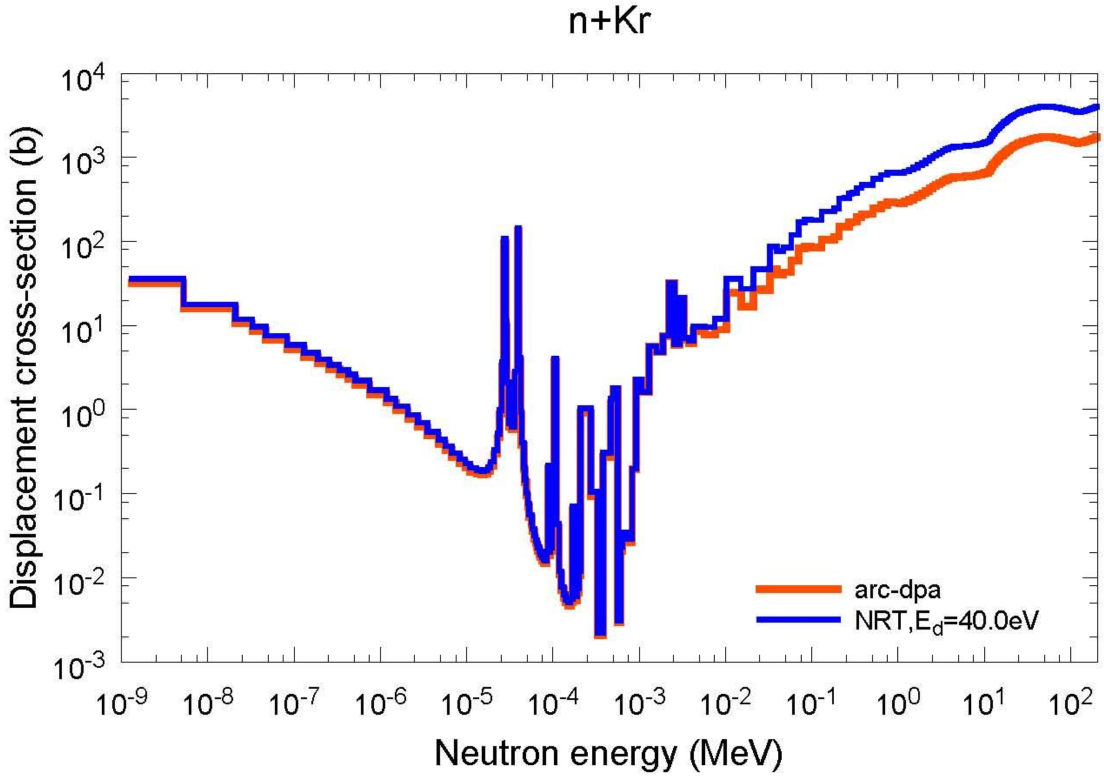
n+Kr
Displacement cross-section (b)
Neutron energy (MeV)
arc-dpa
NRT,E_d=40.0eV

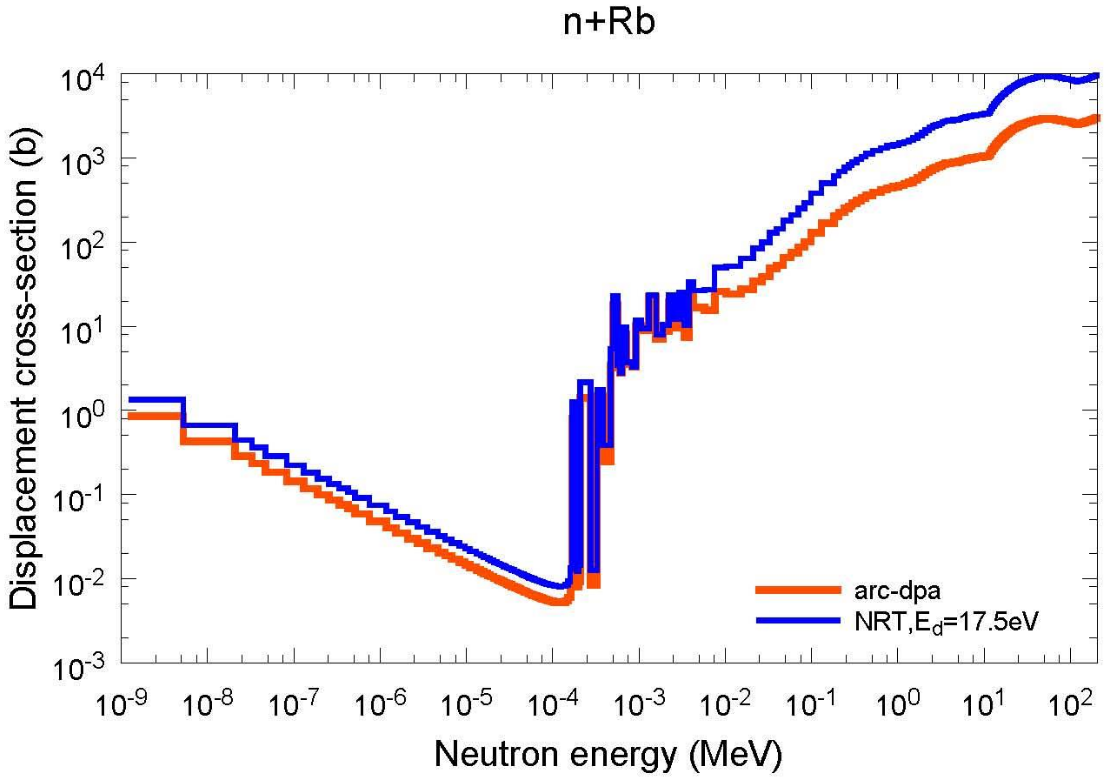
n+Rb
Displacement cross-section (b)
Neutron energy (MeV)
arc-dpa
NRT,E_d=17.5eV

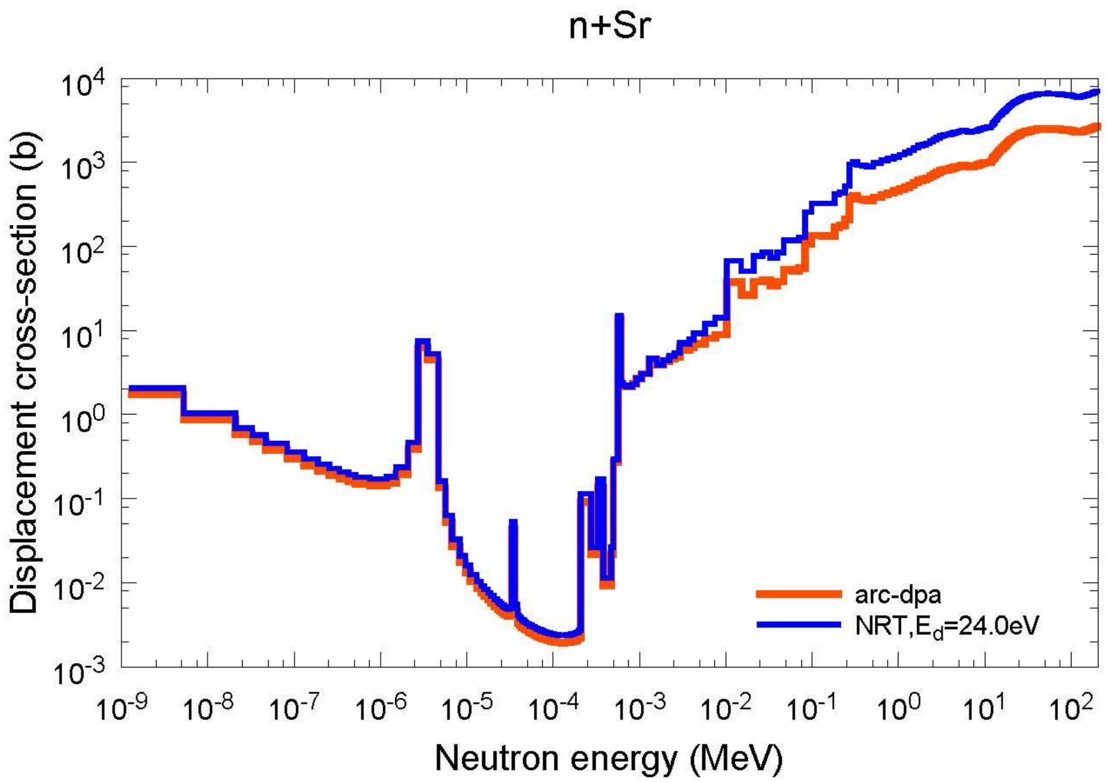
n+Sr
Displacement cross-section (b)
Neutron energy (MeV)
arc-dpa
NRT,E_d=24.0eV

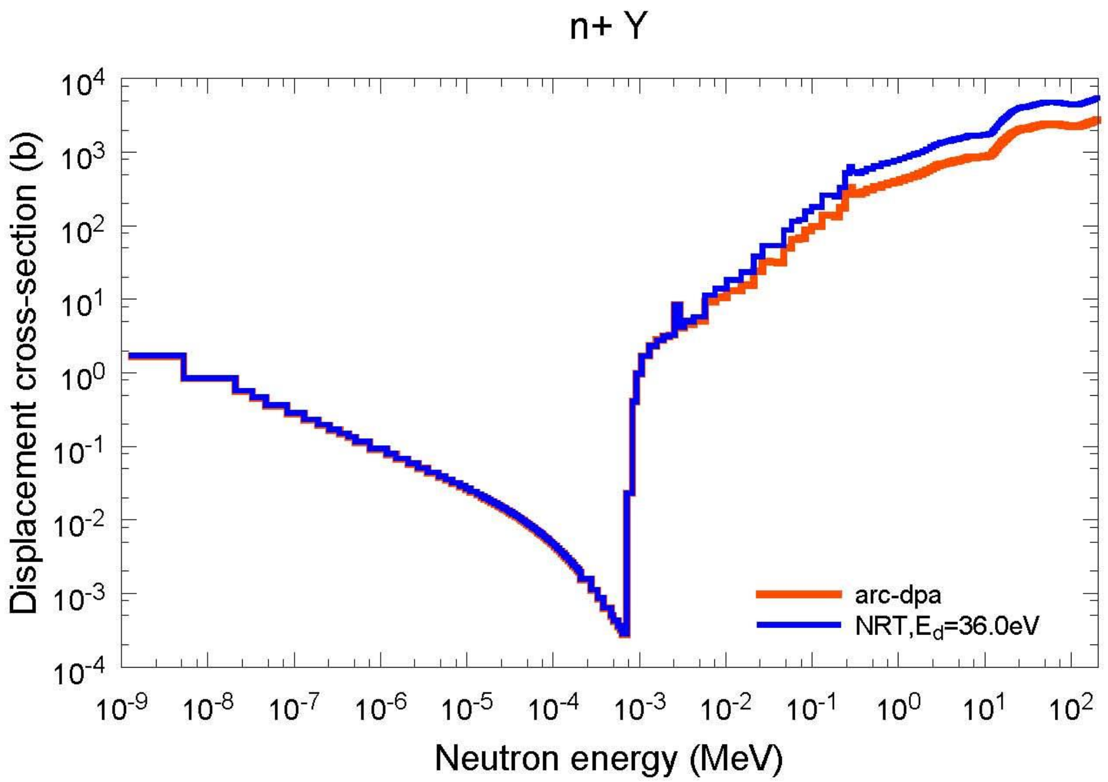
n+ Y
Displacement cross-section (b)
Neutron energy (MeV)
arc-dpa
NRT,E_d=36.0eV

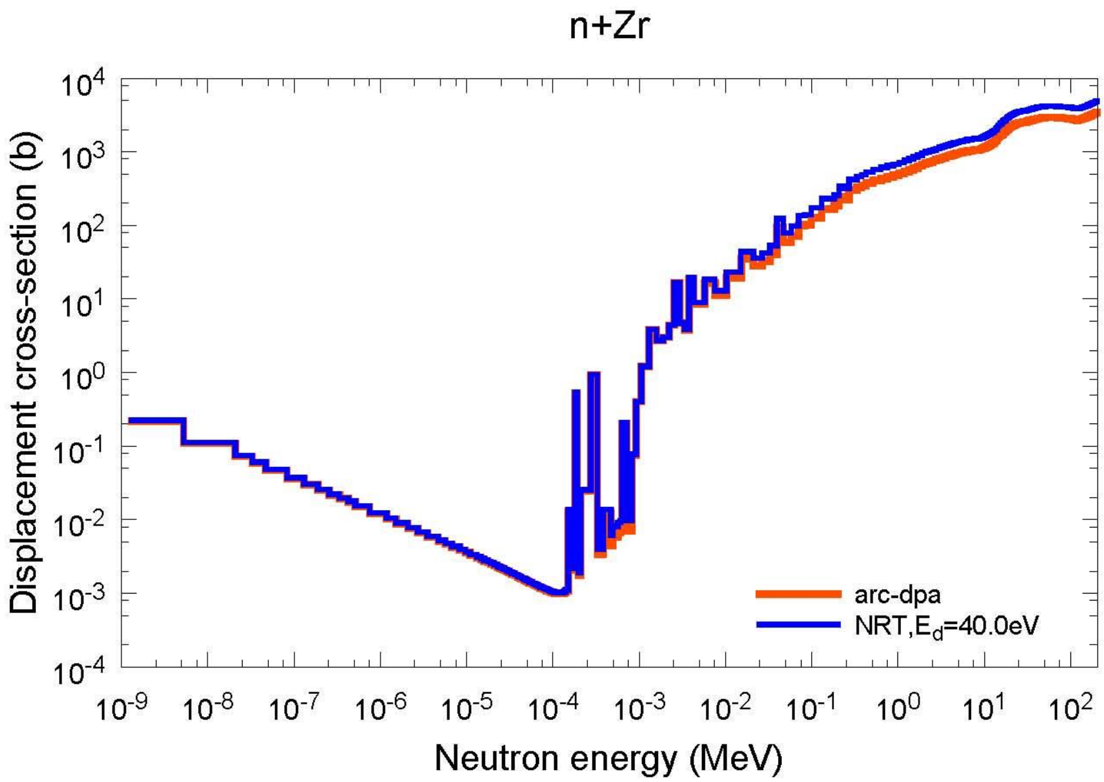
n+Zr
Displacement cross-section (b)
Neutron energy (MeV)
arc-dpa
NRT,E_d=40.0eV

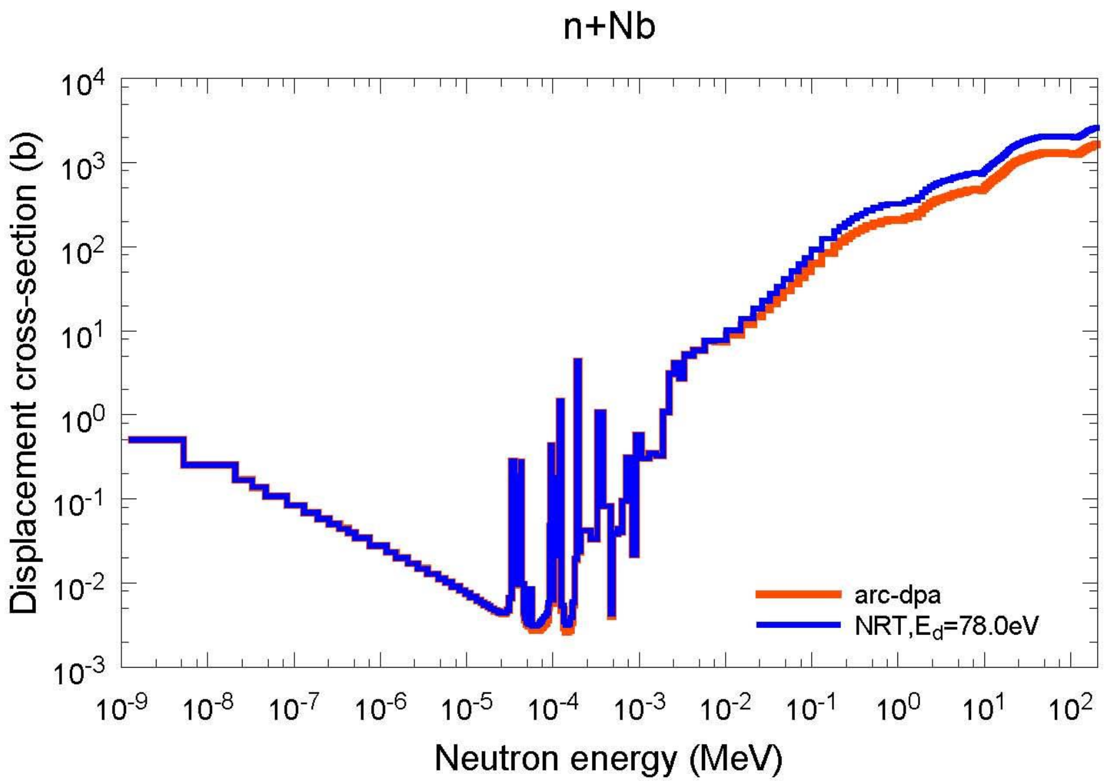
n+Nb
Displacement cross-section (b)
Neutron energy (MeV)
arc-dpa
NRT,E_d=78.0eV

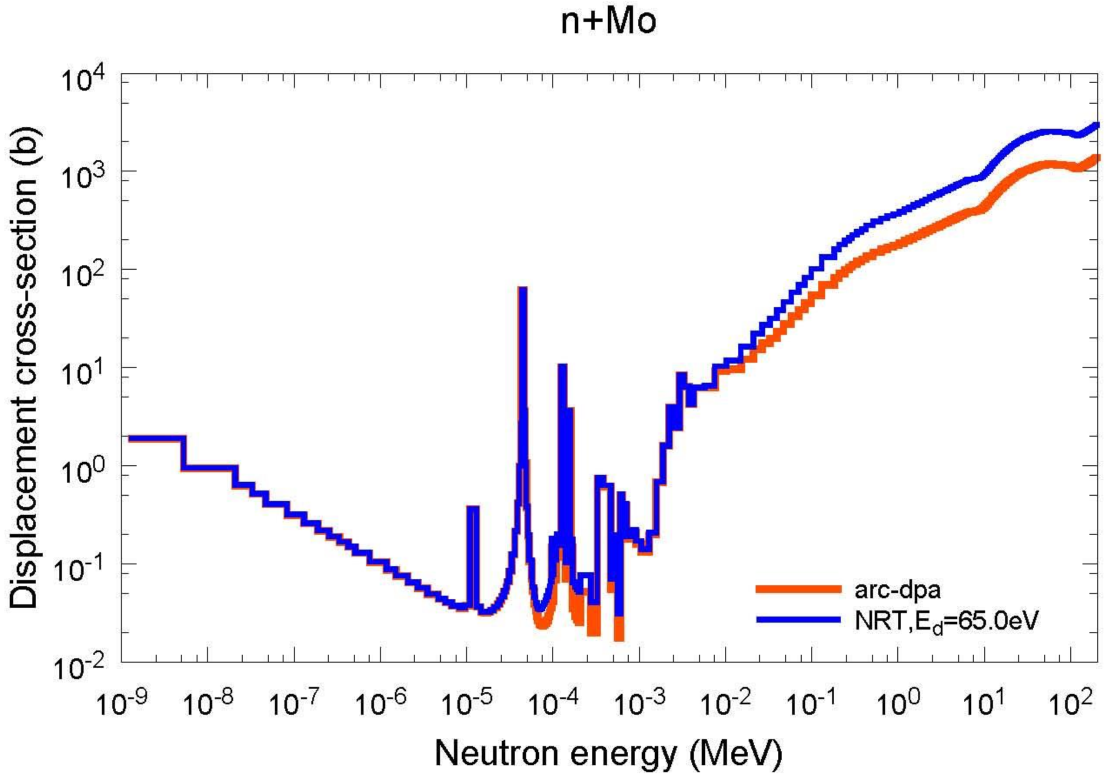
n+Mo
Displacement cross-section (b)
Neutron energy (MeV)
arc-dpa
NRT,E_d=65.0eV

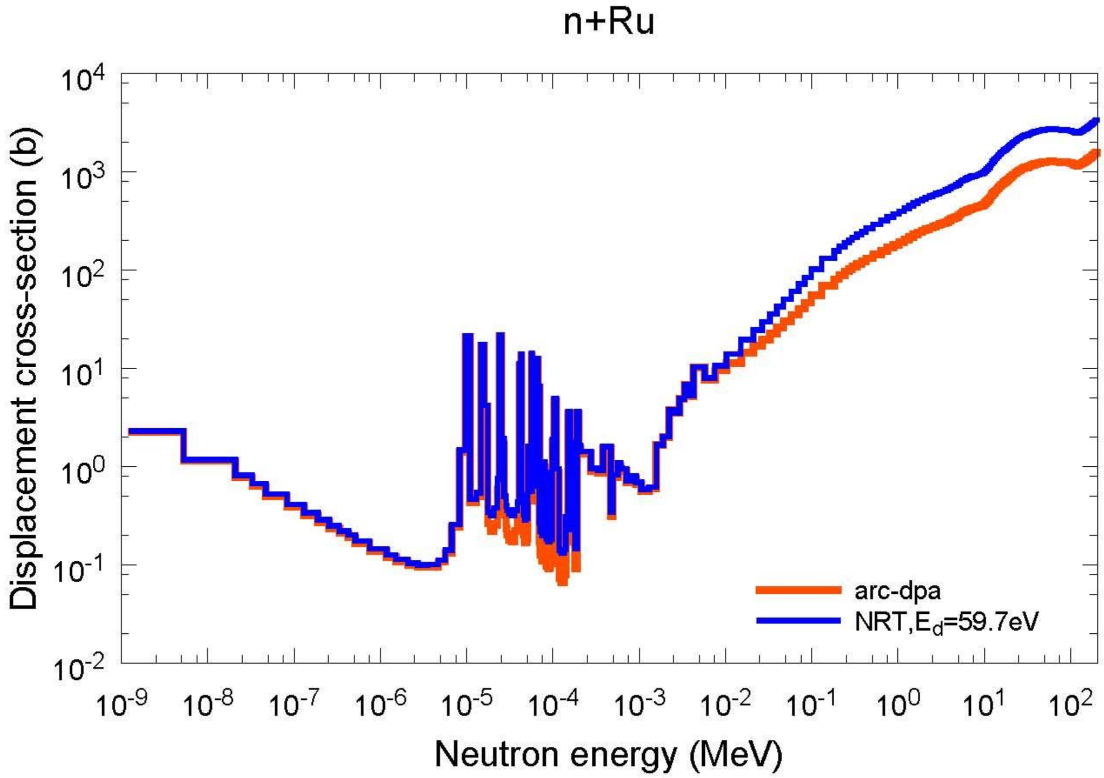
n+Ru
Displacement cross-section (b)
Neutron energy (MeV)
arc-dpa
NRT,E_d=59.7eV

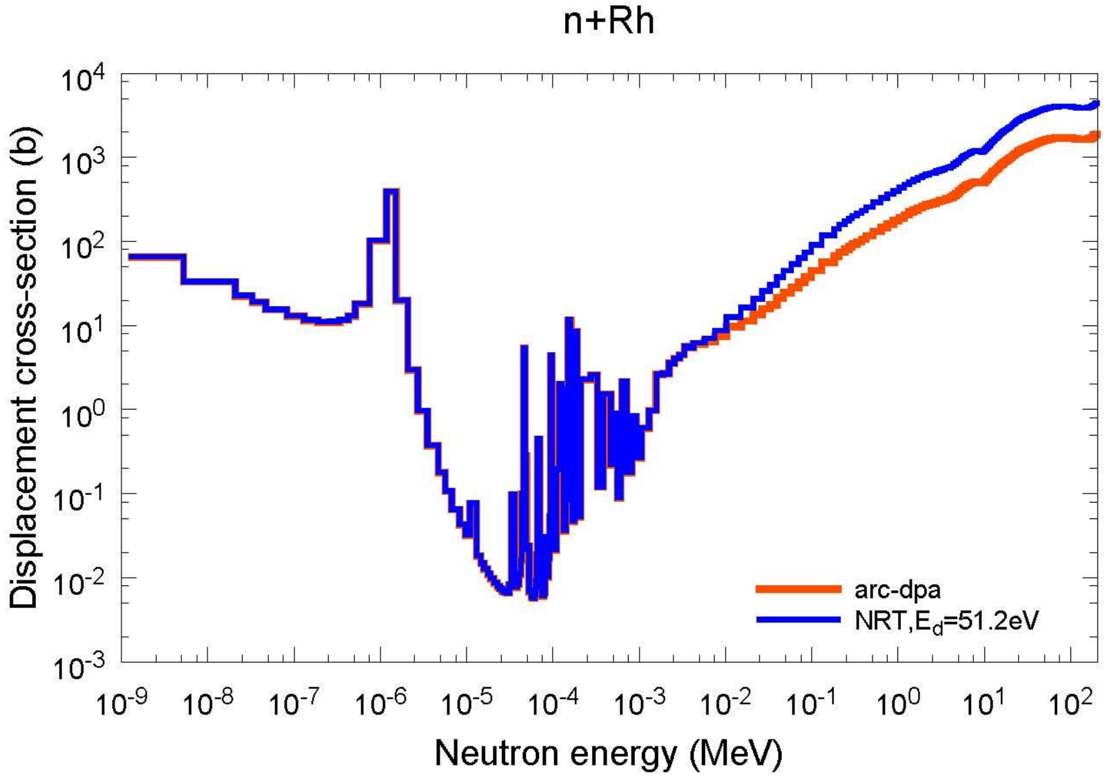
n+Rh
Displacement cross-section (b)
Neutron energy (MeV)
arc-dpa
NRT,E_d=51.2eV

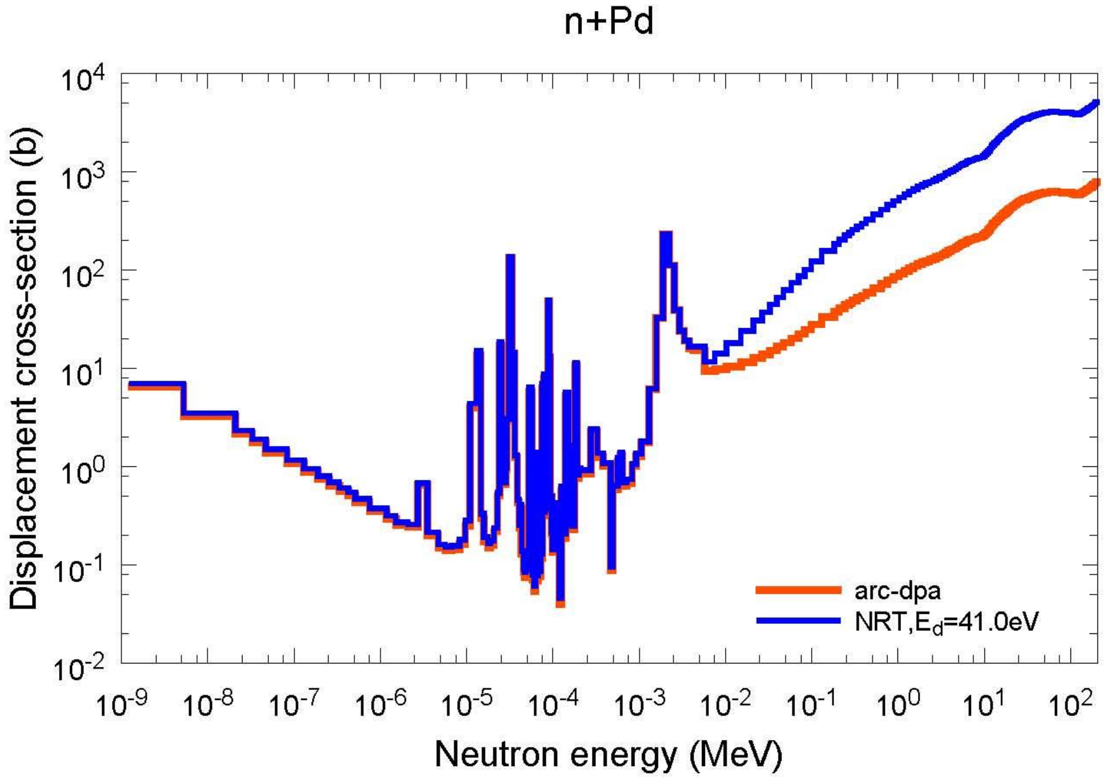
n+Pd
Displacement cross-section (b)
Neutron energy (MeV)
arc-dpa
NRT,E_d=41.0eV

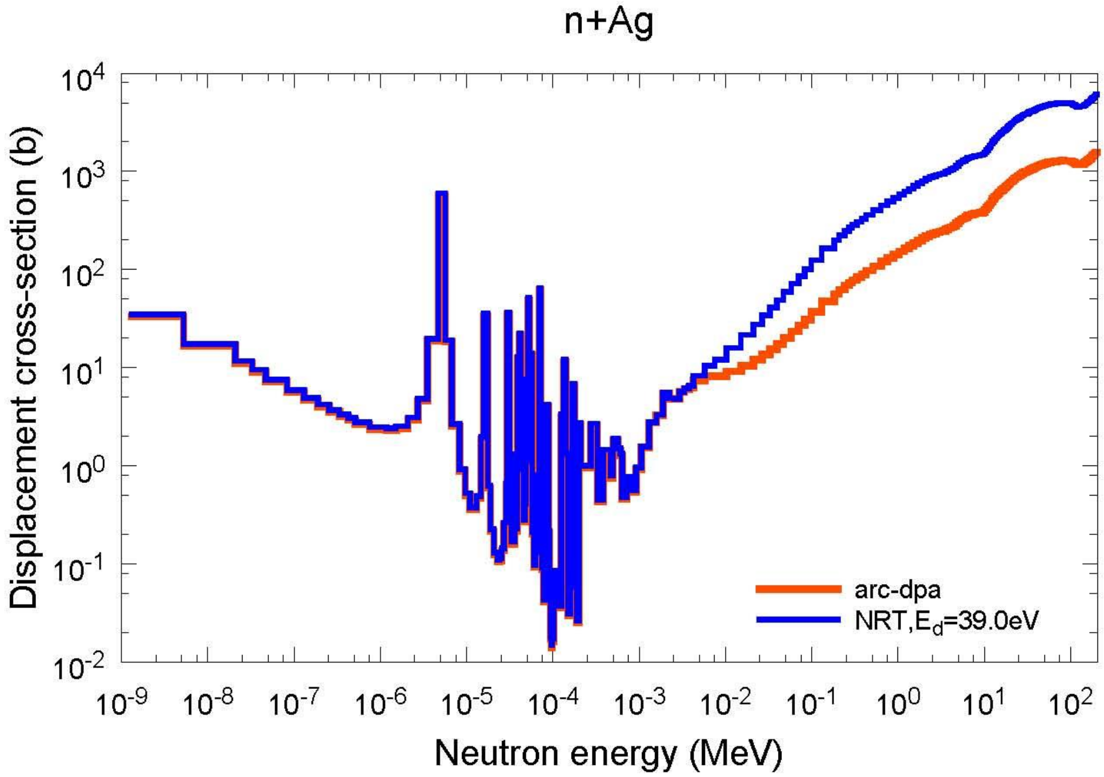
n+Ag
Displacement cross-section (b)
Neutron energy (MeV)
arc-dpa
NRT,E_d=39.0eV

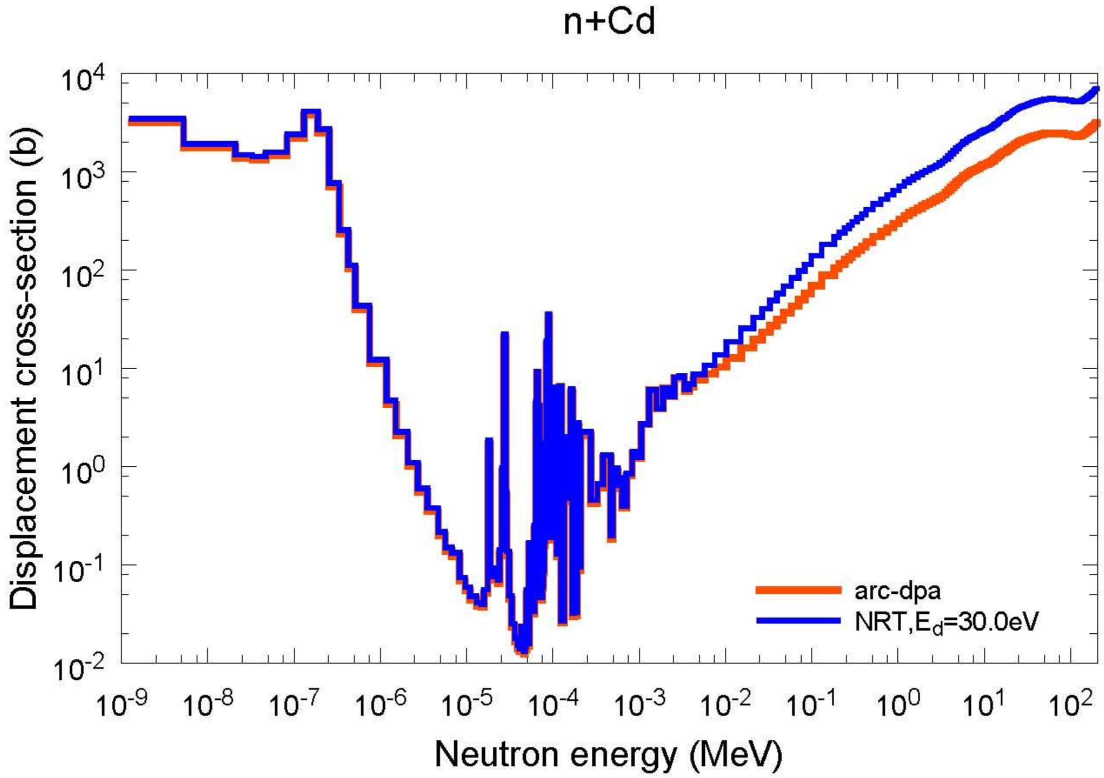
n+Cd
Displacement cross-section (b)
Neutron energy (MeV)
arc-dpa
NRT,E_d=30.0eV

n+In

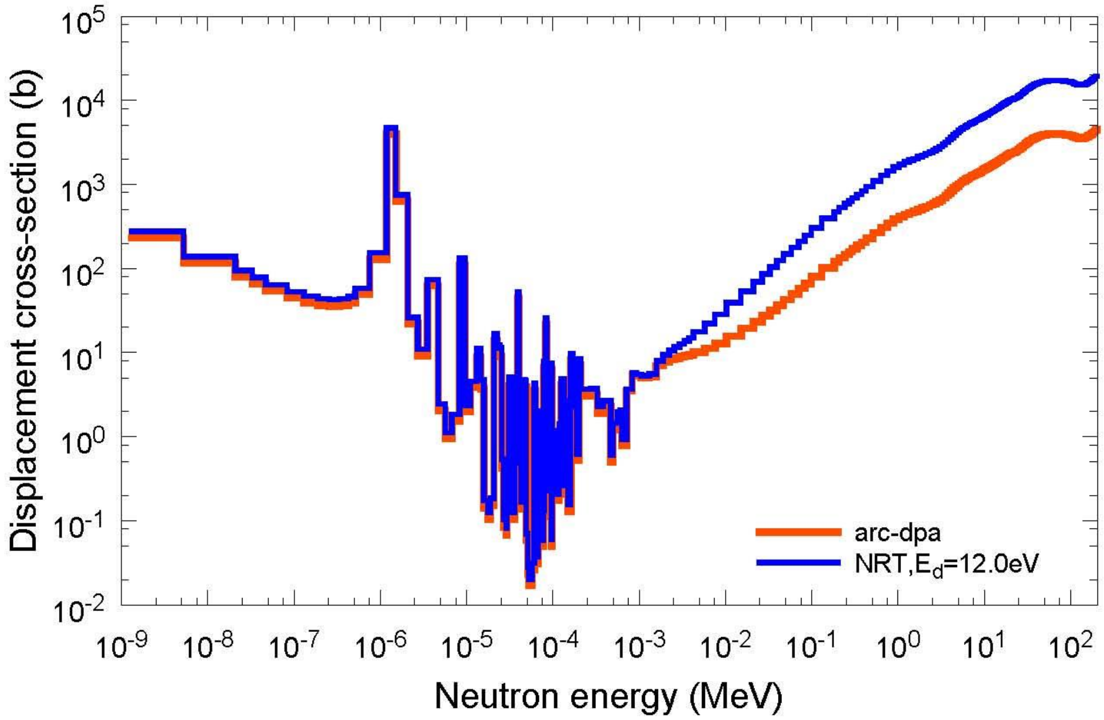

Displacement cross-section (b)
Neutron energy (MeV)
arc-dpa
NRT,E_d=12.0eV

n+Sn

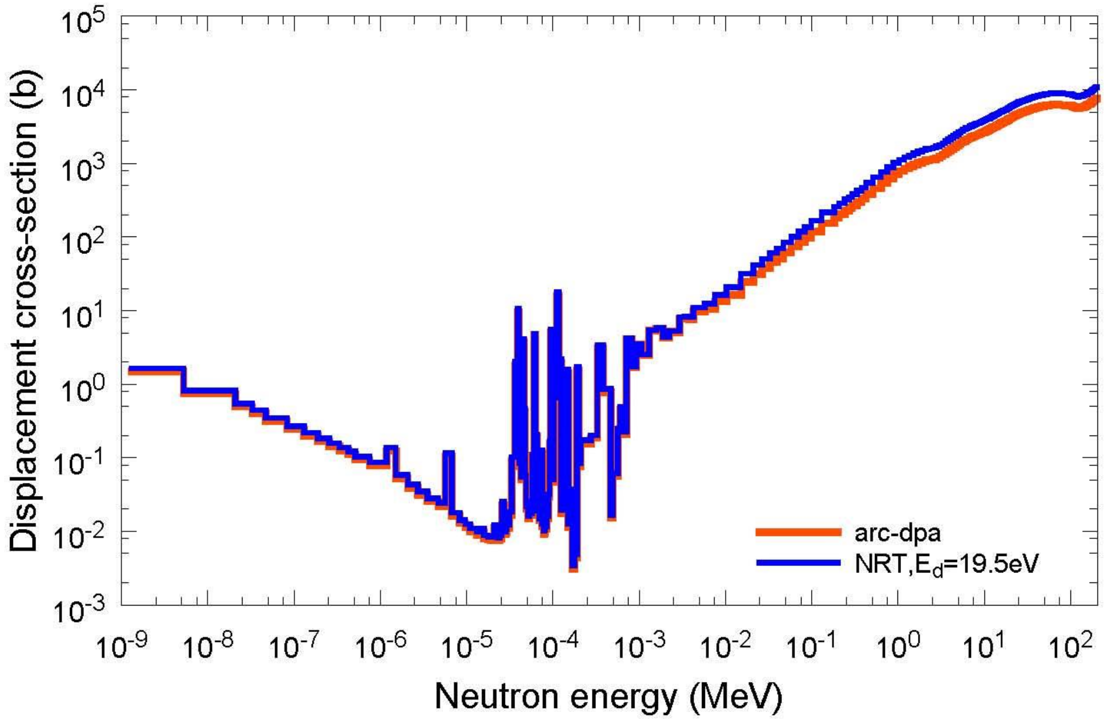

Displacement cross-section (b)
Neutron energy (MeV)
arc-dpa
NRT,E_d=19.5eV

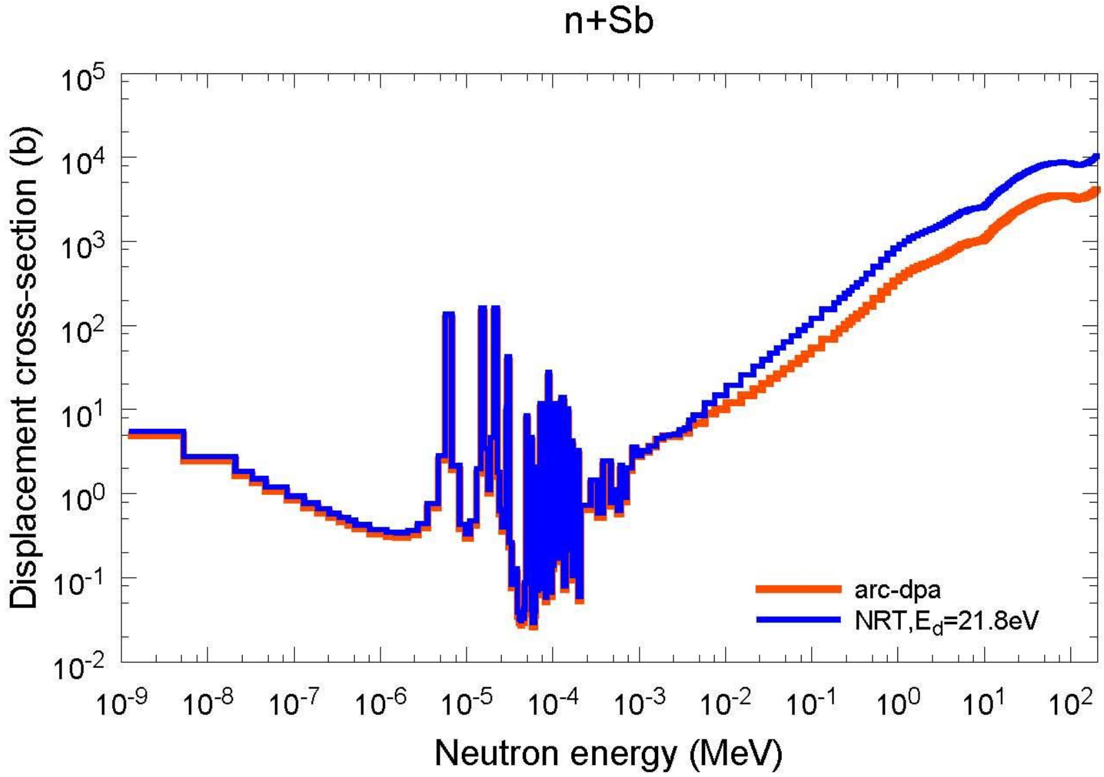
n+Sb
Displacement cross-section (b)
Neutron energy (MeV)
arc-dpa
NRT,E$_d$=21.8eV

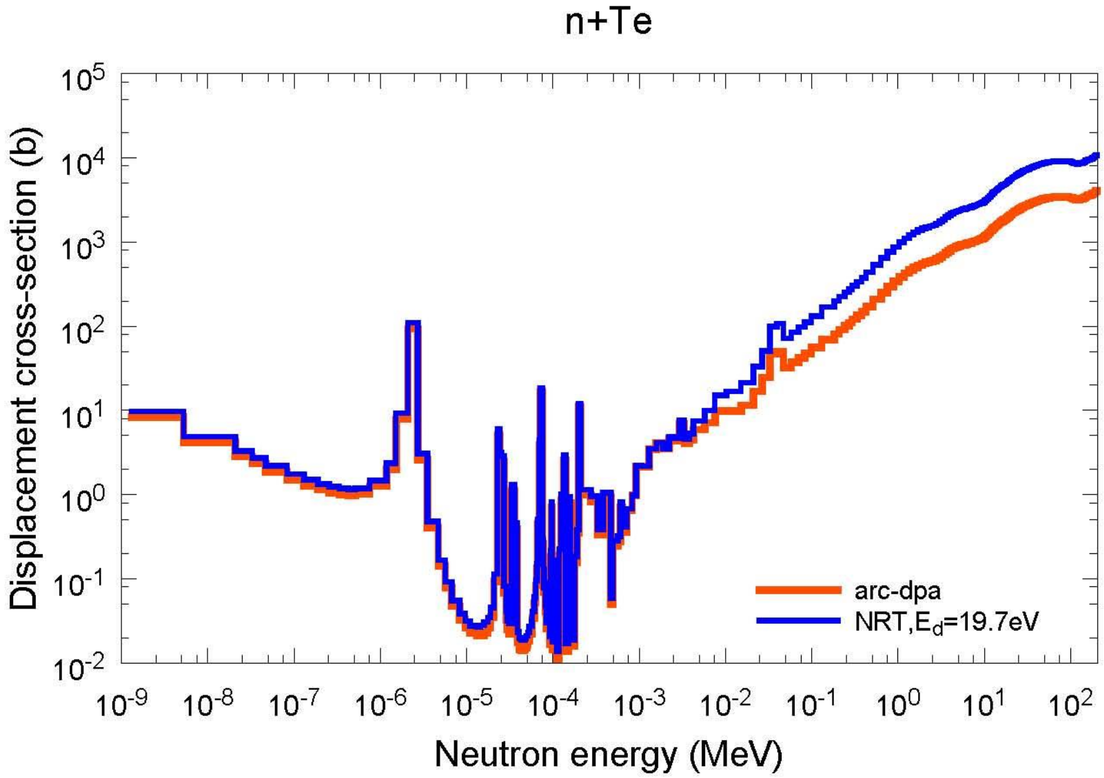
n+Te
Displacement cross-section (b)
Neutron energy (MeV)
arc-dpa
NRT,E$_d$=19.7eV

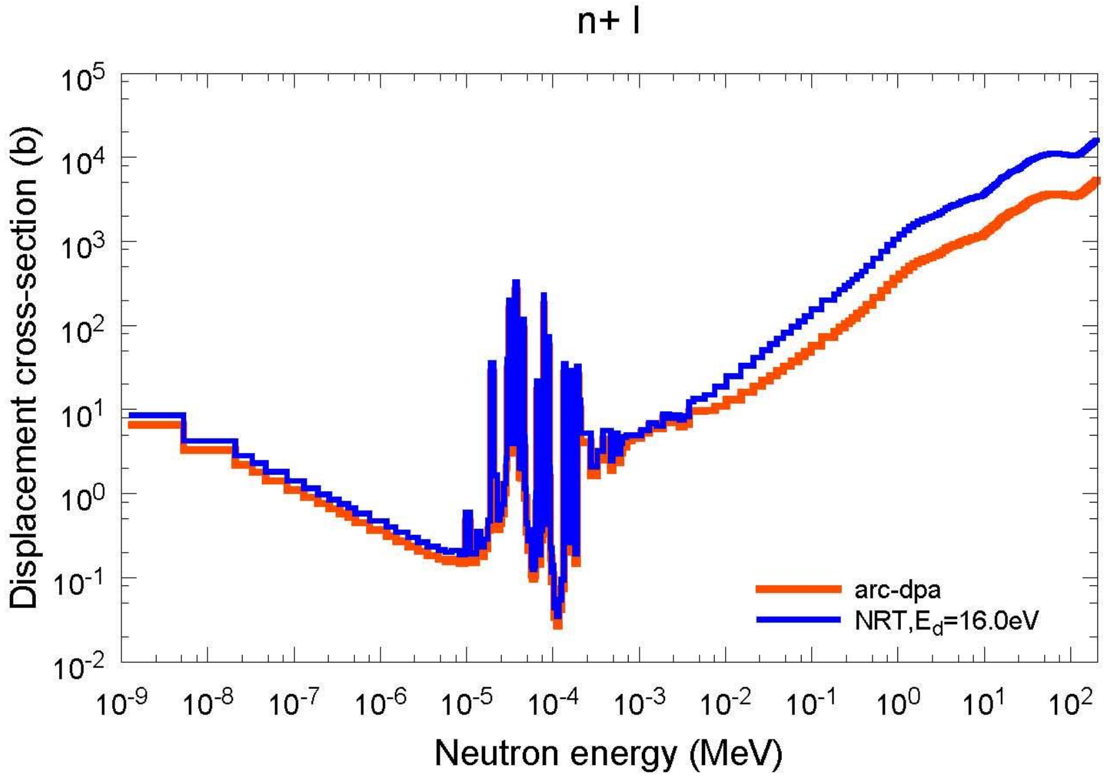
n+ I
Displacement cross-section (b)
10^{5}
10^{4}
10^{3}
10^{2}
10^{1}
10^{0}
10^{-1}
10^{-2}
arc-dpa
NRT,E_d=16.0eV
10^{-9} 10^{-8} 10^{-7} 10^{-6} 10^{-5} 10^{-4} 10^{-3} 10^{-2} 10^{-1} 10^{0} 10^{1} 10^{2}
Neutron energy (MeV)

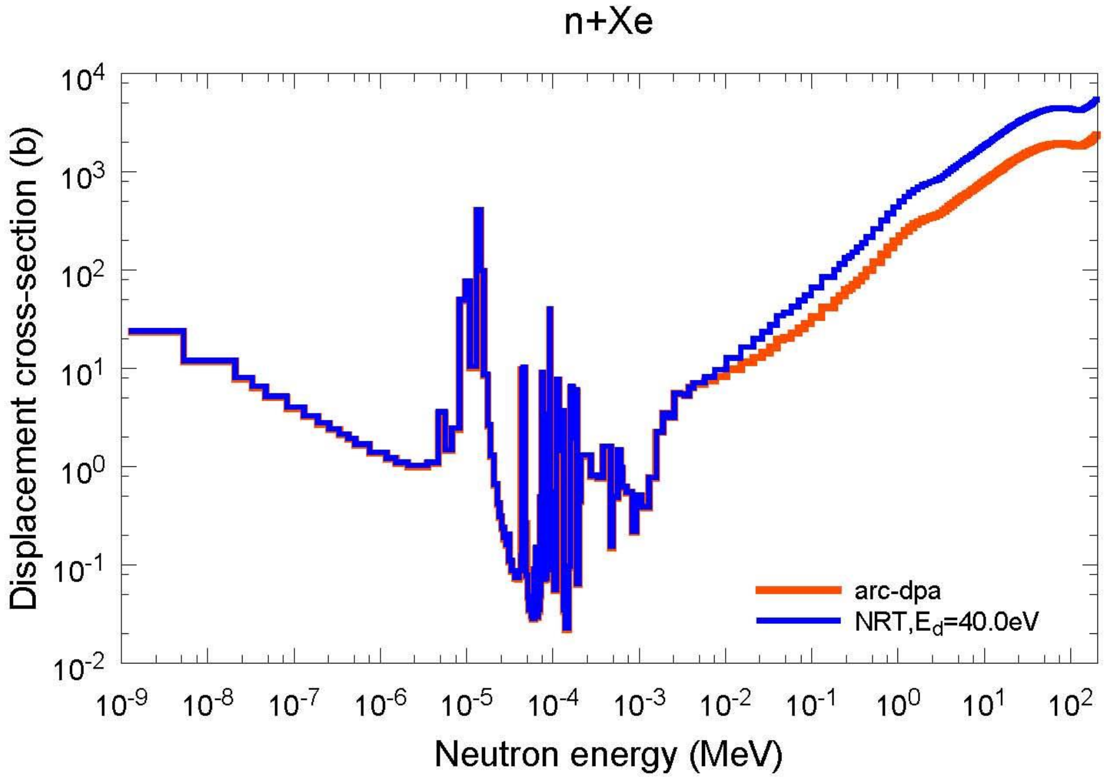
n+Xe
Displacement cross-section (b)
10^{4}
10^{3}
10^{2}
10^{1}
10^{0}
10^{-1}
10^{-2}
arc-dpa
NRT,E_d=40.0eV
10^{-9} 10^{-8} 10^{-7} 10^{-6} 10^{-5} 10^{-4} 10^{-3} 10^{-2} 10^{-1} 10^{0} 10^{1} 10^{2}
Neutron energy (MeV)

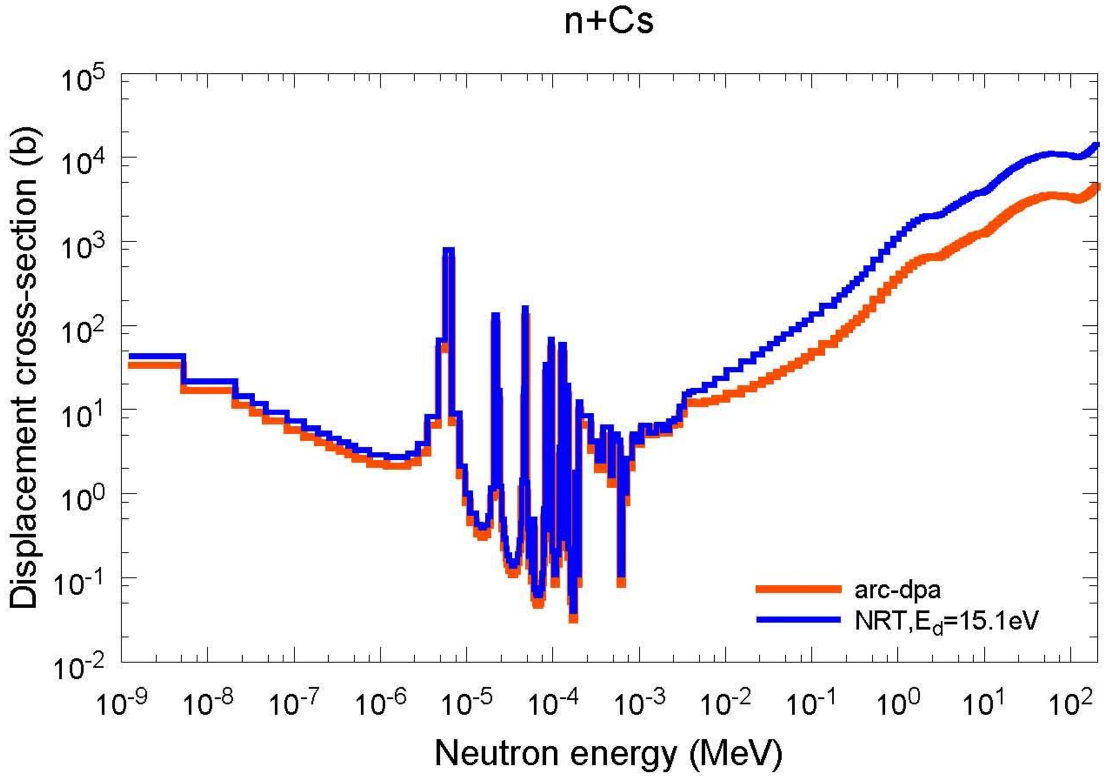
n+Cs
Displacement cross-section (b)
Neutron energy (MeV)
arc-dpa
NRT,E_d=15.1eV

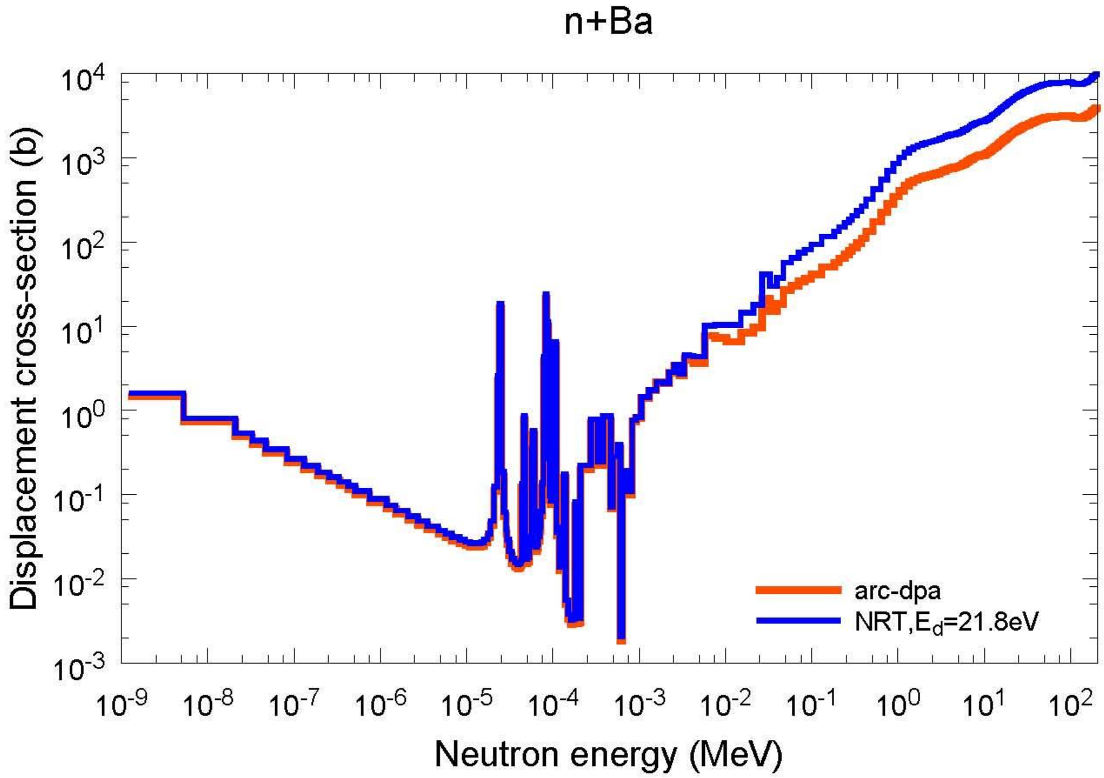
n+Ba
Displacement cross-section (b)
Neutron energy (MeV)
arc-dpa
NRT,E_d=21.8eV

n+La

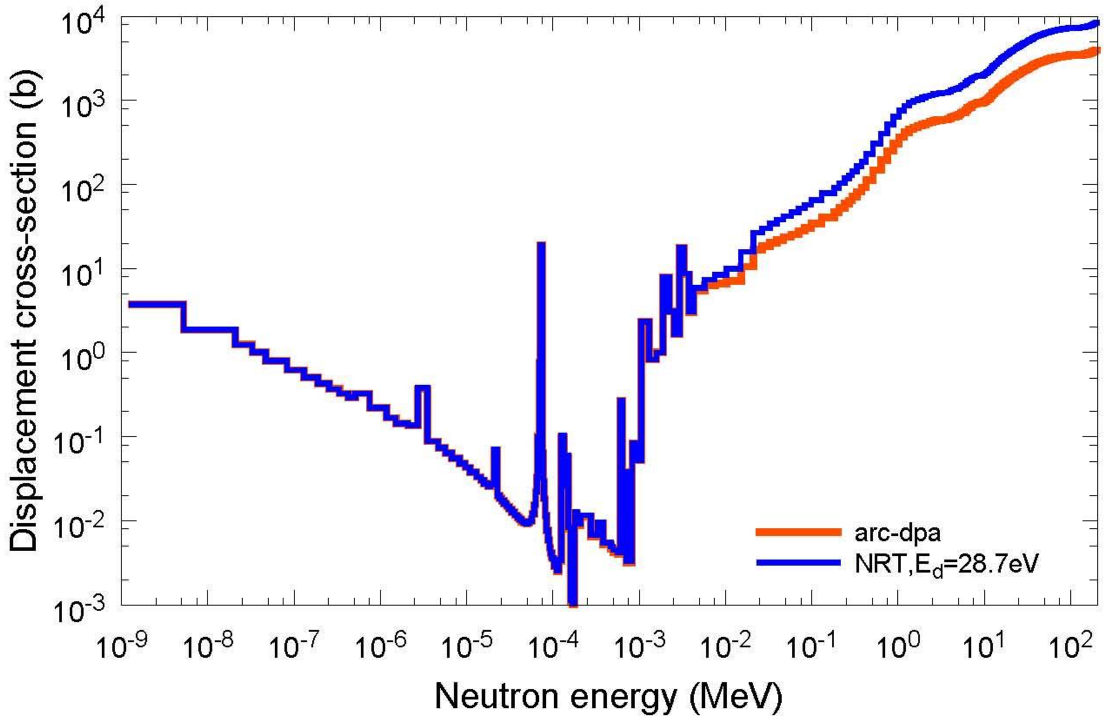
Displacement cross-section (b)
Neutron energy (MeV)
arc-dpa
NRT,E$_d$=28.7eV

n+Ce

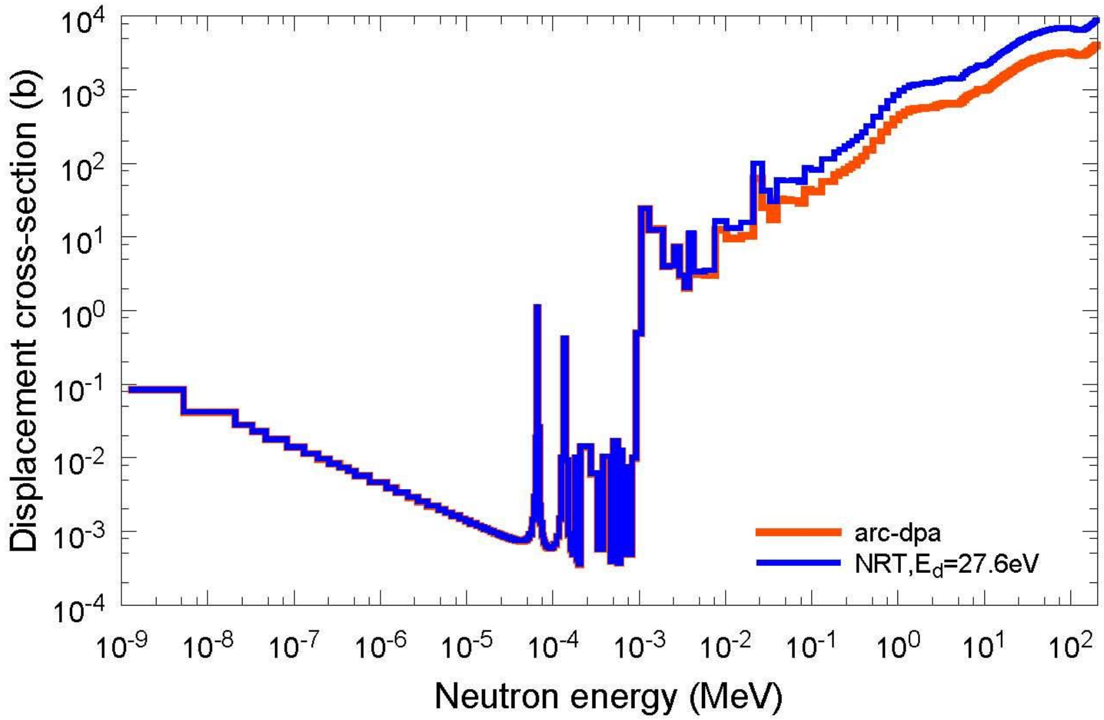
Displacement cross-section (b)
Neutron energy (MeV)
arc-dpa
NRT,E$_d$=27.6eV

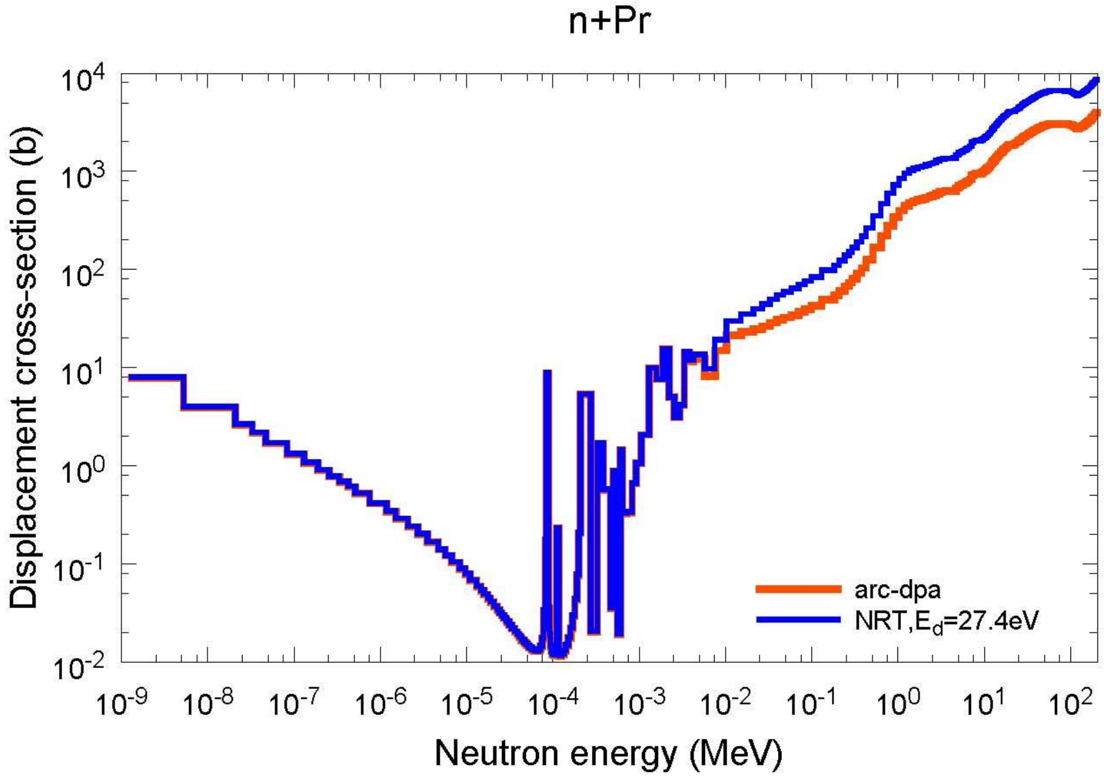
n+Pr
Displacement cross-section (b)
Neutron energy (MeV)
arc-dpa
NRT,E$_d$=27.4eV

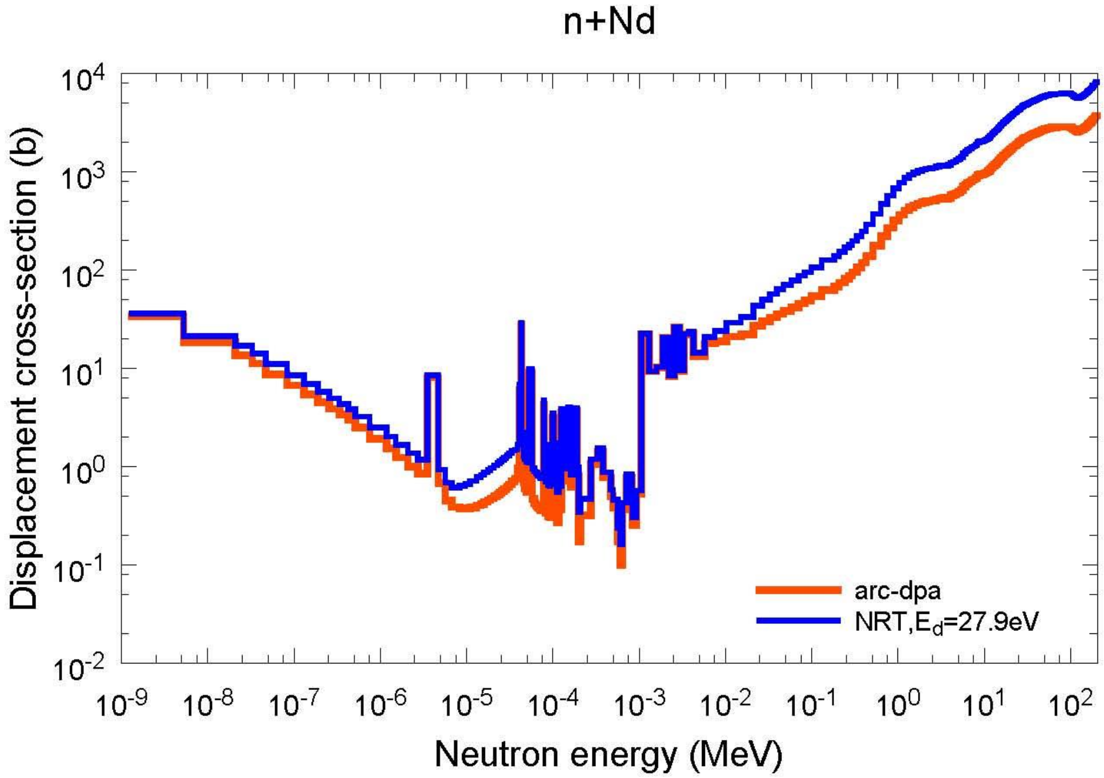
n+Nd
Displacement cross-section (b)
Neutron energy (MeV)
arc-dpa
NRT,E$_d$=27.9eV

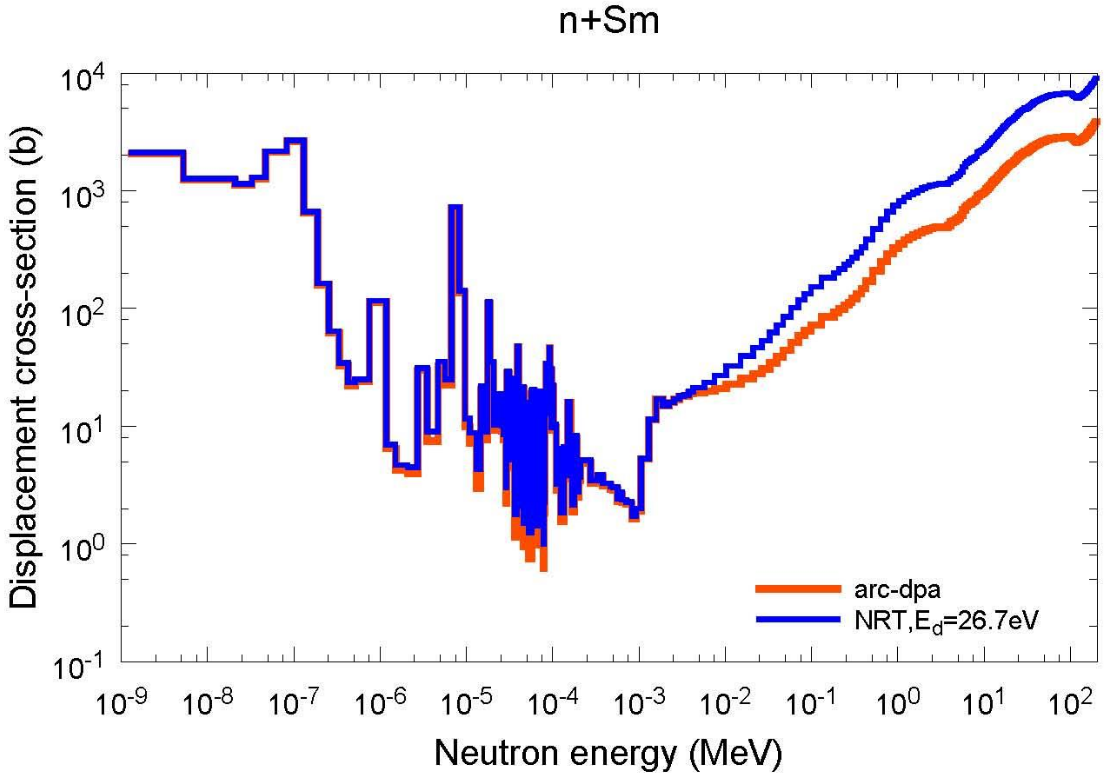
n+Sm
Displacement cross-section (b)
Neutron energy (MeV)
arc-dpa
NRT,E$_d$=26.7eV

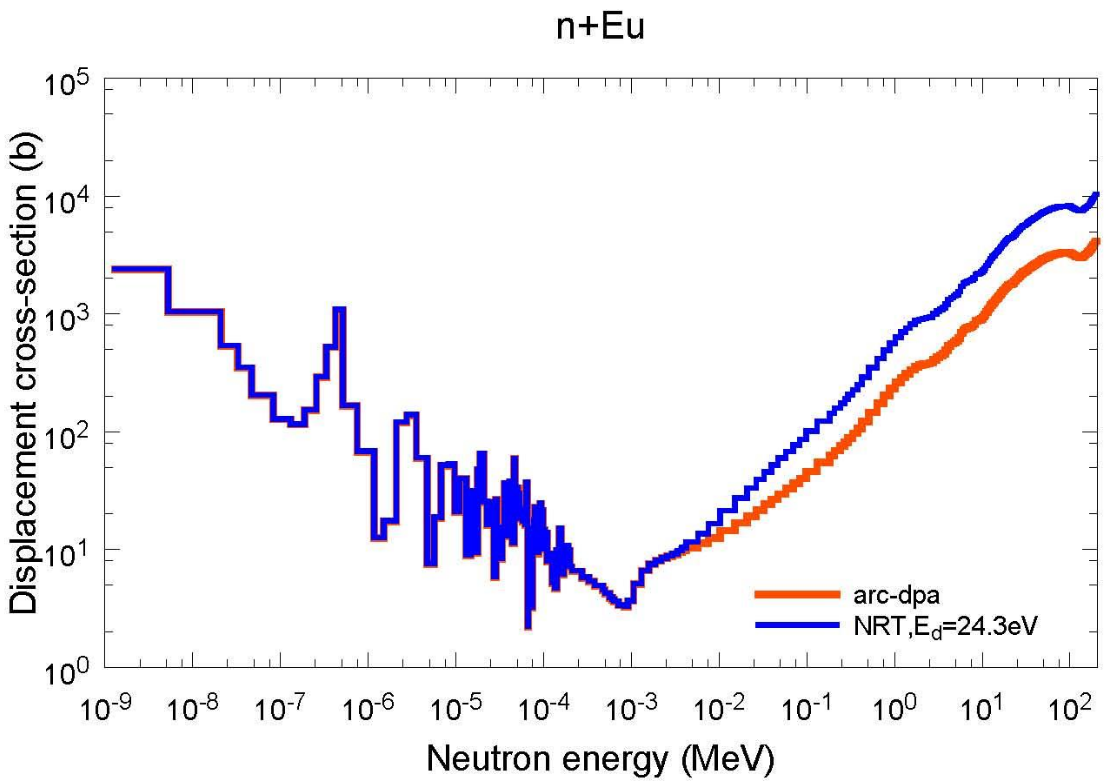
n+Eu
Displacement cross-section (b)
Neutron energy (MeV)
arc-dpa
NRT,E$_d$=24.3eV

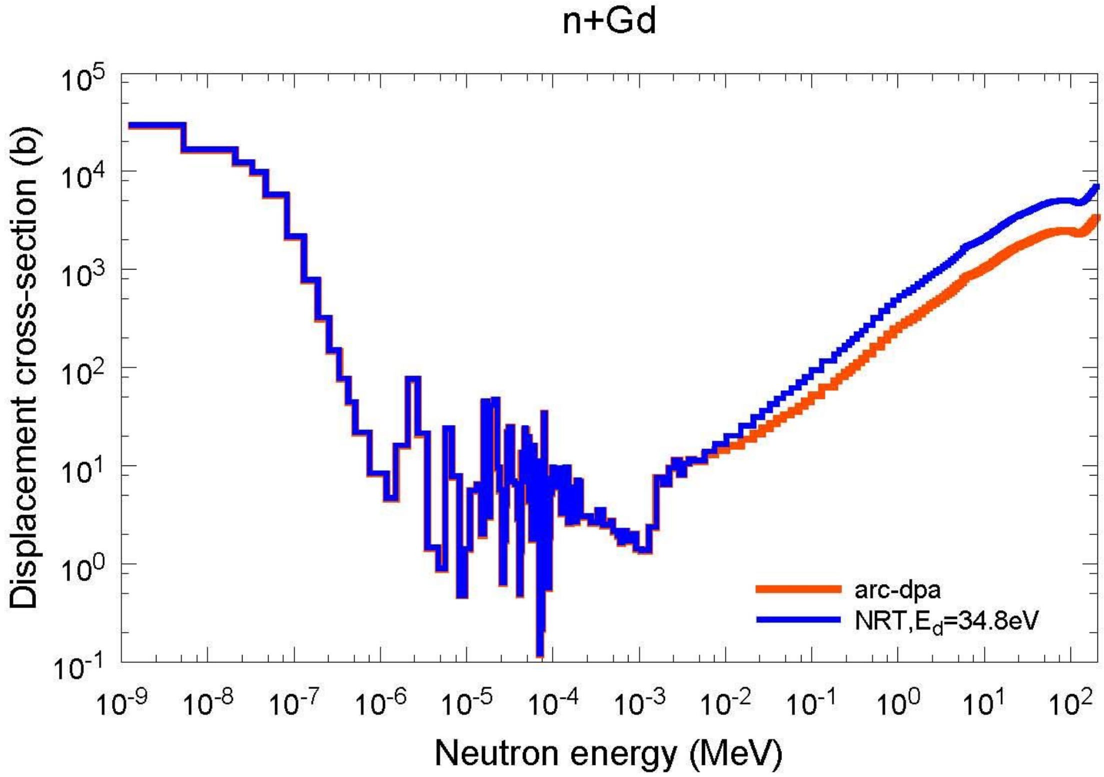
n+Gd
Displacement cross-section (b)
Neutron energy (MeV)
arc-dpa
NRT,E_d=34.8eV
10^{-1}
10^{0}
10^{1}
10^{2}
10^{3}
10^{4}
10^{5}
10^{-9} 10^{-8} 10^{-7} 10^{-6} 10^{-5} 10^{-4} 10^{-3} 10^{-2} 10^{-1} 10^{0} 10^{1} 10^{2}

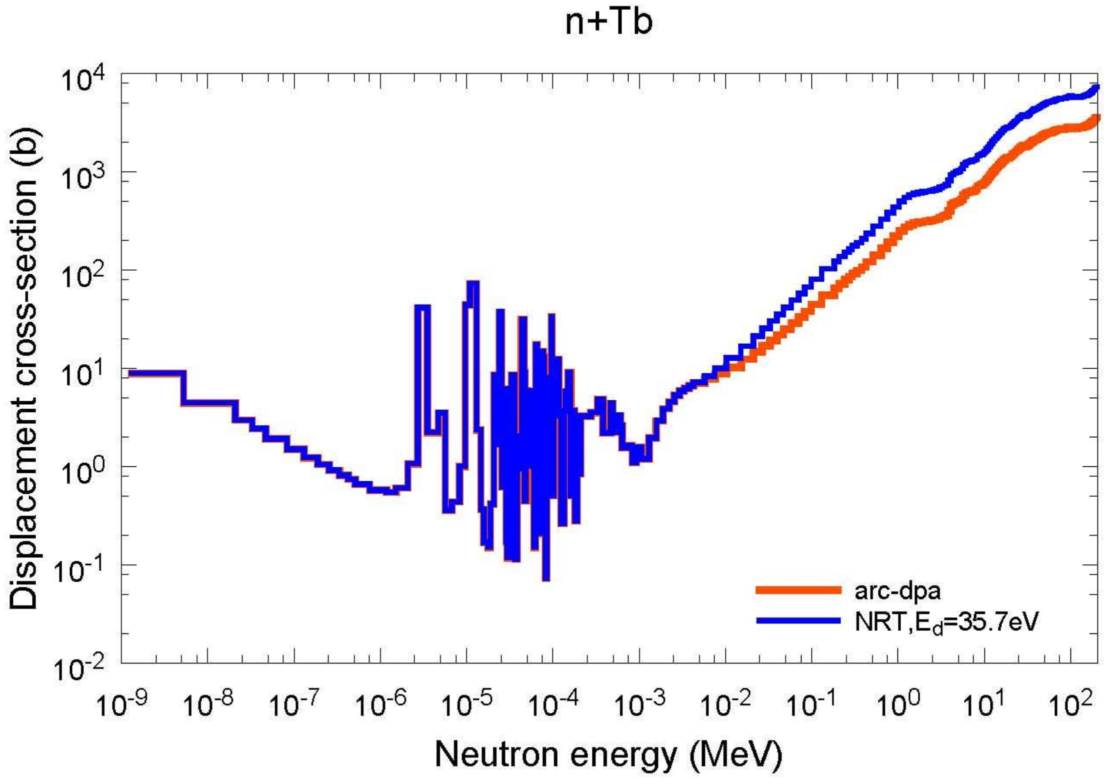
n+Tb
Displacement cross-section (b)
Neutron energy (MeV)
arc-dpa
NRT,E_d=35.7eV
10^{-2}
10^{-1}
10^{0}
10^{1}
10^{2}
10^{3}
10^{4}
10^{-9} 10^{-8} 10^{-7} 10^{-6} 10^{-5} 10^{-4} 10^{-3} 10^{-2} 10^{-1} 10^{0} 10^{1} 10^{2}

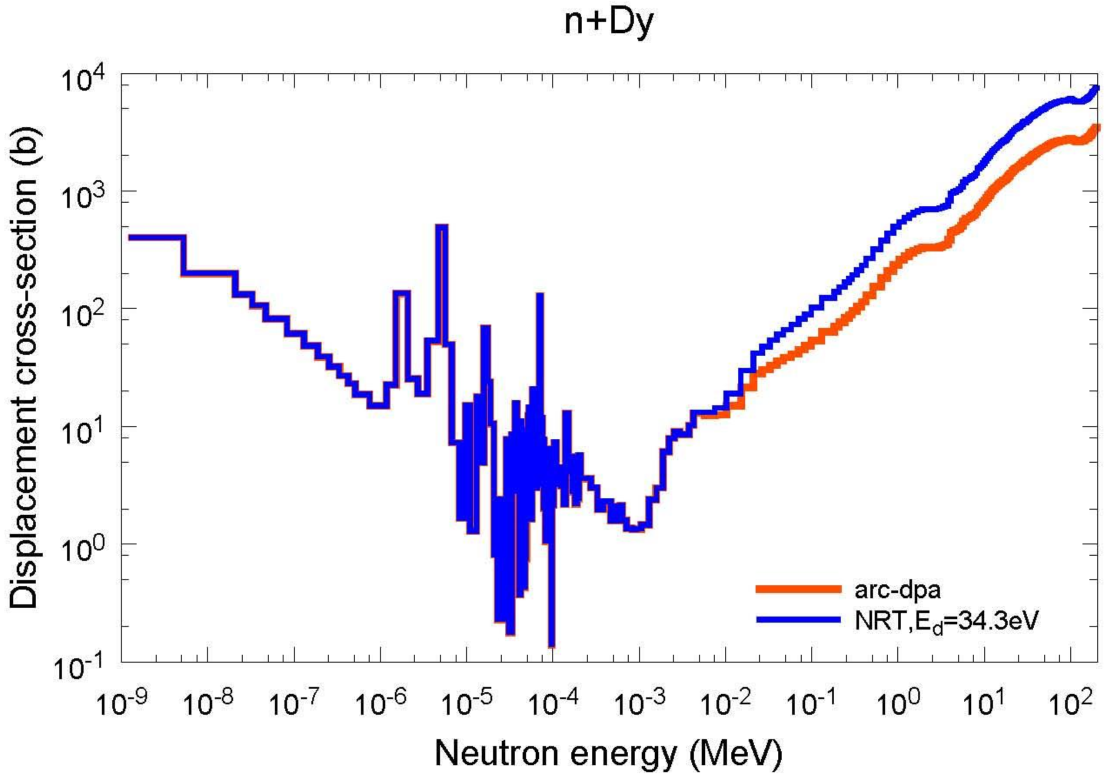

n+Dy
Displacement cross-section (b)
Neutron energy (MeV)
arc-dpa
NRT,E_d=34.3eV

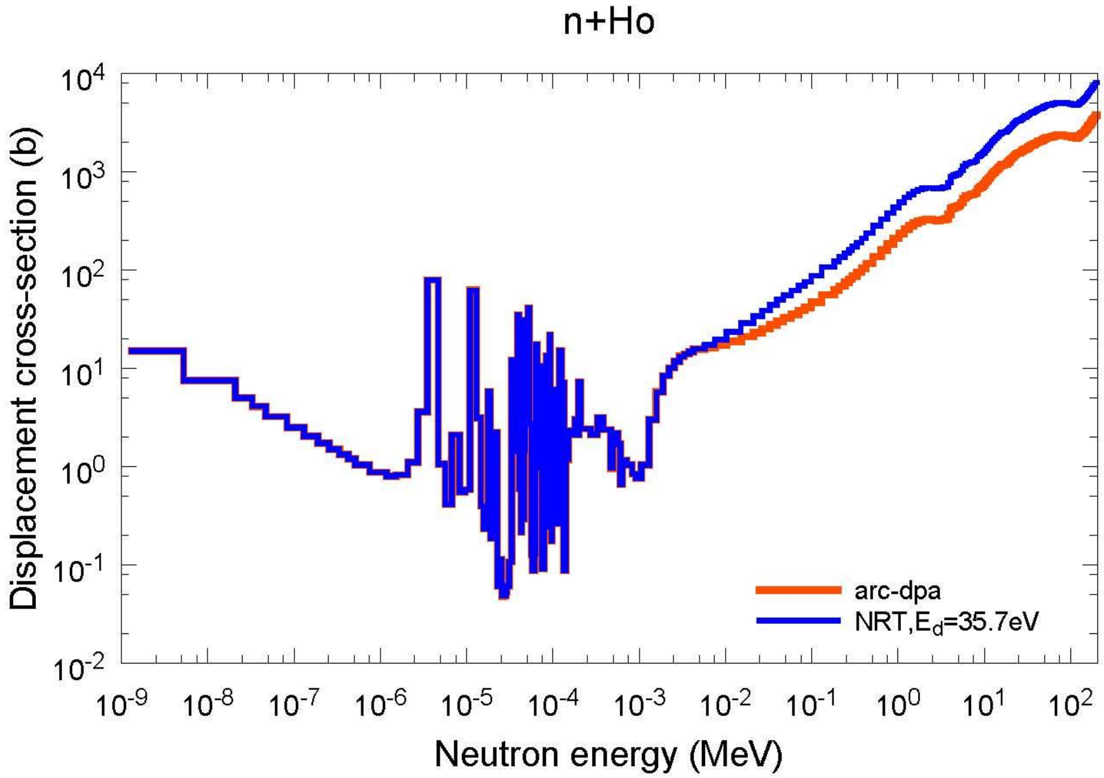

n+Ho
Displacement cross-section (b)
Neutron energy (MeV)
arc-dpa
NRT,E_d=35.7eV

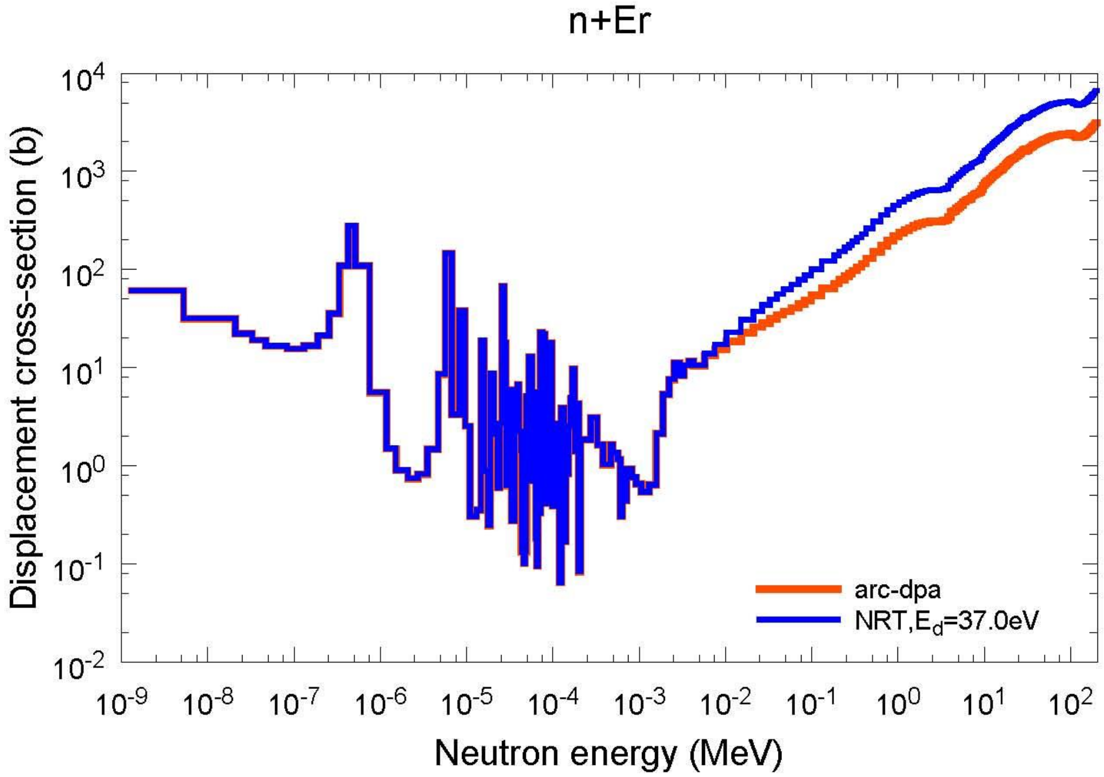

n+Er
Displacement cross-section (b)
Neutron energy (MeV)
arc-dpa
NRT,E$_d$=37.0eV

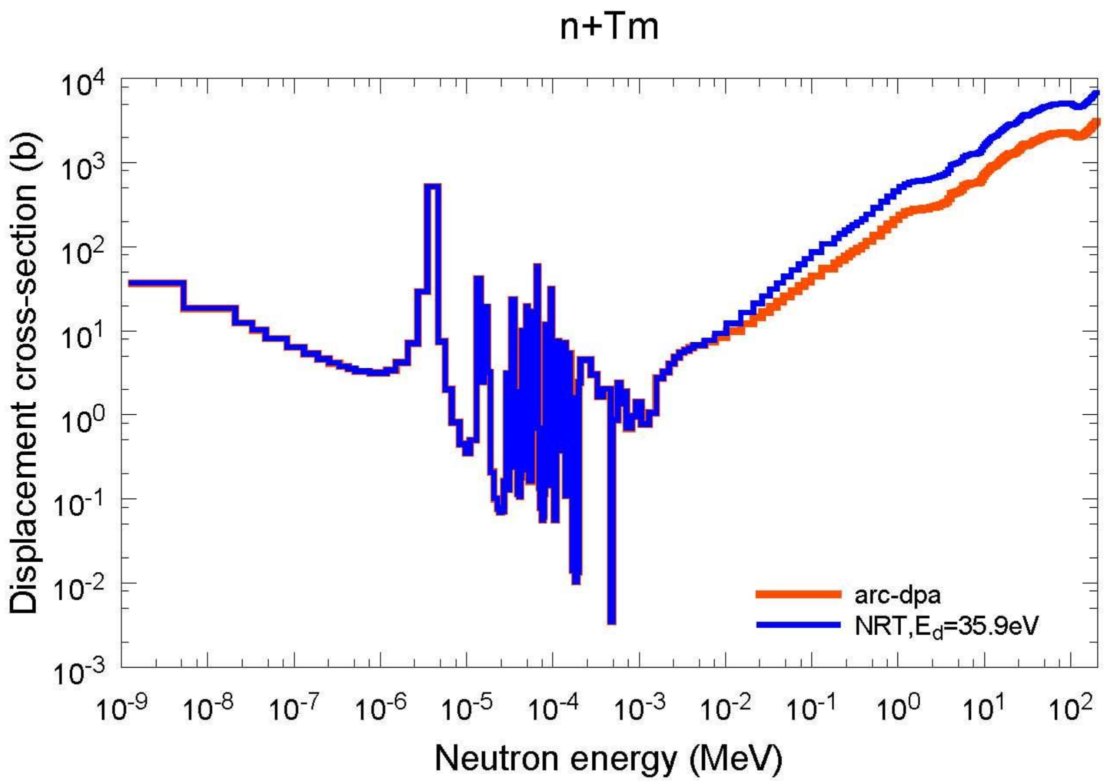

n+Tm
Displacement cross-section (b)
Neutron energy (MeV)
arc-dpa
NRT,E$_d$=35.9eV

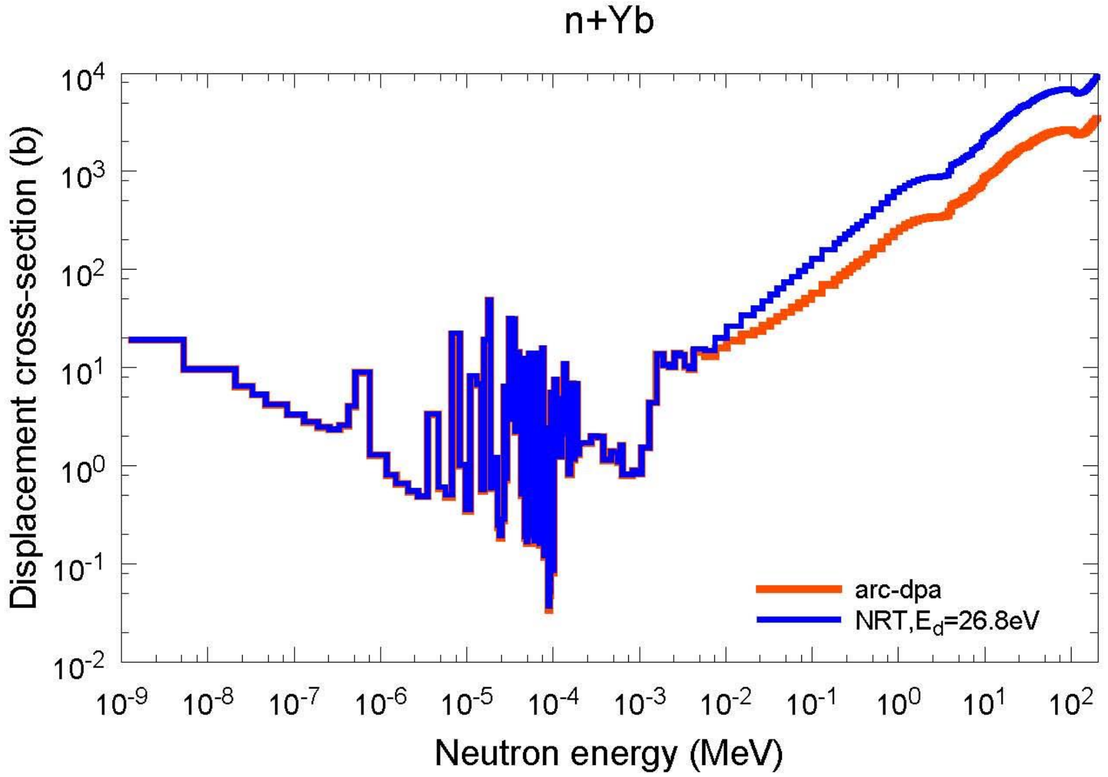
n+Yb
Displacement cross-section (b)
Neutron energy (MeV)
arc-dpa
NRT,E$_d$=26.8eV

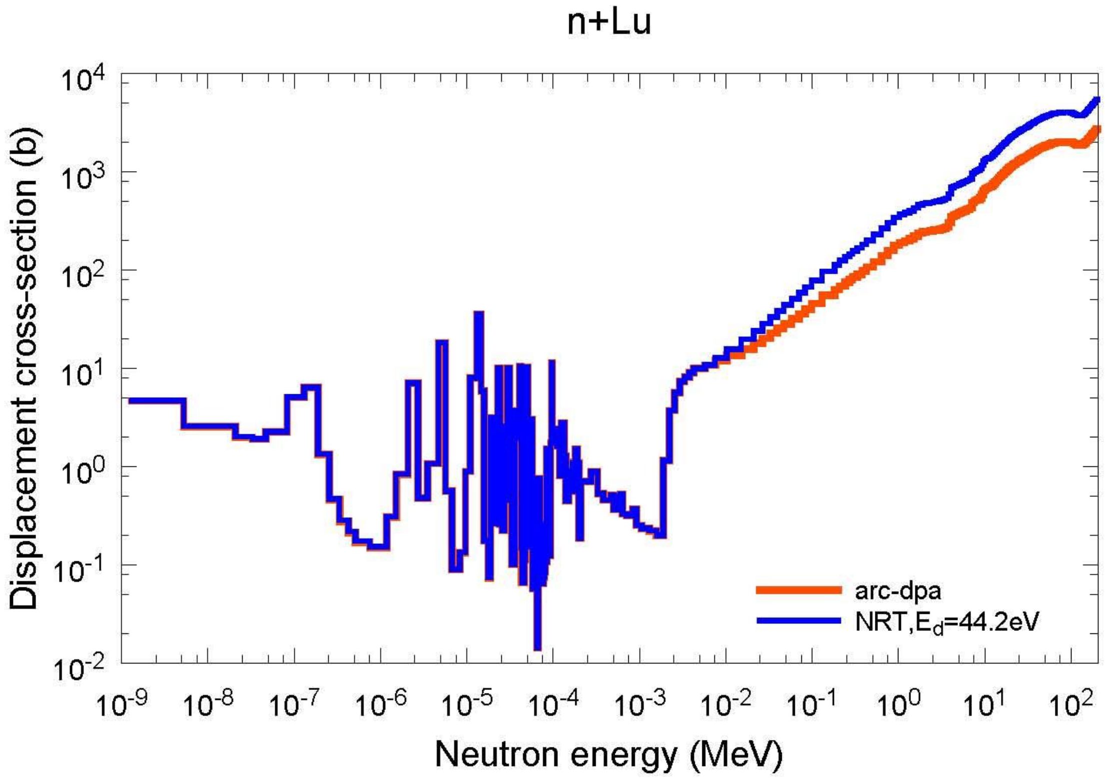
n+Lu
Displacement cross-section (b)
Neutron energy (MeV)
arc-dpa
NRT,E$_d$=44.2eV

n+Hf

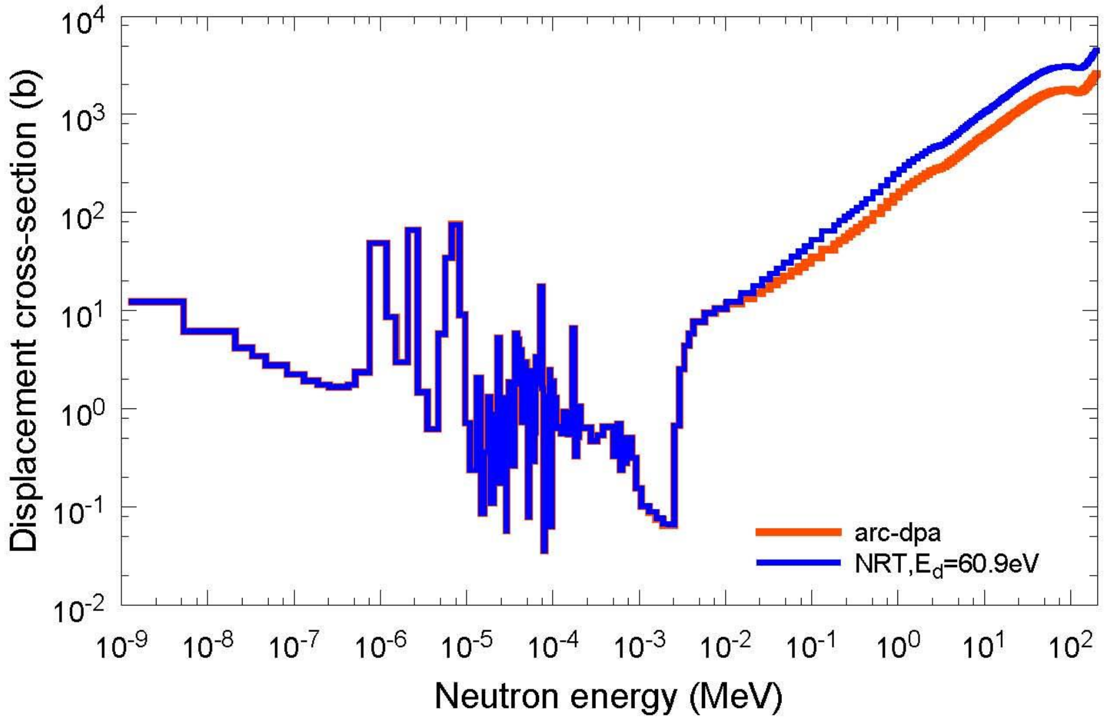

arc-dpa
NRT,E$_d$=60.9eV
Displacement cross-section (b)
Neutron energy (MeV)

n+Ta

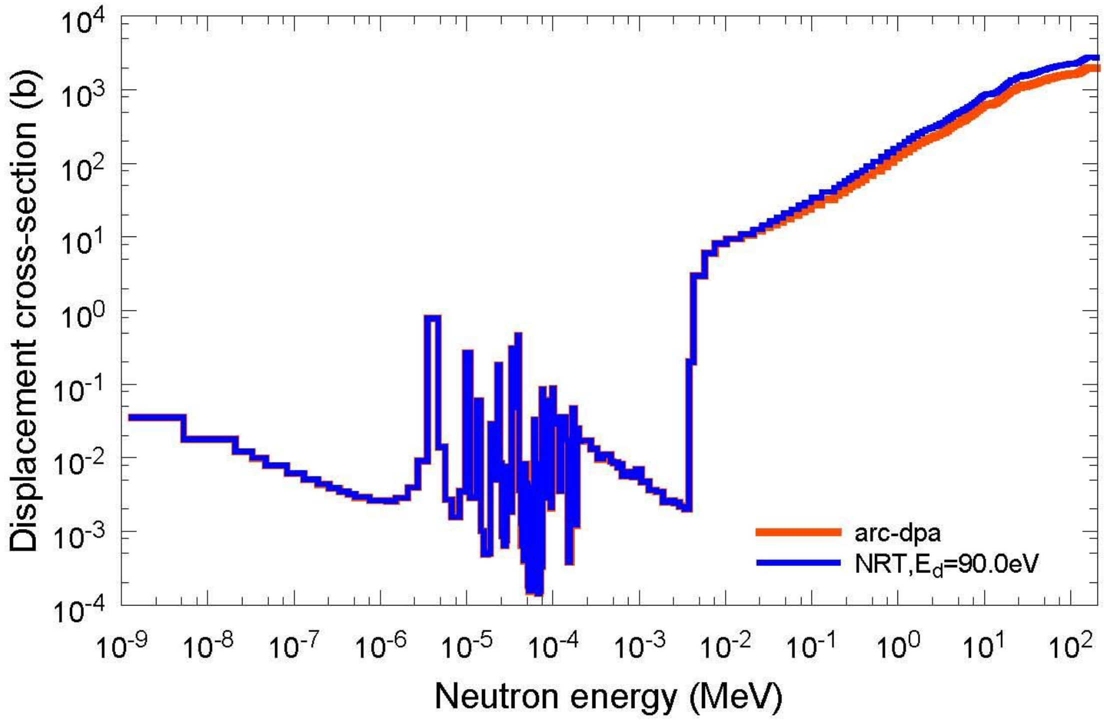

arc-dpa
NRT,E$_d$=90.0eV
Displacement cross-section (b)
Neutron energy (MeV)

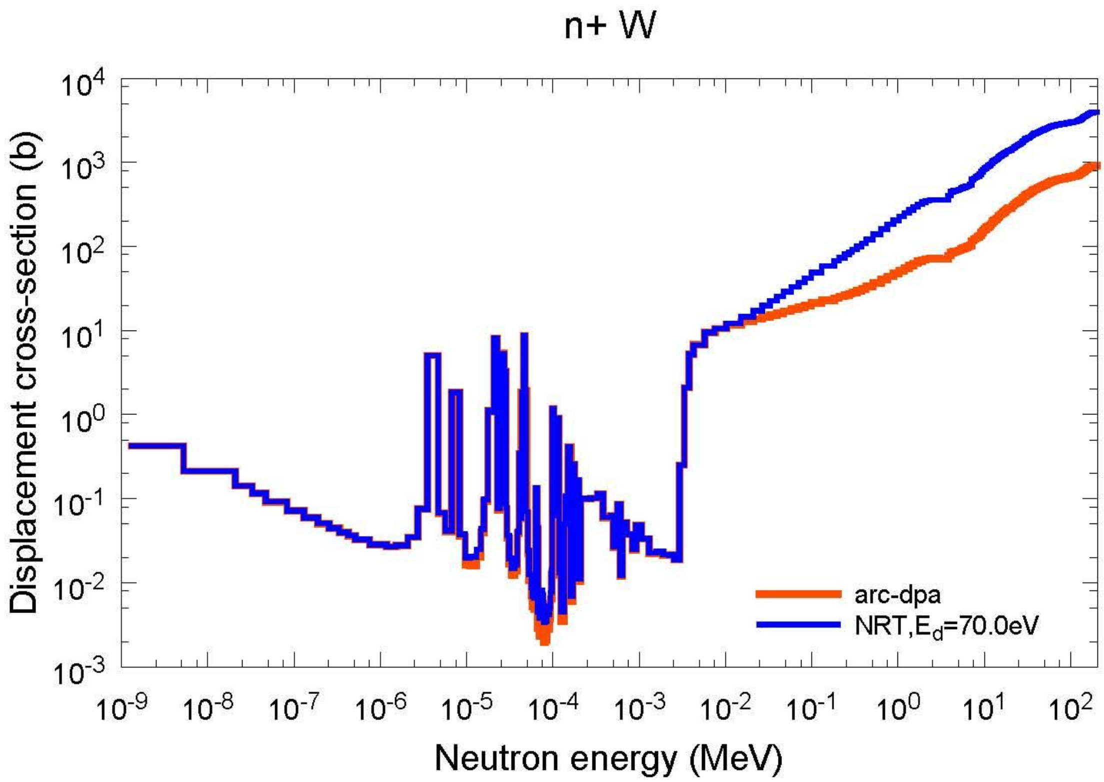
n+ W
Displacement cross-section (b)
Neutron energy (MeV)
arc-dpa
NRT,E$_d$=70.0eV

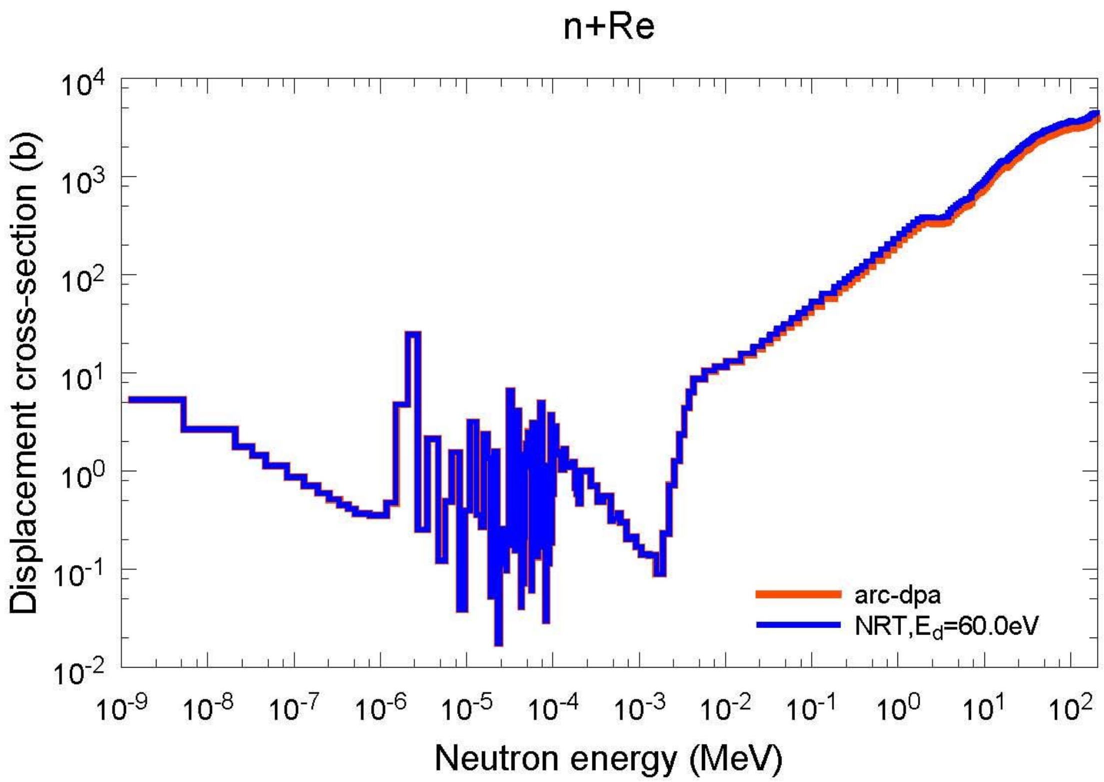
n+Re
Displacement cross-section (b)
Neutron energy (MeV)
arc-dpa
NRT,E$_d$=60.0eV

n+Os

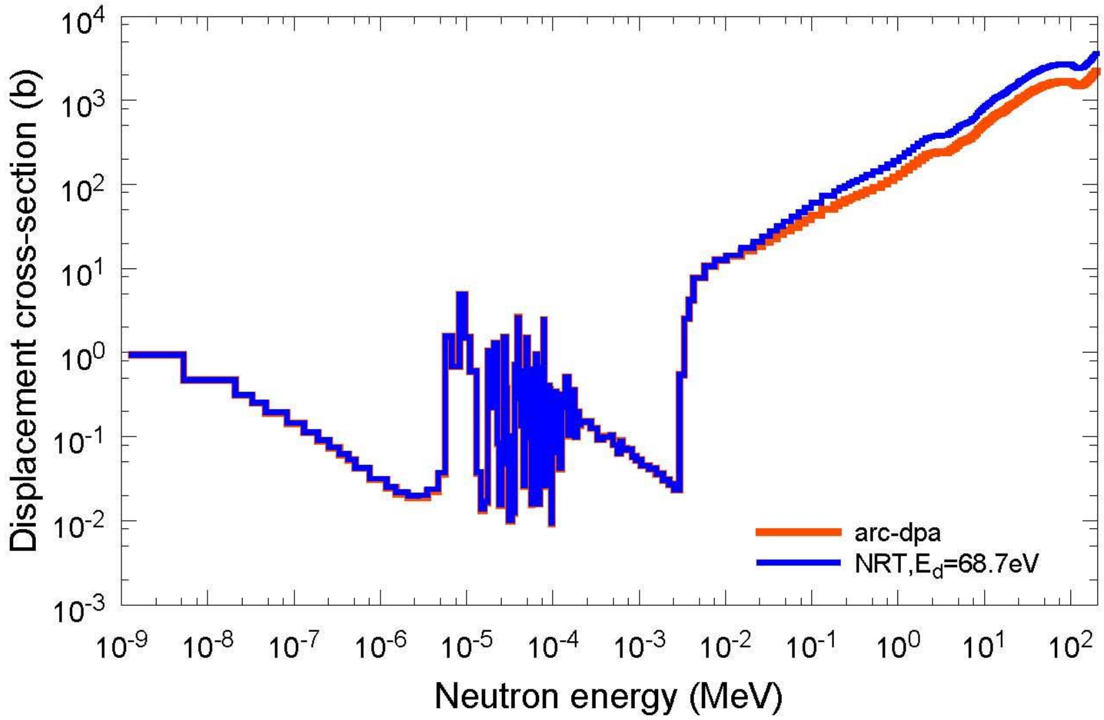
Displacement cross-section (b)
Neutron energy (MeV)
arc-dpa
NRT,E$_d$=68.7eV

n+Ir

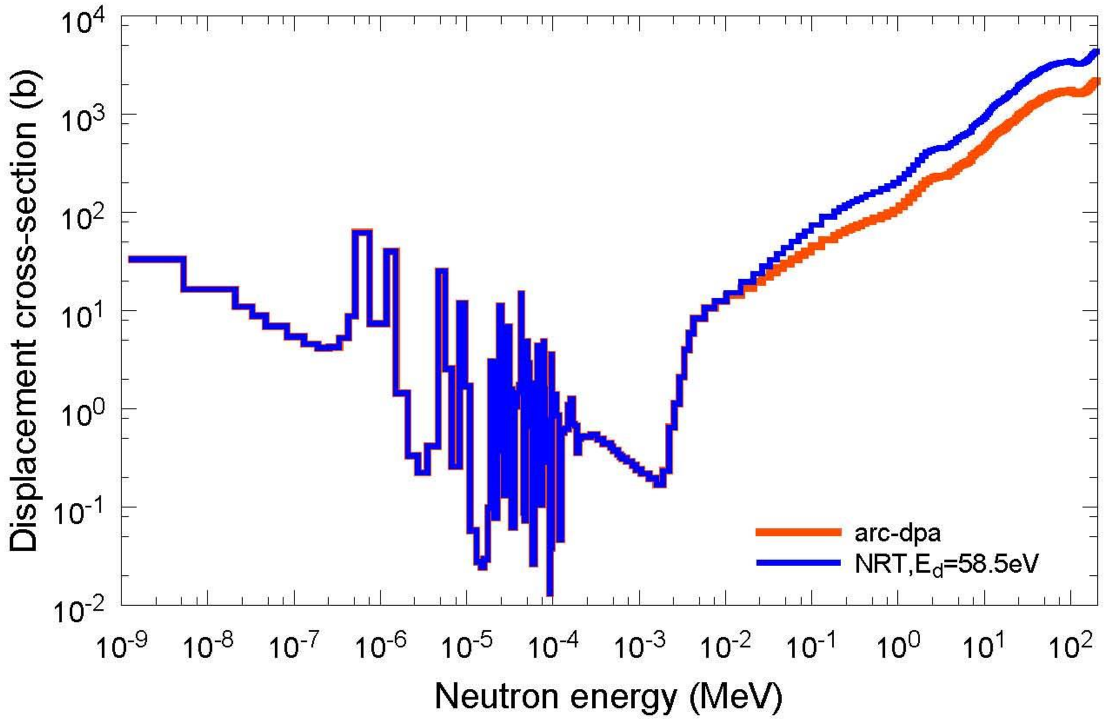
Displacement cross-section (b)
Neutron energy (MeV)
arc-dpa
NRT,E$_d$=58.5eV

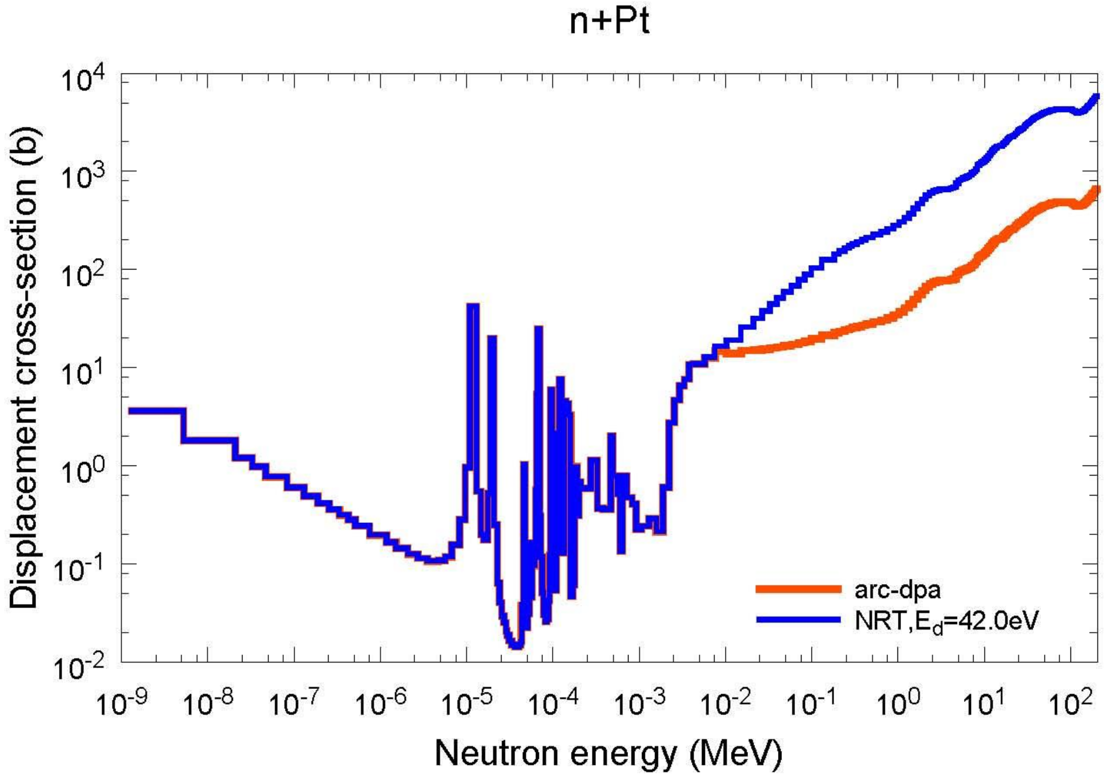
n+Pt
Displacement cross-section (b)
Neutron energy (MeV)
arc-dpa
NRT,E_d=42.0eV

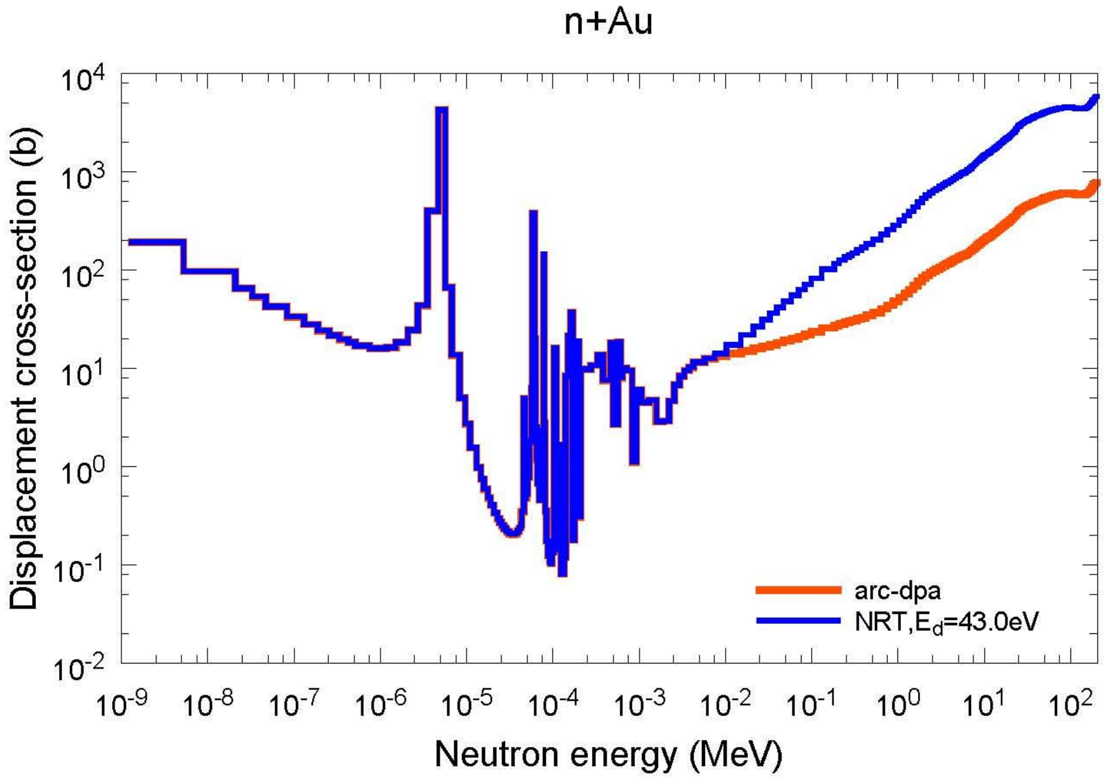
n+Au
Displacement cross-section (b)
Neutron energy (MeV)
arc-dpa
NRT,E_d=43.0eV

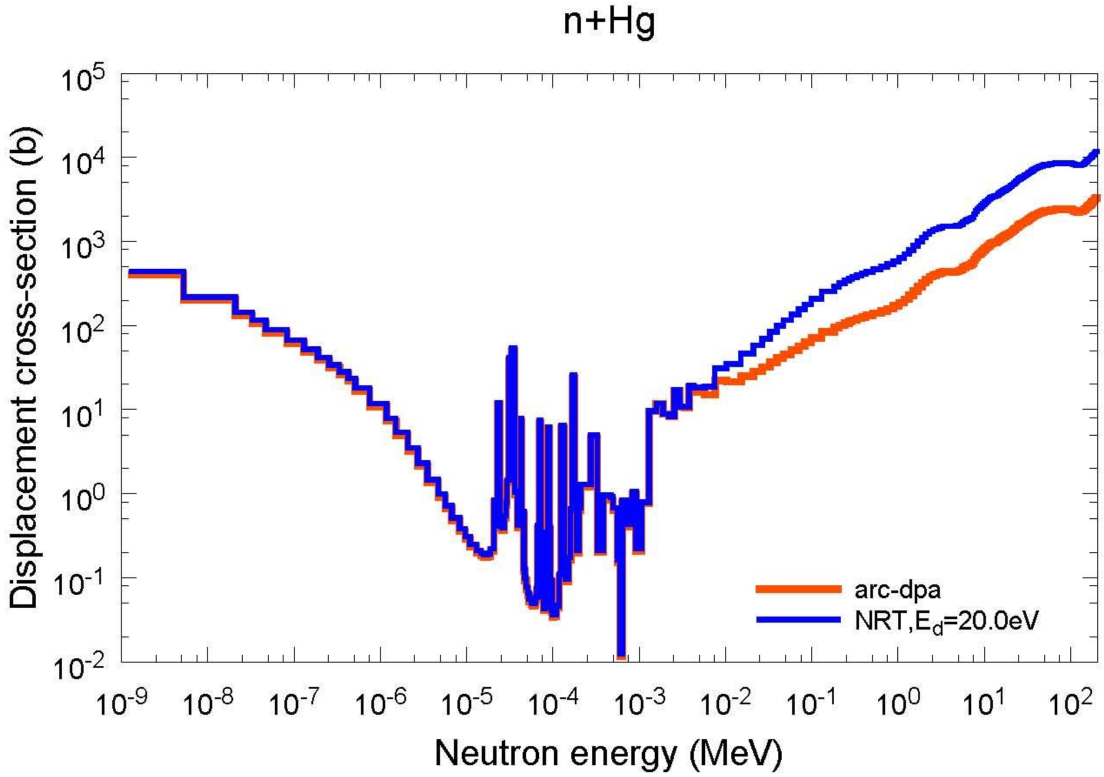
n+Hg
Displacement cross-section (b)
Neutron energy (MeV)
arc-dpa
NRT,E_d=20.0eV

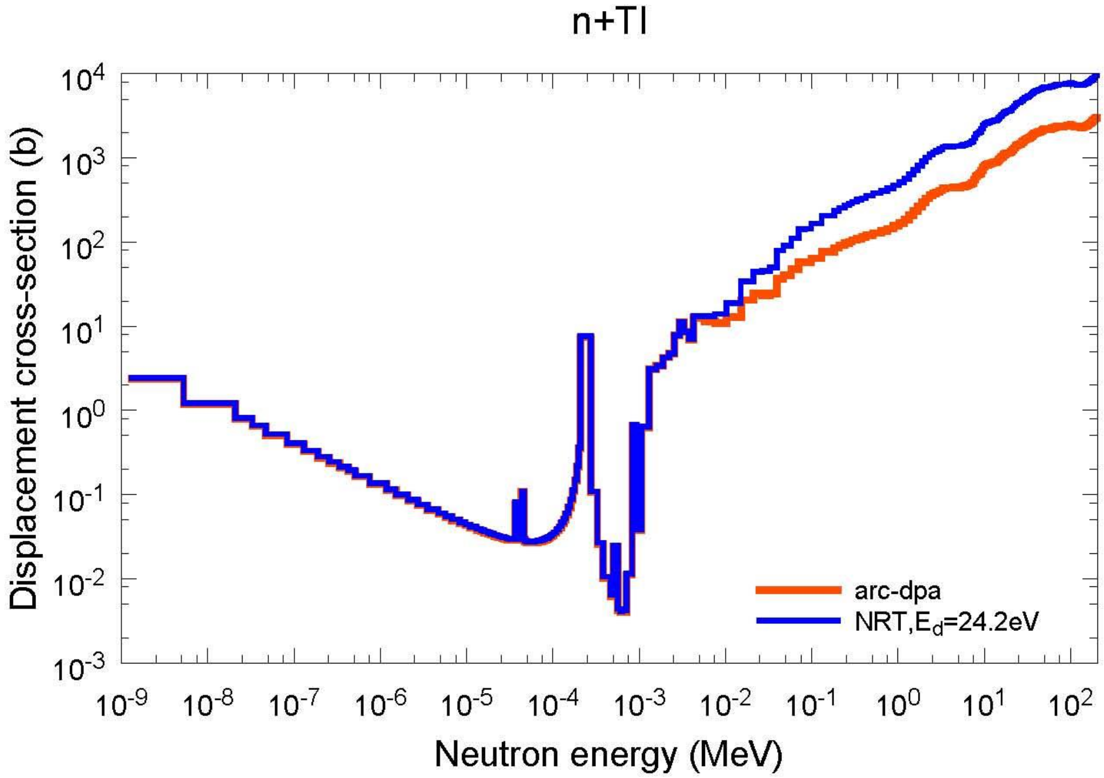
n+Tl
Displacement cross-section (b)
Neutron energy (MeV)
arc-dpa
NRT,E_d=24.2eV

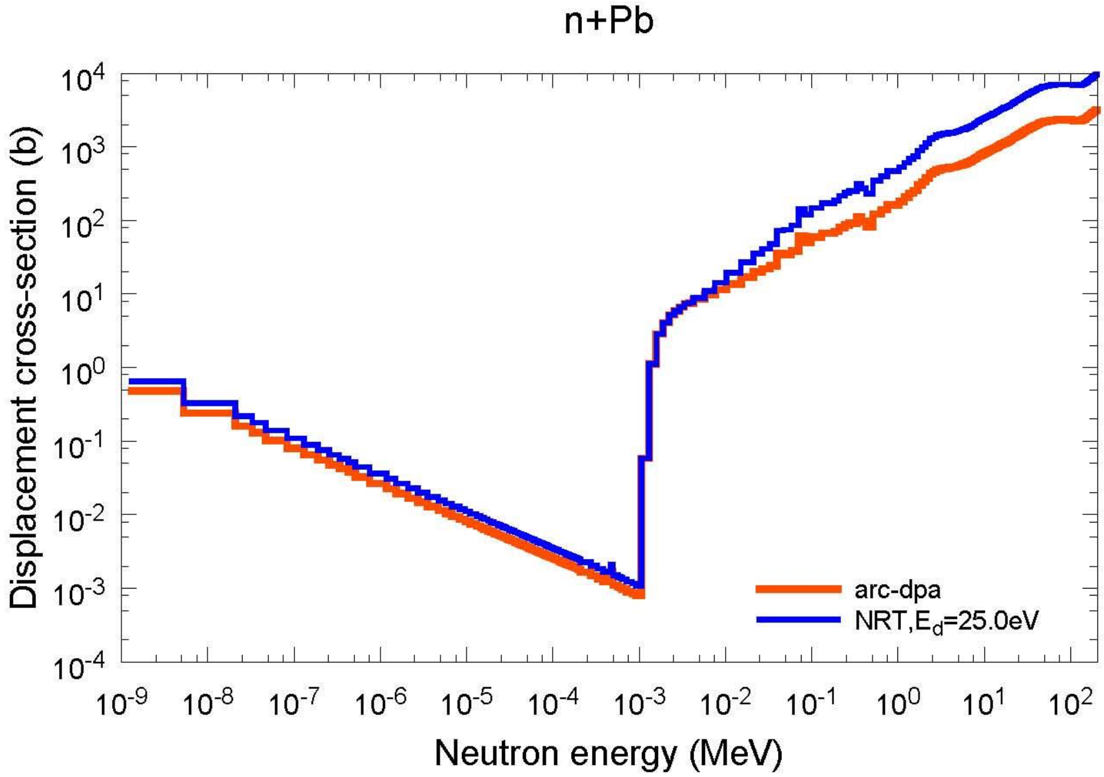

n+Pb
Displacement cross-section (b)
Neutron energy (MeV)
arc-dpa
NRT,E$_d$=25.0eV

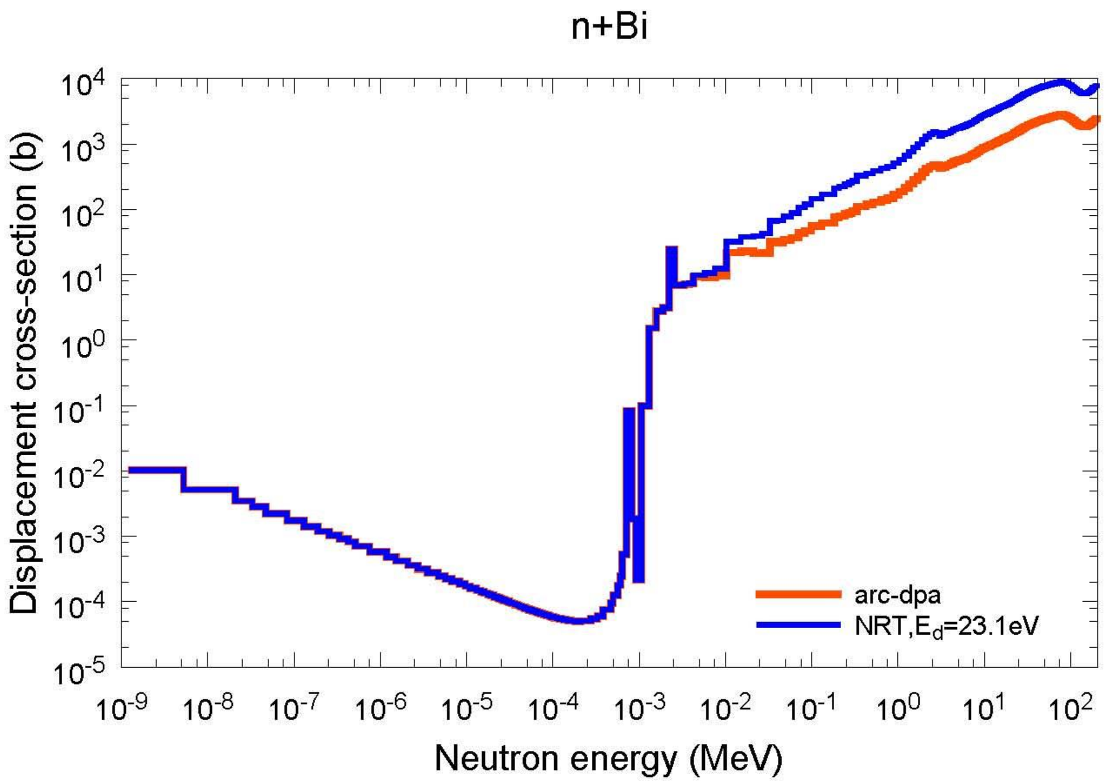

n+Bi
Displacement cross-section (b)
Neutron energy (MeV)
arc-dpa
NRT,E$_d$=23.1eV

KIT Scientific Working Papers
ISSN 2194-1629